

Spectral embedding of inhomogeneous Poisson processes on multiplex networks

Joshua Corneck, Edward A. K. Cohen, and Francesco Sanna Passino

Department of Mathematics, Imperial College London
180 Queen's Gate, SW7 2AZ, London (United Kingdom)

Abstract

In many real-world networks, data on the edges evolve in continuous time, naturally motivating representations based on point processes. Heterogeneity in edge types further gives rise to multiplex network point processes. In this work, we propose a model for multiplex network data observed in continuous-time. We establish two-to-infinity norm consistency and asymptotic normality for spectral-embedding-based estimation of the model parameters as both network size and time resolution increase. Drawing inspiration from random dot product graph models, each edge intensity is expressed as the inner product of two low-dimensional latent positions: one dynamic and layer-agnostic, the other static and layer-dependent. These latent positions constitute the primary objects of inference, which is conducted via spectral embedding methods. Our theoretical results are established under a histogram estimator of the network intensities and provide justification for applying a doubly unfolded adjacency spectral embedding method for estimation. Simulations and real-data analyses demonstrate the effectiveness of the proposed model and inference procedure.

Keywords — continuous-time networks, multiplex networks, point processes, spectral embedding.

1 Introduction

Network models provide a principled way to encode complex patterns of interaction among large collections of interdependent entities. In many modern applications, such data exhibit rich structure, encompassing multiple types of relationships and evolving continuously over time. To capture heterogeneity of connection types, *multiplex* (also known as *multilayer*) networks extend this framework by considering multiple *layers*, each encoding a distinct form of relation among the same set of nodes (De Domenico et al., 2015). By further allowing temporal point processes to exist on the edges of multiplex networks, continuous-time interaction data can be more accurately understood. Such networks naturally arise in many domains (for a survey of common applications, see Goldenberg et al., 2010); for example, on a social media platform, layers may represent “follow” or “retweet” interactions with time-stamps defining a point process (Greene and Cunningham, 2013). Similarly, on a trade network, times of trades could be considered as a point process with layers corresponding to different products (Corneck et al., 2025a).

A common approach for modelling static networks is to associate each node with a low-dimensional latent position governing its connectivity, as in the latent position model of Hoff et al. (2002). The random dot-product graph (RDPG) is a widely studied special case, for which spectral embedding provides a natural and tractable method of inference (Athreya et al., 2018). Spectral embedding has become a central tool in statistical network analysis, providing consistent estimators of latent positions under the stochastic block model (Sussman et al., 2012; Rohe et al., 2010), and enabling tasks such as clustering and community detection (Athreya et al., 2018) via limiting distributional results.

Despite significant advances in the literature on spectral embedding for static and multiplex graphs, few approaches have been developed to handle dynamic multiplex graphs observed in continuous time. In this work, we address this gap by introducing the *multiplex inhomogeneous Poisson process dot-product graph*

(MIPP-DPG), a continuous-time multiplex dot-product model characterised via low-dimensional latent positions. The MIPP-DPG characterises marked point process data as a multiplex, edge-level network point process (NPP), with observations being quadruples describing the time of arrival, the source and recipient nodes, and the corresponding network layer of the arrival. The multiplex NPP is modelled as a collection of conditionally independent, inhomogeneous Poisson processes, with intensities given by an inner product between a dynamic, layer-agnostic position and a static, layer-dependent position. We estimate these positions by binning time to form a histogram estimator of edge intensities and then applying spectral embedding to the resulting matrix. Despite this discretisation step, our theory recovers the continuous-time nature of the latent positions asymptotically. Under non-degeneracy and smoothness conditions, and as the numbers of nodes increase and the time resolution is refined, we prove row-wise two-to-infinity norm consistency and asymptotic normality of the estimated positions. Simulations and a real-data application demonstrate that the method recovers interpretable dynamic and layer-dependent structure.

The remainder of this manuscript is organised as follows. Section 1.1 introduces the related literature and outlines the notation used. Section 2 presents our proposed model and related estimation procedure, before Section 3 introduces the main theoretical results of this work, as well as key results for their proof. In conclusion, Section 4 examines inference with simulated data, with Section 5 then exploring an application of our model to a global air transportation network.

1.1 Background and related literature

A graph is mathematically represented as $\mathcal{G} = (\mathcal{V}, \mathcal{E})$, with a node set $\mathcal{V} := [N]$, where $[N] := \{1, \dots, N\}$, $N \in \mathbb{N}$, and an edge set $\mathcal{E} \subseteq \mathcal{V} \times \mathcal{V}$ that characterises interactions between these nodes. We write $(i, j) \in \mathcal{E}$ if there is a connection between nodes $i, j \in \mathcal{V}$. We say that the graph is undirected if and only if $(i, j) \in \mathcal{E}$ implies $(j, i) \in \mathcal{E}$, otherwise the graph is considered to be directed. A graph can be equivalently represented by its adjacency matrix $\mathbf{A} \in \{0, 1\}^{N \times N}$, with $A_{ij} = \mathbb{I}_{\mathcal{E}}\{(i, j)\}$, where $\mathbb{I}_{\{\cdot\}}$ denotes the indicator function.

A common model for such a directed graph in the single layer setting is the latent position model (LPM; Hoff et al., 2002). In the undirected graph case, each node $i \in \mathcal{V}$ is associated with a latent position vector $X_i \in \mathcal{X} \subseteq \mathbb{R}^d$, where the latent space \mathcal{X} has dimension $d \ll N$. Once equipped with a kernel function $\kappa : \mathcal{X} \times \mathcal{X} \rightarrow [0, 1]$, the latent positions fully characterise the network by expressing the edge probabilities as $\mathbb{P}(A_{ij} = 1) = \kappa(X_i, X_j)$. A popular choice of the kernel function is $\kappa(X_i, X_j) = X_i^\top X_j$, in which case the LPM is referred to as a random dot product graph (RDPG; see, for example, Athreya et al., 2018). Spectral embedding of the adjacency matrices can be used to estimate the latent positions in RDPGs, with the left and right singular vectors of the associated adjacency matrix sorted by the magnitude of the associated singular values (Athreya et al., 2018). Spectral embedding estimators produce uniformly consistent estimates of up to orthogonal or general linear transformation in various RDPG-based models, with asymptotically Gaussian error (Lyzinski et al., 2015; Athreya et al., 2018; Cape et al., 2019a,b; Jones and Rubin-Delanchy, 2020; Gallagher et al., 2024; Baum et al., 2024).

Latent positions in latent space models can be assumed to be either deterministic and unknown, or to be random and unknown (see, for example, the discussion in Section 4.1 of Athreya et al., 2018). In the case of random positions, the latent representations can be sampled independently for each node from a pre-specified distribution on a suitable space. As discussed in Wang et al. (2025), deterministic latent positions are more suited to the case of labelled dynamic networks, meaning that each node has a deterministic identity across time. In unlabelled networks, the focus is on the overall population structure at each time, rather than individual trajectories, and inference is on recovering the latent positions. Contrastingly, in the labelled case, inference is anchored at the node level, aiming to track each node's latent trajectory through time. We will focus on the labelled case and thus assume that our latent positions are *deterministic but unknown*.

Networks that evolve over time are termed *dynamic*, with temporal dependence manifesting in the edge set, the node set, or both. Much of the literature has focused on discrete-time formulations of dynamic networks, where networks are observed through aggregated snapshots, and most theoretical results are established in this setting (see, for example, Sewell and Chen, 2015; Shlomovich et al., 2022; Billio et al., 2024; Athreya et al., 2025). In contrast, many real-world interaction datasets are inherently continuous-time, such as email exchanges within a company (Klimt and Yang, 2004), social media activity (Paranjape et al., 2017), or bike-sharing networks

(Corneck et al., 2025b). Models for such continuous-time data typically view interactions as edge-level NPPs, for example through semiparametric stochastic block models (Matias et al., 2018), Cox process formulations (Perry and Wolfe, 2013), or mutually exciting processes with intensities depending only on node-specific parameters (Sanna Passino and Heard, 2023). An alternative formulation of a dynamic network is to view the network itself as static, but to consider a collection of point processes on the edges (an NPP), with the edge-level point process capturing the temporal dynamics of the data (see, for example, Corneck et al., 2025b; Matias et al., 2018; Modell et al., 2024). It is this formulation on which the MIPP-DPG is modelled.

When the graph \mathcal{G} consists of multiple connection types between its nodes, it is called a *multiplex network*. Each of the L connection types is described by a unique layer, with each layer $\ell \in [L]$ being a graph $\mathcal{G}_\ell = (\mathcal{V}, \mathcal{E}_\ell)$ on a node set common to all layers. A multiplex network \mathcal{G} with L types of connection is mathematically denoted by $\mathcal{G} = (\mathcal{V}, \{\mathcal{E}_1, \dots, \mathcal{E}_L\})$. Methodological development for multiplex networks is relatively recent (Sosa and Betancourt, 2022; Huang et al., 2023; Lei and Lin, 2023). Within the context of RDPG models, a relevant extension is the multilayer RDPG (MRDPG; Jones and Rubin-Delanchy, 2020), where each node is assigned a layer-specific latent position $Y_{\ell j}$, so that the probability of connection between nodes i and j in layer ℓ is $X_i^\top Y_{\ell j}$. The MRDPG admits inference via unfolded adjacency spectral embedding (UASE; Jones and Rubin-Delanchy, 2020), wherein the adjacency matrices of the network are stacked and simultaneously embedded. Asymptotic theoretical properties for UASE have been established, with Gallagher et al. (2021) showing that it yields stable and consistent latent position estimates across layers. More broadly, theoretical properties of the UASE estimator are supported by the extensive theory of spectral embedding for single-layer networks (Athreya et al., 2018).

While multiplex and dynamic networks have each been studied, the setting where both aspects are present has received comparatively limited attention. Examples include the work of Oselio et al. (2014); Hoff (2015); Durante et al. (2017); Loyal and Chen (2023); Wang et al. (2025). Among the available approaches, the dynamic multiplex random dot-product graph (DMRDPG) of Baum et al. (2024) is particularly relevant to this work. The DMRDPG extends the MRDPG to a sequence of discrete-time multiplex graphs. Nodes are assigned a time-dependent latent position X_{it} , for $t \in \mathbb{N}$, so that the probability of connection between nodes i and j in layer ℓ at time point t is $X_{it}^\top Y_{\ell j}$. The authors develop an inference procedure called doubly unfolded adjacency spectral embedding (DUASE; Baum et al., 2024), establishing methodology and theoretical results for the discrete-time and binary edge setting. In this work, we adapt DUASE to the weighted, continuous-time setting by assuming a dot product structure for the edge-process intensity functions, proving that the estimators are asymptotically unbiased with normally distributed errors.

Recent work has introduced spectral methods for continuous-time networks, such as the Intensity Profile Projection (IPP; Modell et al., 2024), which provides representations of nodes in single-layer point process networks, or the Common Subspace Independent Process (COSIP; Romero et al., 2025). However, the literature on continuous-time networks remain largely separate from the RDPG framework that underpins much of the theory for static and discrete-time random graph models. Furthermore, continuous-time approaches of the kind in Modell et al. (2024) and Romero et al. (2025) have not yet been developed for multiplex networks. All available estimation procedures for continuous-time data on networks must involve discretising the observation window. Our work utilises this approach too; however, our theory will recover the continuous-time setting in the limit of a growing network.

1.2 Matrix and norm notation

We write matrices using boldface and vectors and scalars in standard font. For a matrix $\mathbf{M} \in \mathbb{R}^{m \times n}$, we denote its i -th row and j -th column by $M_{i,*} \in \mathbb{R}^n$ and $M_{*,j} \in \mathbb{R}^m$, treated as row and column vectors, respectively. We access the (i, j) -th element of \mathbf{M} as M_{ij} , but when writing the (i, j) -th element of a product $\mathbf{M}_1 \mathbf{M}_2$, we write $(\mathbf{M}_1 \mathbf{M}_2)_{ij}$. When matrices carry subscripts, such as \mathbf{M}_ℓ or $\mathbf{M}_{m\ell}$, we access the (i, j) -th element as $M_{\ell,ij}$ or $M_{m\ell,ij}$. If we consider a block matrix $\mathbf{M} \in \mathbb{R}^{an \times bm}$, we write $\mathbf{M}^{(r,*)}$ to be the $n \times bm$ matrix consisting of the r -th set of n rows, and $\mathbf{M}^{(*,s)}$ to be the $an \times m$ matrix consisting of the s -th set of m columns, and $\mathbf{M}^{(r,s)}$ to be the (r, s) -th $n \times n$ submatrix.

When \mathbf{M} is square, the k -th largest eigenvalue of \mathbf{M} is written as $\lambda_k(\mathbf{M})$, and when $m \neq n$, the k -th largest singular value is written as $\sigma_k(\mathbf{M})$. For $\alpha > 0$, we define the vector norm $\|\cdot\|_\alpha$ on \mathbb{R}^n by $\|x\|_\alpha = (\sum_{i=1}^n |x_i|^\alpha)^{1/\alpha}$. The matrix \mathbf{M} induces a linear operator from \mathbb{R}^n to \mathbb{R}^m , and we define the operator norm of

\mathbf{M} as a mapping from \mathbb{R}^n to \mathbb{R}^m , equipped with $\|\cdot\|_\alpha$ and $\|\cdot\|_\beta$, respectively, as $\|\mathbf{M}\|_{\alpha,\beta} := \sup_{\|\mathbf{x}\|_\alpha=1} \|\mathbf{M}\mathbf{x}\|_\beta$. An important case is the two-to-infinity norm of \mathbf{M} , written $\|\mathbf{M}\|_{2,\infty} := \sup_{\|\mathbf{x}\|_2=1} \|\mathbf{M}\mathbf{x}\|_\infty$, equivalent to $\|\mathbf{M}\|_{2,\infty} = \max_{i \in [m]} \|\mathbf{M}_i\|_2$, the maximum of the Euclidean norm of the rows of \mathbf{M} . In the case that $\alpha = \beta$, the operator norm of the matrix \mathbf{M} is simply written as $\|\mathbf{M}\|_\alpha$. We regularly refer to the spectral norm $\|\mathbf{M}\|_2$, which corresponds to $\lambda_1(\mathbf{M}^\top \mathbf{M})^{1/2} = \sigma_1(\mathbf{M})$. Also of importance is the Frobenius norm of \mathbf{M} , defined as $\|\mathbf{M}\|_F := (\sum_{i=1}^m \sum_{j=1}^n |\mathbf{M}_{ij}|^2)^{1/2}$. We frequently make use of the following inequalities (see, for example, [Cape et al., 2019b](#)):

$$\|\mathbf{M}\|_2 \leq \|\mathbf{M}\|_F \leq \sqrt{\text{rank}(\mathbf{M})} \|\mathbf{M}\|_2, \quad \|\mathbf{M}\|_{2,\infty} \leq \|\mathbf{M}\|_2 \leq \sqrt{m} \|\mathbf{M}\|_{2,\infty}.$$

For an $n \times m$ matrix \mathbf{M} of rank d , we write its skinny singular value decomposition (SVD) as $\mathbf{M} = \mathbf{U}_M \mathbf{\Sigma}_M \mathbf{V}_M^\top$, and we define its incoherence parameter as $\mu(\mathbf{M}) = \max\{\frac{n}{d} \|\mathbf{U}_M\|_{2,\infty}^2, \frac{m}{d} \|\mathbf{V}_M\|_{2,\infty}^2\}$ and its condition number as $\kappa(\mathbf{M}) = \sigma_1(\mathbf{M})/\sigma_d(\mathbf{M})$.

We denote by $\text{GL}(d)$ the general linear group of dimension d , which is the collection of all $d \times d$ invertible matrices. We denote by $\mathbb{O}(d)$ the orthogonal group of dimension d , which is the collection of all matrices $\mathbf{O} \in \mathbb{R}^{d \times d}$ for which $\mathbf{O}^\top \mathbf{O} = \mathbf{O} \mathbf{O}^\top = \mathbf{I}_d$, where we use \mathbf{I}_d to denote the identity matrix of shape $d \times d$. For a collection of matrices $\mathbf{M}_1, \dots, \mathbf{M}_r \in \mathbb{R}^{m \times n}$, we denote their vertical stacking by $[\mathbf{M}_1 \mid \dots \mid \mathbf{M}_r] \in \mathbb{R}^{rm \times n}$ and their horizontal stacking by $[\mathbf{M}_1, \dots, \mathbf{M}_r] \in \mathbb{R}^{m \times rn}$.

1.3 Probabilistic asymptotic notation

For two real valued, non-stochastic functions f and g , we write $f(n) = \mathcal{O}\{g(n)\}$ and $g(n) = \Omega\{f(n)\}$ as $n \rightarrow \infty$ if there exist $N^* \in \mathbb{N}$ and $C^* > 0$ such that $f(n) \leq C^*g(n)$ for all $n > n^*$. If the bound is tight, we write instead $f(n) = o\{g(n)\}$ and $g(n) = \omega\{f(n)\}$. Furthermore, we write $f(n) = \Theta\{g(n)\}$ if $f(n) = \mathcal{O}\{g(n)\}$ and $g(n) = \mathcal{O}\{f(n)\}$. The theoretical results in this work will be shown to hold probabilistically, and in what follows we define the necessary terminology.

An event E is said to hold *almost surely* if $\mathbb{P}(E) = 1$. We say that an event E_n , depending on $n \in \mathbb{N}$, occurs with *overwhelming probability* if, for any $\gamma > 0$, there exists a finite $C_\gamma > 0$ such that $\mathbb{P}(E_n) \geq 1 - C_\gamma n^{-\gamma}$, with C_γ independent of n (see, for example, [Tao and Vu, 2010](#)). Given a real-valued function f and a family of random variables $\{Z_n\}_{n \in \mathbb{N}}$, each defined on some space $(\Omega_n, \mathcal{F}_n, \mathbb{P}_n)$, we write $|Z_n| = \mathcal{O}_{\mathbb{P}_n}\{f(n)\}$ if there exists $n^* \in \mathbb{N}$ and a finite $C > 0$ such that the event $|Z_n| \leq Cf(n)$ holds with overwhelming probability for all $n \geq n^*$.

As noted in [Tao and Vu \(2010\)](#), with overwhelming probability implies eventual almost sure bounds, provided only countably many unions are taken. If we consider the sequence $\{Z_n\}_{n \in \mathbb{N}}$ on the product space $(\Omega, \mathcal{F}, \mathbb{P}) = \prod_{n \in \mathbb{N}} (\Omega_n, \mathcal{F}_n, \mathbb{P}_n)$, then a sample $\omega = (\omega_1, \omega_2, \dots) \in \Omega$ encodes a trajectory $Z_1(\omega_1), Z_2(\omega_2), \dots$, representing the values of $\{Z_n\}_{n \in \mathbb{N}}$ for the sample $\omega \in \Omega$. Since the bound holds for any $\gamma > 0$, we may choose $\gamma > 1$ so that $\sum_n n^{-\gamma} < \infty$. In this setting, Borel-Cantelli implies that overwhelming-probability bounds, combined with polynomial cardinality of events, upgrades our statements to *almost sure eventual bounds*: with probability one, there exists an $n^*(\omega)$ such that $|Z_n(\omega_n)| \leq Cf(n)$ for all $n \geq n^*(\omega)$, in which case we say $|Z_n| = \mathcal{O}\{f(n)\}$ *eventually almost surely*.

2 Multiplex inhomogeneous Poisson process random dot product graphs

In this work, we propose a model for a point process on a multiplex graph $\mathcal{G} = (\mathcal{V}, \{\mathcal{E}_1, \dots, \mathcal{E}_L\})$ with $L \in \mathbb{N}$ layers, where \mathcal{V} is a node set with cardinality $|\mathcal{V}| = N$ shared across all layers, and $\mathcal{E}_\ell \subseteq \mathcal{V} \times \mathcal{V}$ denotes the edge set for layer $\ell \in [L]$. Arrivals of events on the network are viewed as observations of a marked point process consisting of a stream of quadruples $(i_k, j_k, \ell_k, t_k) \in \mathcal{V} \times \mathcal{V} \times [L] \times \mathbb{R}_+$, $k = 1, 2, \dots$, denoting directed interactions from node i_k to node j_k in layer ℓ_k at time t_k , where $t_k \leq t_{k'}$ for $k < k'$. This formulation induces a counting process on each edge (i, j) and layer ℓ , defined as:

$$N_{\ell ij}(t) := \sum_{k=1}^{\infty} \mathbb{I}_{\{(\ell, i, j)\}}\{(i_k, j_k, \ell_k)\} \mathbb{I}_{(0, t]}(t_k). \quad (2.1)$$

We write $\mathbf{N}(t) = [\mathbf{N}^{(*,1)}(t), \dots, \mathbf{N}^{(*,L)}(t)] \in \mathbb{N}^{N \times NL}$ to be the full matrix-valued network counting process, where $\mathbf{N}^{(*,\ell)}(\cdot) \in \mathbb{N}^{N \times N}$ is the matrix of counting processes for all possible edges in layer $\ell \in [L]$, with (i, j) -th entry given by $N_{\ell ij}(\cdot)$, the counting process for the edge (i, j) on layer ℓ . Furthermore, we define the intensity function associated to the counting process $N_{\ell ij}(\cdot)$ as

$$\lambda_{\ell ij}(t) = \lim_{h \downarrow 0} \frac{\mathbb{E} \{ N_{\ell ij}(t+h) - N_{\ell ij}(t) \mid \mathcal{F}_t \}}{h},$$

where $\mathcal{F}_t = \{(i_k, j_k, \ell_k, t_k) : t_k < t\}$ denotes the history of the process in $[0, t]$.

The main contribution of this work is a model for intensity functions of a multi-layer network point process, that we call the *multiplex inhomogeneous Poisson process dot product graph (MIPP-DPG)*, defined in Section 2.1. Additionally, we propose an inference procedure based on spectral embedding methods in Section 2.2, with convenient asymptotic properties that will be illustrated in Section 3.

2.1 Defining the MIPP-DPG

We assume the point processes to be inhomogeneous Poisson, implying that:

$$N_{\ell ij}(t) - N_{\ell ij}(s) \sim \text{Poisson} \left(\int_s^t \lambda_{\ell ij}(u) du \right). \quad (2.2)$$

for all $i, j \in \mathcal{V}$, $\ell \in [L]$ and $0 \leq s < t$, with independent increments across disjoint time intervals. Under this framework, we assume that each node $i \in \mathcal{V}$ in layer $\ell \in [L]$ has two latent positions of dimension $d \ll N$, called $X_i(t) \in \mathbb{R}^d$ and $Y_{\ell i} \in \mathbb{R}^d$. The latent position $X_i(t)$ is a time-varying representation that is shared across layers, whereas $Y_{\ell i}$ a static position that is unique to the layer. The intensity of the Poisson process on the edge $(i, j) \in \mathcal{V} \times \mathcal{V}$ on layer $\ell \in [L]$ is assumed to arise from an inner product of these positions, so that

$$\lambda_{\ell ij}(t) = X_i(t)^\top Y_{\ell j}.$$

The latent positions are thus required to satisfy that $X_i(t)^\top Y_{\ell j} > 0$ for all $(i, j, \ell, t) \in \mathcal{V} \times \mathcal{V} \times [L] \times \mathcal{T}$, where $\mathcal{T} = [0, T]$ is an observation interval. As noted in Section 1.1, we consider the latent positions to be unobserved but non-random quantities. We denote the intensity functions for the full network as $\mathbf{\Lambda}(t) = [\mathbf{\Lambda}^{(*,1)}(t), \dots, \mathbf{\Lambda}^{(*,L)}(t)] \in \mathbb{R}_+^{N \times NL}$, where $\mathbf{\Lambda}^{(*,\ell)}$ is the $N \times N$ matrix of intensities for layer $\ell \in [L]$, with (i, j) -th entry corresponding to $\Lambda_{ij}^{(*,\ell)}(t) = \lambda_{\ell ij}(t)$. We can compactly express $\mathbf{\Lambda}(t)$ at time $t \in \mathcal{T}$ as a matrix product $\mathbf{\Lambda}(t) = \mathbf{X}(t) \mathbf{Y}^\top$, where we define $\mathbf{X}(t) = [X_1(t)^\top \mid \dots \mid X_n(t)^\top] \in \mathbb{R}^{N \times d}$ and $\mathbf{Y} = [Y_{11}^\top \mid \dots \mid Y_{1N}^\top \mid Y_{21}^\top \mid \dots \mid Y_{LN}^\top] \in \mathbb{R}^{NL \times d}$. A network point process that arises in this way is said to be a MIPP-DPG, and we write:

$$\mathbf{N}(t) \sim \text{MIPP-DPG} \{ \mathbf{X}(t), \mathbf{Y} \}.$$

2.2 A spectral estimation procedure for the MIPP-DPG

Given quadruples $(i_k, j_k, \ell_k, t_k) \in \mathcal{V} \times \mathcal{V} \times [L] \times \mathcal{T}$, $k = 1, 2, \dots$, observed on a time interval \mathcal{T} , the inferential objective under the MIPP-DPG is to estimate the latent positions $X_i(t)$ and $Y_{\ell i}$ for all $i \in [N]$, $\ell \in [L]$, $t \in \mathcal{T}$. Without loss of generality, we set $\mathcal{T} = [0, 1]$. For this inferential task, we resort to spectral methods for dynamic multiplex graphs observed at discrete time points, by leveraging doubly unfolded adjacency spectral embedding (DUASE; Baum et al., 2024), a dynamic extension of the UASE approach of Jones and Rubin-Delanchy (2020) for multiplex networks.

Definition 1 (Doubly unfolded adjacency spectral embedding, DUASE; Baum et al., 2024). *Consider a set of adjacency matrices $\{A_{ml}\}_{m \in [M], l \in [L]}$, for $M, L \in \mathbb{N}$, where $A_{ml} \in \{0, 1\}^{N \times N}$ for all pairs $(m, l) \in [M] \times [L]$, where m and ℓ index time and layers, respectively. Define the doubly unfolded adjacency matrix as*

$$\mathbf{A} = \begin{bmatrix} \mathbf{A}_{11} & \cdots & \mathbf{A}_{1L} \\ \vdots & \ddots & \vdots \\ \mathbf{A}_{M1} & \cdots & \mathbf{A}_{ML} \end{bmatrix} \in \{0, 1\}^{NM \times NL}.$$

Consider the singular value decomposition

$$\mathbf{A} = \mathbf{U}\Sigma\mathbf{V}^\top + \mathbf{U}_\perp\Sigma_\perp\mathbf{V}_\perp^\top,$$

where $\Sigma \in \mathbb{R}^{d \times d}$ is a diagonal matrix containing the d largest singular values of \mathbf{A} , $\mathbf{U} \in \mathbb{R}^{NM \times d}$ and $\mathbf{V} \in \mathbb{R}^{NL \times d}$ contain the corresponding left and right singular vectors, respectively, and $\Sigma_\perp, \mathbf{U}_\perp, \mathbf{V}_\perp$ contain the remaining singular values and left and right singular vectors, respectively. Then, the doubly unfolded adjacency spectral embedding of $\{\mathbf{A}_{m\ell}\}_{m \in [M], \ell \in [L]}$ into \mathbb{R}^d is

$$\hat{\mathbf{X}} = \mathbf{U}\Sigma^{1/2} \in \mathbb{R}^{NM \times d} \quad \text{and} \quad \hat{\mathbf{Y}} = \mathbf{V}\Sigma^{1/2} \in \mathbb{R}^{NL \times d}.$$

We refer to $\hat{\mathbf{X}}$ and $\hat{\mathbf{Y}}$ as the left and right doubly unfolded adjacency spectral embeddings, respectively, and we write $(\hat{\mathbf{X}}, \hat{\mathbf{Y}}) = \text{DUASE}(\mathbf{A})$.

In the case that each $\mathbf{A}_{m\ell}$ is a random dot product graph with $\mathbb{E}\{\mathbf{A}_{m\ell}\} = \mathbf{X}^{(m,*)}\mathbf{Y}^{(\ell,*)\top}$, for some $\mathbf{X} \in \mathbb{R}^{NM \times d}$ and $\mathbf{Y} \in \mathbb{R}^{NL \times d}$, DUASE can be shown to consistently recover these latent positions at each discrete time point and layer with overwhelming probability in the sense of the two-to-infinity norm as $N \rightarrow \infty$. In this work, we propose to use a procedure based on DUASE to obtain estimators $\hat{\mathbf{X}}$ and $\hat{\mathbf{Y}}$ for the latent positions $\mathbf{X}(t)$ and \mathbf{Y} of the MIPP-DPG model, proving almost sure consistency in the sense of the two-to-infinity norm of the proposed estimator.

The DUASE estimator is not immediately amenable to inference within the MIPP-DPG modelling framework due to the continuous-time nature of $\mathbf{X}(t)$ and that the graphs under consideration are weighted. As such, we propose to discretise the observation window \mathcal{T} by dividing it into M bins $\{B_m\}_{m=1}^M$, with $B_m := ((m-1)/M, m/M]$, where we let the number of bins M potentially depend on the number of nodes N . We construct estimates $\hat{\mathbf{X}}$ and $\hat{\mathbf{Y}}$ for the MIPP-DPG latent positions by applying DUASE on a histogram estimate of $\mathbf{\Lambda}$, representing the simplest possible approach. Similarly to [Modell et al. \(2024\)](#), we argue that, by providing theoretical results for the case of this simple estimator, we can intuitively justify that our guarantees will be at least as strong in the case that more sophisticated estimation procedures are used. In particular, we construct a histogram estimate of $\lambda_{\ellij}(t)$ as

$$\hat{\lambda}_{\ellij}(t) = \sum_{m=1}^M \hat{\lambda}_{\ellij}^m \mathbb{I}_{B_m}(t),$$

where $\hat{\lambda}_{\ellij}^m$ provides a point estimate for $\lambda_{\ellij}(t)$ on B_m , defined as $\hat{\lambda}_{\ellij}^m := M[N_{\ellij}(m/N) - N_{\ellij}((m-1)/M)]$, where $N_{\ellij}(\cdot)$ is the counting process in [\(2.1\)](#). All components of the histogram estimators for the edge intensities are then stacked into the block matrix $\hat{\mathbf{\Lambda}}$ defined as

$$\hat{\mathbf{\Lambda}} = \begin{bmatrix} \hat{\mathbf{\Lambda}}^{(1,1)} & \dots & \hat{\mathbf{\Lambda}}^{(1,L)} \\ \vdots & \ddots & \vdots \\ \hat{\mathbf{\Lambda}}^{(M,1)} & \dots & \hat{\mathbf{\Lambda}}^{(M,L)} \end{bmatrix} \in \mathbb{R}^{NM \times NL},$$

with each block matrix $\hat{\mathbf{\Lambda}}^{(m,\ell)} \in \mathbb{R}^{N \times N}$ having (i, j) -th entry $\hat{\Lambda}_{ij}^{(m,\ell)} = \hat{\lambda}_{\ellij}^m$. The matrix $\hat{\mathbf{\Lambda}}^{(m,\ell)}$ is used as an estimate $\mathbf{\Lambda}^{(*,\ell)}(t)$ for all $t \in B_m$. Importantly, from the inhomogeneous Poisson process assumption in [\(2.2\)](#), each $\hat{\lambda}_{\ellij}^m/M$ is a Poisson random variable with mean $\int_{B_m} \lambda_{\ellij}(s)ds$. This fact allows us to construct the matrix

$$\bar{\mathbf{\Lambda}} = \begin{bmatrix} \bar{\mathbf{\Lambda}}^{(1,1)} & \dots & \bar{\mathbf{\Lambda}}^{(1,L)} \\ \vdots & \ddots & \vdots \\ \bar{\mathbf{\Lambda}}^{(M,1)} & \dots & \bar{\mathbf{\Lambda}}^{(M,L)} \end{bmatrix} \in \mathbb{R}^{NM \times NL},$$

with block matrices $\bar{\mathbf{\Lambda}}^{(m,\ell)} \in \mathbb{R}^{N \times N}$ having entries $\bar{\Lambda}_{ij}^{(m,\ell)} = \bar{\lambda}_{\ellij}^m$, where we define $\bar{\lambda}_{\ellij}^m =: M \int_{B_m} \lambda_{\ellij}(s)ds$. Note that $\bar{\mathbf{\Lambda}} = \mathbb{E}\{\hat{\mathbf{\Lambda}}\}$, and additionally this time-averaged matrix is seen to arise from a dot product:

$$\bar{\mathbf{\Lambda}}^{(m,*)} = M \int_{B_m} \mathbf{X}(t)\mathbf{Y}^\top dt = \left(M \int_{B_m} \mathbf{X}(t)dt \right) \mathbf{Y}^\top := \tilde{\mathbf{X}}^{(m,*)}\mathbf{Y}^\top,$$

where we write the average of $\mathbf{X}(t)$ over bin B_m as

$$\tilde{\mathbf{X}}^{(m,*)} := M \int_{B_m} \mathbf{X}(t) dt \in \mathbb{R}^{N \times d},$$

so that $\bar{\Lambda} = \tilde{\mathbf{X}} \mathbf{Y}^\top$, with

$$\tilde{\mathbf{X}} = [\tilde{\mathbf{X}}^{(1,*)} \mid \dots \mid \tilde{\mathbf{X}}^{(M,*)}] \in \mathbb{R}^{NM \times d}.$$

Building off of the theoretical properties of DUASE in the binary case presented in [Baum et al. \(2024\)](#), we will show that doubly unfolded left and right embeddings of $\hat{\Lambda}$ to provide asymptotically good estimates of $\hat{\mathbf{X}}$ and $\hat{\mathbf{Y}}$ in the sense of the two-to-infinity norm. Therefore, we propose to use the following estimates for the latent positions under the MIPP-DPG model:

$$(\hat{\mathbf{X}}, \hat{\mathbf{Y}}) = \text{DUASE}(\hat{\Lambda}), \quad \hat{\mathbf{X}} \in \mathbb{R}^{NM \times d}, \quad \hat{\mathbf{Y}} \in \mathbb{R}^{NL \times d}. \quad (2.3)$$

3 Theoretical results

In this section, we present key theoretical results about recovery of the MIPP-DPG latent positions via the proposed DUASE estimator. In particular, we extend existing theoretical results for DUASE from the binary to the weighted setting, and demonstrate that the estimators recover the continuous dynamic when an appropriate limit is taken. These results are natural extensions of the results of [Jones and Rubin-Delanchy \(2020\)](#); [Gallagher et al. \(2024\)](#); [Baum et al. \(2024\)](#) to weighted, multiplex graphs observed in continuous time.

Consistency is derived in the sense of the two-to-infinity norm, which is a particularly meaningful metric in the context of our model as it is the natural norm to capture the maximum error between the set of estimates of the latent positions and the truth under the MIPP-DPG. Consider DUASE estimates $\hat{\mathbf{Y}}$ for \mathbf{Y} , and $\hat{\mathbf{X}}$ for $\mathbf{X}(t)$ across the set of bins, such that $\hat{\mathbf{X}}^{(m,*)}$ estimates $\mathbf{X}(t)$ on B_m , *cf.* (2.3). We can look to bound the following norms as $N \rightarrow \infty$:

$$\max_{m \in [M]} \sup_{t \in B_m} \|\hat{\mathbf{X}}^{(m,*)} \mathbf{W}_X^N - \mathbf{X}(t)\|_{2,\infty} \quad \text{and} \quad \|\hat{\mathbf{Y}} \mathbf{W}_Y^N - \mathbf{Y}\|_{2,\infty}, \quad (3.1)$$

for sequences of matrices $\mathbf{W}_X^N, \mathbf{W}_Y^N \in \text{GL}(d)$. Here, we talk of sequences as \mathbf{W}_X^N and \mathbf{W}_Y^N will change with N . \mathbf{W}_X^N and \mathbf{W}_Y^N are defined as the product of an orthogonal and a general linear transformation, *cf.* Section C. They arise because the true latent positions are fundamentally unidentifiable in both scale and orientation. This is clear by noting that, for any $\mathbf{Q} \in \mathbb{O}(d)$, $\mathbf{X}(t)\mathbf{Q}$ and $\mathbf{Y}\mathbf{Q}$ give rise to the same inner product as the untransformed latent positions. Furthermore, scaling $\mathbf{X}(t)$ by s and \mathbf{Y} by $1/s$ and will result in the same inner product and thus the same intensity matrix.

The second norm in (3.1) is a standard target in related RDPG literature (see, for example, [Athreya et al., 2018](#); [Jones and Rubin-Delanchy, 2020](#); [Gallagher et al., 2024](#); [Baum et al., 2024](#)), whereas the first is a continuous-time adaptation, similar in nature to that of [Modell et al. \(2024\)](#). In particular, a bound on the first norm would bound the ‘‘worst case scenario’’, and will account for errors introduced through discretisation. It should be emphasised that despite binning the observation windows, our theory will recover the continuous setting as we can allow $M \rightarrow \infty$, provided the rate is sufficiently slow in comparison with the growth of N . These statements will be made more precise shortly.

Before stating the main theoretical results, we discuss the necessary assumptions on the latent positions required to obtain these properties. We divide the assumptions into two classes, related to variance and bias of the proposed DUASE estimator for the latent positions. These assumption naturally occur from the following bias-variance decomposition of the bound on the first of the two norms in (3.1):

$$\begin{aligned} \max_{m \in [M]} \sup_{t \in B_m} \|\hat{\mathbf{X}}^{(m,*)} \mathbf{W}_X^N - \mathbf{X}(t)\|_{2,\infty} \leq \\ \|\hat{\mathbf{X}} \mathbf{W}_{X,2}^N - \tilde{\mathbf{X}}\|_{2,\infty} + \max_{m \in [M]} \sup_{t \in B_m} \|\tilde{\mathbf{X}}^{(m,*)} \mathbf{W}_{X,1}^N - \mathbf{X}(t)\|_{2,\infty}, \end{aligned} \quad (3.2)$$

with $\mathbf{W}_X^N = \mathbf{W}_{X,2}^N \mathbf{W}_{X,1}^{N,\top}$, $\mathbf{W}_{X,1}^N, \mathbf{W}_{X,2}^N \in \text{GL}(d)$. Similarly, variance assumptions are needed to establish properties for the decay of the term $\|\hat{\mathbf{Y}}\mathbf{W}_2^N - \mathbf{Y}\|_{2,\infty}$ in (3.1). Assumptions on the latent positions needed for the variance components of the bounds to decay in N are summarised in Assumption 1.

Assumption 1 (Variance assumptions). *The latent positions $\mathbf{X}(t)$ and \mathbf{Y} of the MIPP-DPG satisfy all the following assumptions:*

- i. (Bounded and integrable) $\|\mathbf{X}(t)\|_{2,\infty}, \|\mathbf{Y}\|_{2,\infty} = \mathcal{O}(1)$ for $N \rightarrow \infty$, and $\mathbf{X}(t)$ is integrable on \mathcal{T} ,
- ii. (Stable moments) There exist $\mathbf{Q}_X, \mathbf{Q}_Y \succ 0$ such that, for $N \rightarrow \infty$, we have entrywise convergence:

$$\frac{1}{NM_N} \tilde{\mathbf{X}}^\top \tilde{\mathbf{X}} \rightarrow \mathbf{Q}_X, \quad \frac{1}{NL_N} \mathbf{Y}^\top \mathbf{Y} \rightarrow \mathbf{Q}_Y,$$

- iii. (Growth of M_N and L_N) $M_N = o(N^{1/2}/\log^4 N)$ and $L_N = o(N^{1/2})$.

Here we have changed notation to introduce N subscripts onto M and L to emphasise their dependence on the number of nodes, N . Assumption 1.i is on the behaviour of the integrability of the time-dependent latent positions and the boundedness of the positions in general. It is analogous to Assumption ii in [Gallagher et al. \(2024\)](#) and Assumption 1 in [Modell et al. \(2024\)](#). Assumption 1.ii is on the limiting behaviour of the collection of latent positions. Assumptions of this form in the case of random positions is standard in the literature (see, for example [Athreya et al., 2018](#); [Jones and Rubin-Delanchy, 2020](#); [Baum et al., 2024](#)). Assumption 1.iii is on the growth rate of the number of bins and the number of layers. These are analogous to the requirements of the growth of T_n and K_n in [Baum et al. \(2024\)](#). The required behaviour of M_N and L_N are such that the derived two-to-infinity norm bound decays in N . The number of bins M_N should be interpreted as controlling the sparsity of $\hat{\Lambda}$. The maximum growth rate of M_N is analogous to the maximum decay rate of the sparsity parameter in the work of [Baum et al. \(2024\)](#). The number of layers L_N need not to grow to obtain asymptotic consistency, whereas M_N is only required to grow for the bias term to vanish, and is not required to grow for the recovery of each $Y_{\ell j}$.

We note that Assumptions 1.i and 1.ii provide the following proposition (proved in Appendix E.1) that characterises the behaviour of the matrix of latent positions in the limit.

Proposition 1 (Behaviour of latent position matrices). *Under Assumptions 1.i and 1.ii, as $N \rightarrow \infty$, we have*

$$\sigma_i(\tilde{\mathbf{X}}) = \Theta(M_N^{1/2} N^{1/2}), \quad \sigma_i(\mathbf{Y}) = \Theta(L_N^{1/2} N^{1/2}), \quad \sigma_i(\bar{\Lambda}) = \Theta(M_N^{1/2} L_N^{1/2} N),$$

for all $i \in [d]$, and $\sigma_{d+1}(\bar{\Lambda}) = 0$. Furthermore, we have that $\kappa(\tilde{\mathbf{X}})$, $\kappa(\mathbf{Y})$, $\mu(\tilde{\mathbf{X}})$, $\mu(\mathbf{Y}) = \mathcal{O}(1)$, where κ and μ denote the condition number and incoherence parameter, respectively, as defined in Section 1.1.

Under Assumption 1 (combined with additional technical assumptions detailed in Sections 3.1 and 3.2), we derive theoretical results that demonstrate the asymptotic consistency of DUASE applied to the MIPP-DPG and a subsequent central limit theorem.

3.1 Asymptotic consistency

The first main theoretical result involves asymptotic consistency of the DUASE estimator for the MIPP-DPG latent positions. In order to prove the result, an additional assumption on the behaviour of the latent positions $\mathbf{X}(t)$, $t \in \mathcal{T}$ is needed on the bias term arising from the decomposition in (3.2). Two options are described in Assumption 2.

Assumption 2 (Bias assumptions). *The latent positions $\mathbf{X}(t)$ of the MIPP-DPG model satisfy one of the following assumptions:*

- i. (Rotation-free Lipschitz continuity) For each $s, t \in \mathcal{T}$, and for each $N \in \mathbb{N}$, there exists a $K_N = o(M_N)$ such that:

$$\|\mathbf{X}(t) - \mathbf{X}(s)\|_{2,\infty} \leq K_N |t - s|,$$

ii. (Subspace Lipschitz continuity) Define the projector $\mathbf{P}(\cdot)$ as

$$\mathbf{P}(t) = \mathbf{X}(t)\{\mathbf{X}(t)^\top \mathbf{X}(t)\}^{-1}\mathbf{X}(t)^\top.$$

For each $s, t \in \mathcal{T}$, and for each $N \in \mathbb{N}$, there exists $K_{N,1}, K_{N,2} = o(M_N)$ such that

- (Subspace smoothness) $\|\mathbf{P}(t) - \mathbf{P}(s)\|_2 \leq K_{N,1}|t - s|$ and
- (Coordinate smoothness) $\|\mathbf{P}(t)\{\mathbf{X}(t) - \mathbf{X}(s)\}\|_{2,\infty} \leq K_{N,2}|t - s|$,

Assumption 2.i is a strong assumption that asserts that there is a global coordinate system in which the latent positions evolve smoothly. This is a statement on the orientation and scale up to an overall fixed right-orthogonal matrix. On the other hand, Assumption 2.ii is a statement in two parts on the dynamics of the latent positions $\mathbf{X}(t)$. The first part, involving subspace smoothness, says that the subspace spanned by the columns of $\mathbf{X}(t)$ moves Lipschitz-continuously in time, measured on the Grassmann manifold via projector distance. Intuitively, it corresponds to a bound on the angular velocity of the latent position directional structure. On the other hand, the second part, involving coordinate smoothness, is a bound on how far the coordinates at time s are from the best representation in the subspace at time t . It gives a bound on how fast the coordinates move in the space at time t . Combined, the two conditions in Assumption 2.ii give a rotation-invariant and interpretable notion of temporal smoothness for dynamic latent positions. Note that Assumption 2.ii is strictly weaker than Assumption 2.i.

An important observation to make here is that the Lipschitz constants in Assumption 2 as allowed to grow with N , provide they grow no faster than M_N . This weakens the assumption, as we are not demanding the existence of a universal constant to govern the smoothness, but instead allow the dynamics to become less smooth as the nextwork grows.

Under Assumptions 1 and 2, we can then establish asymptotic consistency. The result is stated in Theorem 1.

Theorem 1 (Two-to-infinity norm bound). *Suppose that $\mathbf{N}(t)$ is a counting process arising from a MIPP-DPG on $\mathcal{T} = (0, 1]$ with N nodes, L_N layers, intensity matrix $\mathbf{\Lambda}(t)$ and latent position matrices $\mathbf{X}(t)$ and \mathbf{Y} , as defined in Section 2.1. Let $\hat{\mathbf{\Lambda}}$ be the histogram estimator of $\mathbf{\Lambda}$ using M_N bins, and $\hat{\mathbf{X}}$ and $\hat{\mathbf{Y}}$ be estimators obtained as defined in Section 2.2. Then, if Assumption 1, is met, there exists sequences of matrices $\mathbf{W}_X^N, \mathbf{W}_Y^N \in \text{GL}(d)$, such that*

$$\begin{aligned} \max_{m \in [M_N]} \sup_{t \in B_m} \|\hat{\mathbf{X}}^{(m,*)} \mathbf{W}_X^N - \mathbf{X}(t)\|_{2,\infty} &= \mathcal{O}\left(M_N L_N^{-1/2} N^{-1/2} \log^{3/2}(N)\right) + B_N, \\ \|\hat{\mathbf{Y}} \mathbf{W}_Y^N - \mathbf{Y}\|_{2,\infty} &= \mathcal{O}\left(M_N^{1/2} N^{-1/2} \log^{3/2}(N)\right), \end{aligned}$$

eventually almost surely, where B_N is:

1. $\mathcal{O}(K_N M_N^{-1})$ under Assumption 2.i,
2. $\mathcal{O}((K_{N,1} + K_{N,2}) M_N^{-1})$ under Assumption 2.ii.

The proof of Theorem 1 is provided in Appendix C. It should be noted that Theorem 1 quantifies that a growing M_N increases the variance term of our estimator, but decreases the bias. This is an intuitive result as larger M_N corresponds to a smaller bin width, thereby reproducing the classical bias–variance tradeoff in histogram density estimation. A similar result is observed in the non-asymptotic result of Modell et al. (2024).

3.2 Central limit theorem

The second result, stated in Theorem 2, is a statement on the asymptotic normality of a studentised vector of differences between the estimated and true latent positions. In addition to Assumption 1, a further weak technical assumption, stated in Assumption 3, is required.

Assumption 3 (Rank preservation and sufficient density). *There exists N_1 such that, whenever $N > N_1$, there exists two sets of d indices $i_1, \dots, i_d \in [NM_N]$ and $j_1, \dots, j_d \in [NL_N]$ such that:*

1. the set $\{Y_{j_k,*}\}_{k=1}^d$ are linearly independent and $\tilde{X}_{i,*}^{(m,*)} Y_{j_k,*}^\top > 0$ for all $k = 1, \dots, d$,

2. the set $\{\tilde{X}_{i_k,*}\}_{k=1}^d$ are linearly independent and $\tilde{X}_{i_k,*}Y_{i,*}^\top > 0$ for all $k = 1, \dots, d$.

Assumption 3 ensures that, for large enough N , for any node in the network we can always find two sets of d indices (not necessarily distinct) such that the the intensities on the edges from that node to these indices are positive, and the corresponding latent positions are linearly independent. The existence of such a finite set of indices in the limit of growing N is intuitively reasonable, and guarantees that matrices arising in our central limit theorem are invertible. Under this additional assumption, then the following studentised CLT holds:

Theorem 2 (Studentised asymptotic normality). *Suppose that $\mathbf{N}(t)$ is a counting process arising from a MIPP-RDPG on $(0, 1]$ with N nodes, L_N layers, intensity matrix $\Lambda(t)$ and latent position matrices $\mathbf{X}(t)$ and \mathbf{Y} , as defined in Section 2.1. Let $\hat{\Lambda}$ be the histogram estimator of Λ using M_N bins, and $\hat{\mathbf{X}}$ and $\hat{\mathbf{Y}}$ be estimators obtained as defined in Section 2.2. Then, if Assumptions 1 and 3 are met, there exists sequences of matrices $\mathbf{W}_X^N, \mathbf{W}_Y^N \in \text{GL}(d)$, such that, for $N \rightarrow \infty$,*

$$N^{1/2}L_N^{1/2}(\mathbf{Q}_X^{-1}\mathbf{C}_{i,m}^N\mathbf{Q}_X^{-1})^{-1/2}(\hat{\mathbf{X}}^{(m,*)}\mathbf{W}_X^N - \tilde{\mathbf{X}}^{(m,*)})_{i,*}^\top \rightarrow \mathcal{N}(0, \mathbf{I}_d),$$

$$N^{1/2}M_N^{1/2}(\mathbf{Q}_Y^{-1}\mathbf{D}_{i,\ell}^N\mathbf{Q}_Y^{-1})^{-1/2}(\hat{\mathbf{Y}}^{(m,*)}\mathbf{W}_Y^N - \tilde{\mathbf{Y}}^{(m,*)})_{i,*}^\top \rightarrow \mathcal{N}(0, \mathbf{I}_d),$$

in distribution, where the matrices $\mathbf{C}_{i,m}^N$ and $\mathbf{D}_{i,\ell}^N$ take the form

$$\mathbf{C}_{i,m}^N = \frac{1}{NL_N} \sum_{j=1}^{NL_N} (\tilde{X}_{i,*}^{(m,*)} Y_{j,*}^\top) Y_{j,*}^\top Y_{j,*}, \quad \mathbf{D}_{i,\ell}^N = \frac{1}{NM_N} \sum_{j=1}^{NM_N} (\tilde{X}_{j,*} Y_{i,*}^{(\ell,*)\top}) \tilde{X}_{j,*}^\top \tilde{X}_{j,*},$$

and are invertible provided Assumption 3 holds.

The result is proved in Appendix D. It should be noted that $\lim_{N \rightarrow \infty} \mathbf{C}_{i,m}^N$ and $\lim_{N \rightarrow \infty} \mathbf{D}_{i,m}^N$ need not necessarily exist without further strong assumptions on the third moments of our latent positions. Assumptions 1.i and 1.ii are sufficient to ensure that these limits are finite, but Assumption 3 is required to ensure that they are invertible. As the limit need not exist, Theorem 2 is stated in a studentised form.

4 Simulation studies

In order to demonstrate the performance of the proposed estimator for the latent position of the MIPP-DPG, we construct two simulation studies. Both studies use a block structure intensity matrix to examine recovery of an underlying group structure. Section 4.1 examines a smoothly evolving dynamic latent position and the interplay between network size and granularity in the recovery of the latent positions. The study of Section 4.2 examines a similar setting, but where we introduce discontinuities into the latent positions to qualitatively assess how a violation of Assumption 2 affects recovery.

4.1 Block structure MIPP-DPG

We consider a simulation study with a smooth intensity matrix $\Lambda(t)$ taking a block structure, based on an extension of the dynamic multiplex stochastic block of Baum et al. (2024). We assume that the nodes are assigned to one of $G_1 \in \mathbb{N}$ groups when functioning as a source node, and to one of $G_2 \in \mathbb{N}$ groups when acting as a destination. We define a collection of functions $\mu_g(t) : \mathcal{T} \rightarrow \mathbb{R}^d$ for each $g \in [G_1]$, and constant vectors $\gamma_q^\ell \in \mathbb{R}^d$ for each $\ell \in [L]$ and $q \in [G_2]$. Each node $i \in \mathcal{V}$ is assigned to a group for its temporal dynamics $z_i \in [G_1]$ and to a group for its layer-specific behaviour $v_i^\ell \in [G_2]$. We then define the node-specific latent positions as $X_i(t) = \mu_{z_i}(t)$ and $Y_{\ell j} = \gamma_{v_j}^\ell$. In this example, we consider $d = 2$ and functions $\mu_g(t)$ of the form:

$$\mu_g(t) = [c_{1,g} + R_g \sin(2\pi t + \theta_g) \quad c_{2,g} + R_g \cos(2\pi t + \theta_g)]^\top, \quad (4.1)$$

where $c_{1,g}, c_{2,g}, R_g, \theta_g \in \mathbb{R}$ for $g \in [G_1]$ are group-dependent constants. For the layer-specific latent positions, we use:

$$\gamma_q^\ell = [d_q^\ell + \cos(\phi_q^\ell) \quad d_q^\ell + \sin(\phi_q^\ell)]^\top, \quad (4.2)$$

where d_q^ℓ, ϕ_q^ℓ for $\ell \in [L]$ and $q \in [G_2]$ are again constants depending on the group.

We examine the recovery of the latent positions $\{X_i(t)\}_{i=1}^N$ via the DUASE-based estimator in a graph with $L = 3$ layers generated using the group-specific positions in Equations (4.1) and (4.2). The nodes are distributed among $G_1 = 3$ groups, such that the first two groups each receive 40% of the nodes, and the third group receives the remaining 20%. For the layer groups, we take $G_2 = 3$, but merge groups 1 and 2 in the second layer and groups 2 and 3 in the third. For the group-specific time-varying latent positions $\mu_g(t)$, we take the following parameters for $g \in \{1, 2, 3\}$: $R_g = 5g$, $c_{1,g} = 2R_g + 1$, $c_{2,g} = 2R_g + 1$, $\theta_g = g\pi$. On the other hand, for the layer-specific latent positions γ_q^ℓ , in the first layer we take $d_q^1 = q$, $\phi_q^1 = \pi/q$, for the second we take $d_1^2 = d_2^2 = 2$, $d_3^2 = 4$ and $\phi_1^2 = \phi_2^2 = \pi/2$, $\phi_3^2 = \pi/3$, and for the third $d_1^3 = 3$, $d_2^3 = d_3^3 = 5$ and $\phi_1^3 = \pi/2$, $\phi_2^3 = \phi_3^3 = \pi/6$. We simulate networks with $N \in \{100, 200, 500\}$ and run the DUASE inference procedure described in Section 2.2 for $M \in \{10, 25, 50\}$ to examine the effect of decreasing bin width and increasing the number of nodes on the recovery of the latent positions. Results are reported in Figures 1a and 1b.

In each panel of Figure 1a, the different coloured crosses show the true simulation values of $\mu_1(t)$, $\mu_2(t)$ and $\mu_3(t)$ at the centres of each bin B_m . The small points show the estimates of each $X_i(t)$ for the bin B_m and the triangles the group-specific means of these estimates. We have aligned the estimated latent positions with the truth using orthogonal Procrustes to aid visualisation. We see that increasing M in general leads to worse estimates of the latent positions, but that the decrease in the estimation quality is smaller for larger N . This aligns with the statement of Theorem 1. In Figure 1b, we produce an analogous plot for the recovery of $\{\gamma_q^\ell\}_{q,\ell=1}^3$, for the case when $M = 10$. We see that the merging of groups in layers 2 and 3 is correctly detected.

4.2 Discontinuous MIPP-DPG

We now consider discontinuities in our latent positions that violate Assumption 2. We examine a simulation study similar to Section 4.1, but with an intensity matrix $\Lambda(t)$ that is discontinuous. In this example, we again consider $d = 2$, and functions $\mu_g(t)$ of the form

$$\mu_g(t) = [c_{1,g} + R_g \sin(2\pi t + \theta_g) \quad c_{2,g} + R_g \cos(2\pi t + \theta_g) + \delta(t)]^\top,$$

where $c_{1,g}, c_{2,g}, R_g, \theta_g \in \mathbb{R}$ for $g \in [G_1]$ are the same as in Section 4.1, and $\delta_g : \mathbb{R}_+ \rightarrow \mathbb{R}_+$ is the following step function:

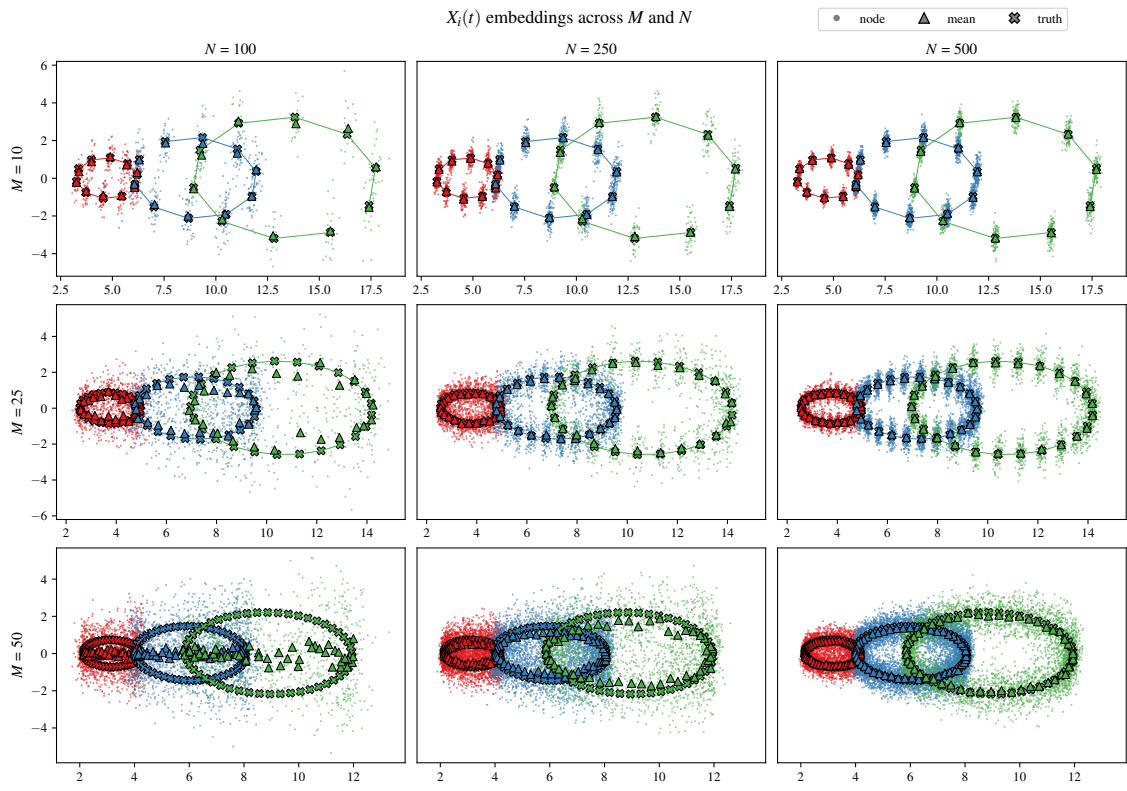
$$\delta_g(t) = \begin{cases} 0, & 0 < t \leq \tau_1, \\ 0.4R_g, & \tau_1 < t \leq \tau_2, \\ -0.3R_g, & \tau_2 < t \leq \tau_3, \\ 0.7R_g, & \tau_3 < t \leq 1, \end{cases}$$

for step locations $\tau_1, \tau_2, \tau_3 \in \mathbb{R}_+$ with $\tau_1 < \tau_2 < \tau_3$. We select $\tau_1 = 0.25$, $\tau_2 = 0.5$ and $\tau_3 = 0.75$. This function is discontinuous and thus violates Assumption 2. A plot of this function (after alignment) is seen in Figure 2a. For the layer-specific latent positions, we use the same functions as in Section 4.1.

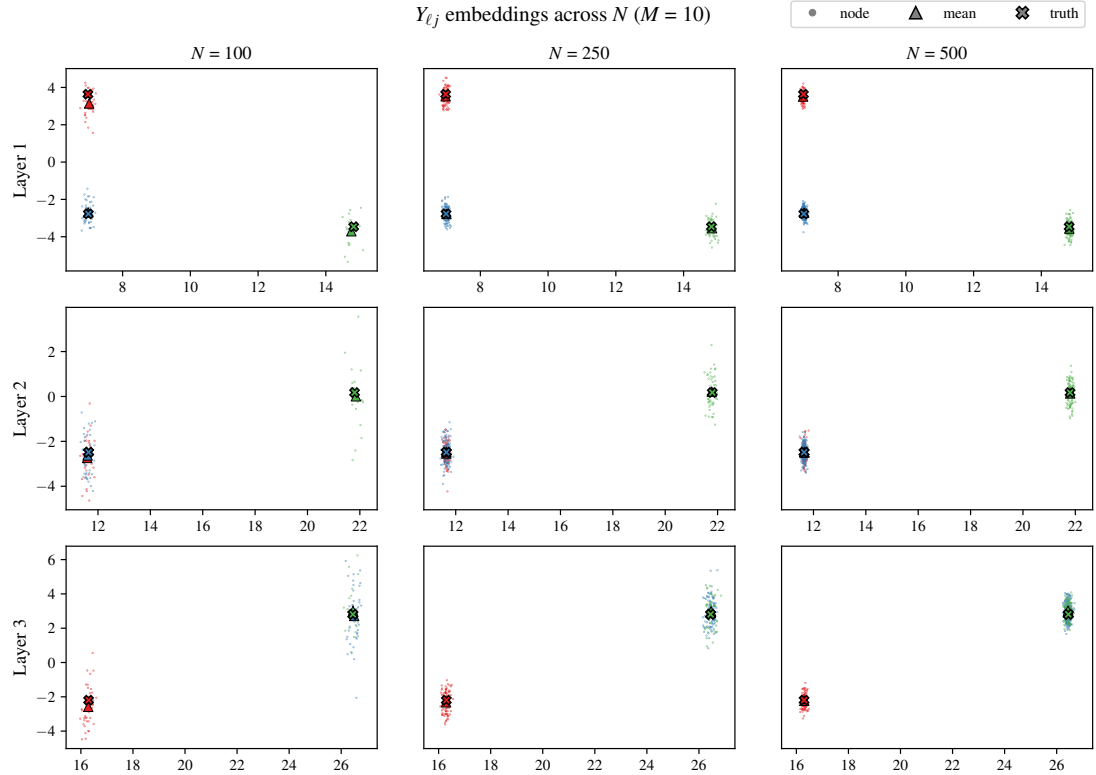
In each panel of Figure 2b, the different colours and symbols are as described in Section 4.1, for a choice of $M = 50$. Again, we observe that increasing N leads to improved recovery of the underlying latent positions. The discontinuities do not affect recovery for $N = 250$ and $N = 500$; however, for $N = 100$ nodes, recovery is poor for such a large value of M , as in Section 4.1.

5 Application to a global air transportation network

We provide a real-data application of the proposed method on a global air transportation network. We analyse the crowdsourced OpenSky Network for the month of April in 2021, which details every recorded flights between airports across the globe (Strohmeier et al., 2021). Each flight consists of an origin and destination airport, the aircraft model for the flight and time stamps of when the first and last message was received from the flight by the OpenSky Network. We process the network by restricting to the 10 most used aircraft models across the dataset and use these to construct $L = 10$ layers. We consider a set of $N = 567$ airports having 5 or more in or



(a) $\hat{X}_i(t)$ for networks of different sizes and with different numbers of bins.



(b) $\hat{Y}_{\ell j}(t)$ for each layer for networks of different sizes, $M = 10$.

Figure 1: Estimated and true latent positions for the simulation study described in Section 4.1, for different values of the number of nodes N and number of bins M .

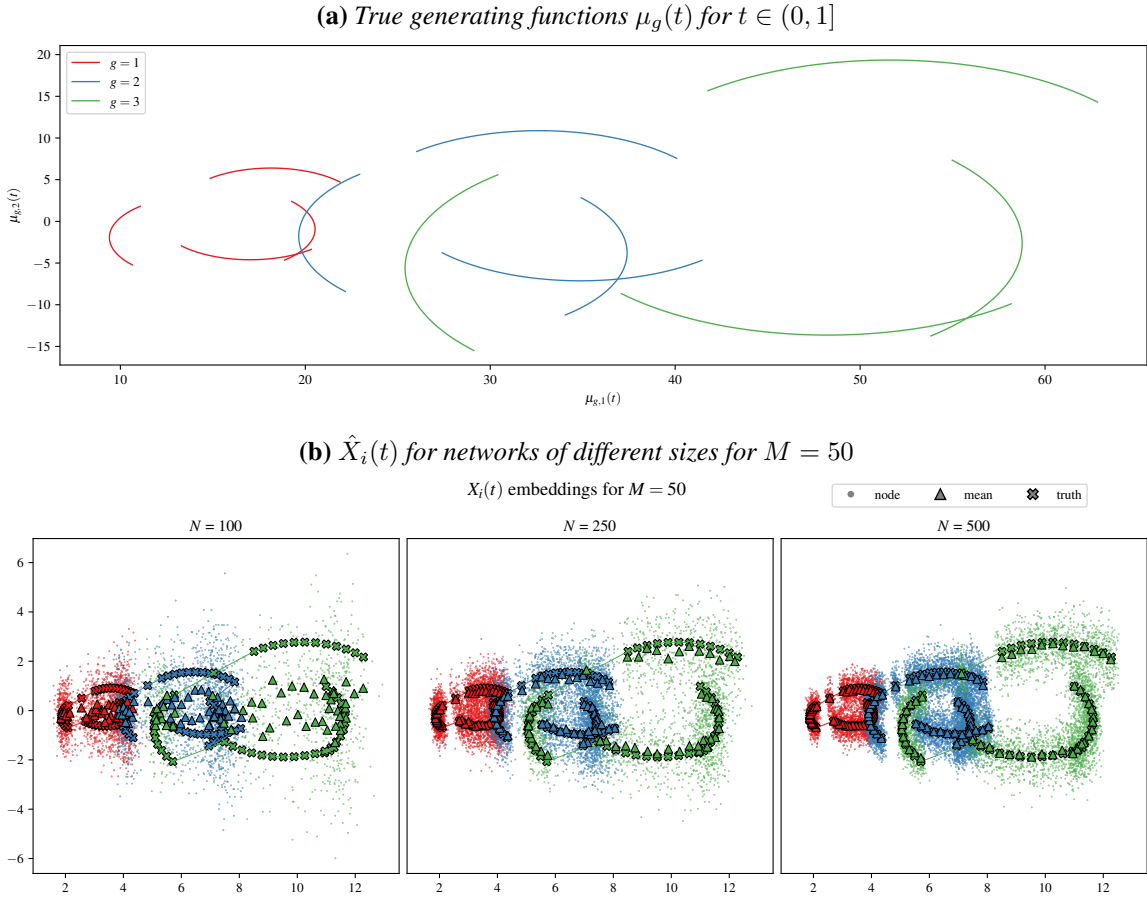


Figure 2: Estimated and true latent positions for the simulation study described in Section 4.2, for different values of the number of nodes N and number of bins $M = 50$.

out flights over the month. Quadruples (i_k, j_k, ℓ_k, t_k) consist of directed flights between airports i_k and j_k on an aircraft of type ℓ_k , landed at time t_k . We run the DUASE inference procedure described in Section 2.2 with a choice of $d = 10$ and binning into $M = 28$ bins. This choice corresponds to the days of the month, and we pick d by inspecting the scree plot of singular values of the resulting matrix $\hat{\Lambda}$.

We consider each element of the resulting sequence $\{\hat{X}^{(m,*)}\}_{m=1}^M$ as the realisation of N multivariate d -dimensional time series at the m -th time point, and examine clustering the nodes using these. To cluster the embedding time series, we implement a simple approach. We normalise each dimension by centring and dividing by its standard deviation, and subsequently smooth it using a box kernel with a window of width 5, obtaining estimates $\{\check{X}^{(m,*)}\}_{m=1}^M$. To cluster the time series, we define the node-specific matrices $\check{X}_i = [\check{X}_i^{(1,*)\top} \mid \dots \mid \check{X}_i^{(M,*)\top}] \in \mathbb{R}^{M \times d}$, summarising the time-varying latent positions of node i within all bins. We then construct a pairwise distance matrix $D \in \mathbb{R}_{\geq 0}^{N \times N}$ with entries $D_{ij} = \|\check{X}_i - \check{X}_j\|_F$, and then implement an agglomerative, hierarchical clustering algorithm using average linkage and $K = 6$ clusters, with dissimilarity D . This choice of K is made to compare our clusters to the continents that the nodes are situated in.

In Figures 3a and 3b, we use t-SNE, a popular non-linear dimension reduction tool, to visualise the resulting low-dimensional embedding vectors. Figure 3a shows the two-dimensional t-SNE embedding of the matrix $[\hat{X}^{(1,*)}, \dots, \hat{X}^{(M,*)}] \in \mathbb{R}^{N \times M^d}$, coloured in the left panel by the continent of the node, and in the right panel by the cluster assigned to the node by the hierarchical clustering procedure described above. Note that this visualisation embeds the entire trajectories all at once, and independent t-SNE representations of each of the estimates for each bin would not be interpretable due to the randomness in the t-SNE procedure. Figure 3b shows an analogous plot for $\hat{Y}^{(\ell,*)}$ for two choice of aircrafts, identified by the typecodes A319 and A321. When coloured by continent, the plots exhibit clear geographic structure: airports from the same continent form

largely contiguous regions. When coloured by the output of our clustering algorithm, several clusters align closely with these continental groups (notably those corresponding to the main European and North-American regions), whereas others cut across continents and instead group airports with similar functional roles in the network (e.g. intercontinental hubs versus regional airports). This indicates that, while geographic location is strongly reflected in the flow-induced geometry, the clustering captures additional structure beyond continents, organising airports according to their traffic patterns rather than purely their physical position.

6 Conclusion and discussion

This paper introduced the multiplex inhomogeneous Poisson process dot product graph (MIPP-DPG), a model for multiplex networks with continuous-time interaction data. Theorems 1 and 2 show that, under mild conditions, doubly unfolded adjacency spectral embedding (DUASE; Baum et al., 2024) yields latent position estimators that are asymptotically consistent and asymptotically normal. Our theory allows the number of discretization bins to grow with the number of nodes, thereby recovering the continuous setting. This is demonstrated in our two simulation studies. Furthermore, the asymptotic normality result is particularly relevant for downstream community detection, an important topic in network literature, as it provides theoretical support for fitting Gaussian mixture models to the embedded positions when clustering nodes. Despite requiring Lipschitz continuity in the latent dynamics, our second simulation established that DUASE is able to recover the latent positions even when the assumptions required for our theoretical guarantees were violated. In an application to a real-world air traffic network, we demonstrated that inference under our model was able to recover latent structure beyond simple geography.

Some paths for future research naturally arise as a result of this work. An interesting avenue would be to explore when the network structure is not assumed to be known, and how spectral methods can be adapted to infer both the latent positions and the network structure itself. Another route would be to investigate more complex point process models, such as a self-exciting process.

Acknowledgements

Joshua Corneck acknowledges funding from the Engineering and Physical Sciences Research Council (EPSRC), grant number EP/S023151/1. Ed Cohen acknowledges funding from the EPSRC NeST Programme, grant number EP/X002195/1. Francesco Sanna Passino acknowledges funding from the EPSRC, grant number EP/Y002113/1.

Code

The Python code for implementing the methods proposed in this article and reproducing the results is available in the GitHub repository [joshcorneck/MIPP-DPG](https://github.com/joshcorneck/MIPP-DPG).

References

- Athreya, A., Fishkind, D. E., Tang, M., et al. (2018) Statistical inference on random dot product graphs: a survey. *Journal of Machine Learning Research*, **18**, 1–92.
- Athreya, A., Lubberts, Z., Park, Y., and Priebe, C. (2025) Euclidean mirrors and dynamics in network time series. *Journal of the American Statistical Association*, **120**, 1025–1036.
- Baum, M., Sanna Passino, F., and Gandy, A. (2024) Doubly unfolded adjacency spectral embedding of dynamic multiplex graphs. *arXiv e-prints*, arXiv:2410.09810.
- Billio, M., Casarin, R., and Iacopini, M. (2024) Bayesian markov-switching tensor regression for time-varying networks. *Journal of the American Statistical Association*, **119**, 109–121.

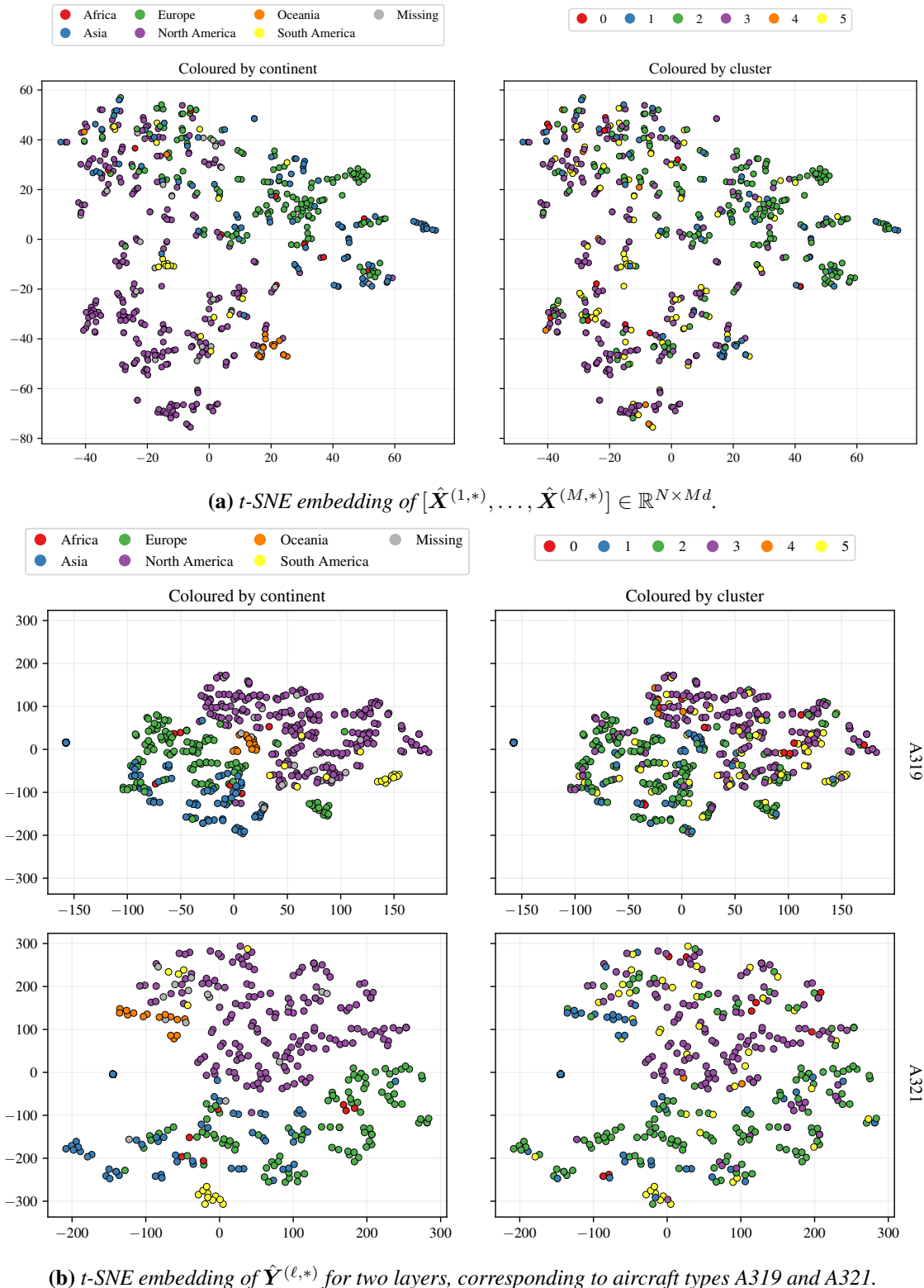


Figure 3: t-SNE embeddings of the inferred airport latent vectors, shown (a) after stacking the dynamic position across time and (b) for two representative layers. Each point represents an airport in the 2D t-SNE space. Points are coloured by continent (left column) and by inferred cluster membership (right column).

Cape, J., Tang, M., and Priebe, C. E. (2019a) Signal-plus-noise matrix models: eigenvector deviations and fluctuations. *Biometrika*, **106**, 243–250.

Cape, J., Tang, M., and Priebe, C. E. (2019b) The two-to-infinity norm and singular subspace geometry with applications to high-dimensional statistics. *The Annals of Statistics*, **47**, 2405–2439.

Chen, Y., Chi, Y., Fan, J., and Ma, C. (2021) Spectral methods for data science: A statistical perspective. *Foundations and Trends® in Machine Learning*, **14**, 566–806.

Corneck, J., Cohen, E. A. K., Martin, J. S., et al. (2025a) Simultaneous global and local clustering in multiplex networks with covariate information. *Journal of Complex Networks*.

Corneck, J., Cohen, E. A. K., Martin, J. S., and Sanna Passino, F. (2025b) Online Bayesian changepoint detection for network Poisson processes with community structure. *Statistics and Computing*, **35**, 75.

De Domenico, M., Nicosia, V., Arenas, A., and Latora, V. (2015) Structural reducibility of multilayer networks. *Nature Communications*, **6**, 6864.

Durante, D., Mukherjee, N., and Steorts, R. C. (2017) Bayesian learning of dynamic multilayer networks. *Journal of Machine Learning Research*, **18**, 1414–1442.

Fang, G., Ward, O. G., and Zheng, T. (2024) Online estimation and community detection of network point processes for event streams. *Statistics and Computing*, **34**.

Gallagher, I., Jones, A., Bertiger, A., Priebe, C. E., and and, P. R.-D. (2024) Spectral embedding of weighted graphs. *Journal of the American Statistical Association*, **119**, 1923–1932.

Gallagher, I., Jones, A., and Rubin-Delanchy, P. (2021) Spectral embedding for dynamic networks with stability guarantees. In *Proceedings of the 35th International Conference on Neural Information Processing Systems, NIPS '21*. Red Hook, NY, USA: Curran Associates Inc.

Goldenberg, A., Zheng, A. X., Fienberg, S. E., and Airoldi, E. M. (2010) A survey of statistical network models. *Foundations and Trends® in Machine Learning*, **2**, 129–233.

Greene, D. and Cunningham, P. (2013) Producing a unified graph representation from multiple social network views. *Proceedings of the 3rd Annual ACM Web Science Conference, WebSci 2013*, **2**.

Hoff, P. D. (2015) Multilinear tensor regression for longitudinal relational data. *The Annals of Applied Statistics*, **9**, 1169–1193.

Hoff, P. D., Raftery, A. E., and and, M. S. H. (2002) Latent space approaches to social network analysis. *Journal of the American Statistical Association*, **97**, 1090–1098.

Horn, R. A. and Johnson, C. R. (2012) *Matrix Analysis*. Cambridge; New York: Cambridge University Press, 2nd edn.

Huang, S., Weng, H., and Feng, Y. (2023) Spectral clustering via adaptive layer aggregation for multi-layer networks. *Journal of Computational and Graphical Statistics*, **32**, 1170–1184.

Jones, A. and Rubin-Delanchy, P. (2020) The multilayer random dot product graph. *arXiv e-prints*, arXiv:2007.10455.

Klimt, B. and Yang, Y. (2004) The Enron corpus: A new dataset for email classification research. In *Machine Learning: ECML 2004* (eds. J.-F. Boulicaut, F. Esposito, F. Giannotti and D. Pedreschi), 217–226. Berlin, Heidelberg: Springer Berlin Heidelberg.

Lei, J. and Lin, K. Z. (2023) Bias-adjusted spectral clustering in multi-layer stochastic block models. *Journal of the American Statistical Association*, **118**, 2433–2445.

Loyal, J. D. and Chen, Y. (2023) An eigenmodel for dynamic multilayer networks. *Journal of Machine Learning Research*, **24**.

Lyzinski, V., Tang, M., Athreya, A., Park, Y., and Priebe, C. (2015) Community detection and classification in hierarchical stochastic blockmodels. *IEEE Transactions on Network Science and Engineering*, **PP**.

Matias, C. and Miele, V. (2017) Statistical clustering of temporal networks through a dynamic stochastic block model. *Journal of the Royal Statistical Society Series B: Statistical Methodology*, **79**, 1119–1141.

Matias, C., Rebafka, T., and Villers, F. (2018) A semiparametric extension of the stochastic block model for longitudinal networks. *Biometrika*, **105**, 665–680.

Modell, A., Gallagher, I., Ceccherini, E., Whiteley, N., and Rubin-Delanchy, P. (2024) Intensity profile projection: A framework for continuous-time representation learning for dynamic networks. In *Advances in Neural Information Processing Systems 36* (eds. A. Oh, T. Naumann, A. Globerson, K. Saenko, M. Hardt and S. Levine), 23259–23296. Curran Associates, Inc.

Osorio, B., Kulesza, A., and Hero, A. O. (2014) Multi-layer graph analysis for dynamic social networks. *IEEE Journal of Selected Topics in Signal Processing*, **8**, 514–523.

Paranjape, A., Benson, A. R., and Leskovec, J. (2017) Motifs in temporal networks. In *Proceedings of the Tenth ACM International Conference on Web Search and Data Mining*, WSDM '17, 601–610. New York, NY, USA: Association for Computing Machinery.

Perry, P. O. and Wolfe, P. J. (2013) Point process modelling for directed interaction networks. *Journal of the Royal Statistical Society Series B: Statistical Methodology*, **75**, 821–849.

Rohe, K., Chatterjee, S., and Yu, B. (2010) Spectral clustering and the high-dimensional stochastic blockmodel. *The Annals of Statistics*, **39**.

Romero, R., Bie, T. D., Heard, N. A., and Modell, A. (2025) Multiresolution analysis and statistical thresholding on dynamic networks. In *Advances in Neural Information Processing Systems 38 (NeurIPS 2025)*.

Sanna Passino, F. and Heard, N. A. (2023) Mutually exciting point process graphs for modeling dynamic networks. *Journal of Computational and Graphical Statistics*, **32**, 116–130.

Schönemann, P. H. (1966) A generalized solution of the orthogonal Procrustes problem. *Psychometrika*, **31**, 1–10.

Sewell, D. K. and Chen, Y. (2015) Latent space models for dynamic networks. *Journal of the American Statistical Association*, **110**, 1646–1657.

Shlomovich, L., Cohen, E. A. K., and Adams, N. (2022) A parameter estimation method for multivariate binned Hawkes processes. *Statistics and Computing*, **32**, 98.

Sosa, J. and Betancourt, B. (2022) A latent space model for multilayer network data. *Computational Statistics & Data Analysis*, **169**, 107432.

Strohmeier, M., Olive, X., Lübbe, J., Schäfer, M., and Lenders, V. (2021) Crowdsourced air traffic data from the opensky network 2019–2020. *Earth System Science Data*, **13**, 357–366.

Sussman, D. L., Tang, M., Fishkind, D. E., and Priebe, C. E. (2012) A consistent adjacency spectral embedding for stochastic blockmodel graphs. *Journal of the American Statistical Association*, **107**, 1119–1128.

Tao, T. and Vu, V. (2010) Random matrices: Universality of local eigenvalue statistics up to the edge. *Communications in Mathematical Physics*, **298**, 549–572.

Tropp, J. A. (2015) An introduction to matrix concentration inequalities. *Foundations and Trends® in Machine Learning*, **8**, 1–230.

Vershynin, R. (2018) *High-Dimensional Probability: An Introduction with Applications in Data Science*. Cambridge Series in Statistical and Probabilistic Mathematics. Cambridge University Press.

Wang, F., Li, W., Madrid Padilla, O. H., Yu, Y., and Rinaldo, A. (2025) Multilayer random dot product graphs: estimation and online change point detection. *Journal of the Royal Statistical Society Series B: Statistical Methodology*.

Wedin, P.-Å. (1972) Perturbation bounds in connection with singular value decomposition. *BIT*, **12**, 99–111.

Yu, Y., Wang, T., and Samworth, R. (2014) A useful variant of the davis–kahan theorem for statisticians. *Biometrika*, **102**.

A Prerequisites for Theorems 1 and 2

To minimise notation, for the duration of this Appendix, we denote the spectral norm by $\|\cdot\|$, dropping the subscript.

A.1 Background on Poisson processes and subexponential random variables

A (simple) temporal point process on a time domain $\mathcal{T} \subseteq \mathbb{R}$ is a random process whose realisation is a list of discrete times $\mathcal{H} = \{t_k\} \subset \mathcal{T}$. Associated with a temporal point process is a counting process $N(\cdot) \in \mathbb{N}$. For $a < b$, the counting process is valued $N((a, b]) = \sum_{t_k \in \mathcal{H}} \mathbb{I}_{(a, b]}(t_k)$ so that it counts the number of events in $(a, b]$. Here we write $\mathbb{I}\{\cdot\}$ for the indicator function. We will write $N(t)$ to mean $N((0, t])$. In this work, we will refer to $N(\cdot)$ as the point process. When a point process comes with additional information, that value is referred to as a mark.

The intensity of $N(\cdot)$, denoted by $\lambda(\cdot)$, is the expected number of arrivals per unit time, defined as $\lambda(t) = \lim_{h \rightarrow 0} \mathbb{P}(N((t, t+h]) > 0)/h$. If $N((a, b]) \sim \text{Poisson}(\int_a^b \lambda(t) dt)$ and $N((a, b])$ and $N((c, d])$ are independent random variables whenever $(a, b] \cap (c, d] = \emptyset$, we refer to $N(\cdot)$ as an inhomogeneous Poisson process (IPP). If $\lambda(t) \equiv \lambda$ for all t , then it is an homogeneous Poisson process (HPP). If a collection of IPPs $N_1(\cdot), \dots, N_m(\cdot)$ are independent with intensities $\lambda_1, \dots, \lambda_m$, then $\sum_r N_r(\cdot)$ is an IPP with intensity $\sum_r \lambda(\cdot)$.

A real-valued random variable X is subexponential if its Orlicz/subexponential norm $\|\cdot\|_{\psi_1}$ is finite, where we define:

$$\|X\|_{\psi_1} := \inf \{K > 0 : \mathbb{E}\{|X|/K\} \leq 2\}.$$

An important equivalent definition is to have that there exists $K_1 > 0$ such that:

$$\mathbb{P}(|X| \geq t) \leq 2 \exp\{-t/K_1\} \quad \text{for all } t \geq 0.$$

This is a statement on the decay rate of the tail probabilities of X . We have the following lemma that shows that a centred Poisson random variable is subexponential. The fact that a centred Poisson random variable is subexponential will be used frequently to prove the theorems in this work.

Lemma 1 (Poisson tail bound). *Let $X \sim \text{Poisson}(\lambda)$. Then*

$$\mathbb{P}(|X - \lambda| \geq t) \leq 2 \exp\left(-\frac{t^2}{2(\lambda + t/3)}\right).$$

A.2 Network point processes

To allow for continuous-time interactions in a network, a point process can be placed on the network edges. The point processes are often modelled as Poisson (Matias and Miele, 2017; Fang et al., 2024; Corneck et al., 2025b; Modell et al., 2024), but examples of self-exciting processes have also been considered (Perry and Wolfe, 2013; Sanna Passino and Heard, 2023). Under such models, a marked point process is observed, consisting of, in the case of a multiplex network, a stream of quadruples $(\ell_k, i_k, j_k, t_k) \in [L_N] \times \mathcal{E}_{\ell_k} \times \mathbb{R}_+$, $k = 1, 2, \dots$, denoting directed interactions from node i_k to node j_k in layer ℓ_k at time t_k , where $t_k \leq t_{k'}$ for $k < k'$. The associated edge-specific counting process is denoted by $N_{\ell i j}(\cdot)$, where, for all $\ell \in [L_N]$ and all $(i, j) \in \mathcal{E}_\ell$,

$$N_{\ell i j}(t) := \sum_k \mathbb{I}_{\{(\ell, i, j)\}}\{(\ell_k, i_k, j_k)\} \mathbb{I}_{(0, t]}(t_k).$$

A.3 Wedin's $\sin\Theta$ theorem and subspace distances

The following theorem is classical in matrix perturbation theory. The exposition here will follow the description of Chen et al. (2021). Given two d -dimensional subspaces \mathcal{U} and \mathcal{U}^* in \mathbb{R}^n , one can represent by matrices \mathbf{U} and \mathbf{U}^* whose columns form orthonormal bases of \mathcal{U} and \mathcal{U}^* , respectively. There are a number of ways of measuring distance between two subspaces, any valid choice of which will account for a global rotation ambiguity: that

UR for any $R \in \mathbb{O}(d)$ will also form an orthonormal bases for \mathcal{U} , and so even when the two subspaces coincide, a rotation could make their distance non-zero unless accounted for. The following notions of distance will be used in the proofs that follow:

- Distance with optimal rotation:

$$\min_{R \in \mathbb{O}(r)} \|UR - U^*\|,$$

- Distance with projection matrices:

$$\|UU^\top - U^*U^{*\top}\|,$$

- Distance with principal angles: let $\sigma_1 \geq \dots \geq \sigma_r \geq 0$ be the singular values of $U^\top U^*$. All singular angles fall within the interval $[0, 1]$. One can thus define the principal angles:

$$\theta_i := \arccos(\sigma_i), \quad \text{for all } 1 \leq i \leq r,$$

which will all lie in $[0, \pi/2]$. The distance between the two subspaces can then be defined as $\|\sin \Theta\|$, where $\Theta = \text{diag}(\sin(\sigma_1), \dots, \sin(\sigma_r))$.

Despite the difference in appearance of these distance measure, it can be shown that they are all equivalent up to constant multiplicative factors. As such, in the context of asymptotic bounds, they will all be used interchangeably.

[Wedin \(1972\)](#) proved the following theorem that controls the perturbation of the left and right subspaces when examining noisy observations of a matrix.

Theorem 3 (Wedin's $\sin \Theta$ Theorem; e.g. Theorem 2.9 in [Chen et al., 2021](#)). *Let M^* and $M = M^* + E$ be two matrices in $\mathbb{R}^{n_1 \times n_2}$ and denote by U^*, U (respectively, V^*, V) the matrices whose columns contain the top d left (respectively, right) singular vectors of M^* , M , respectively. If $\|E\| < \sigma_d(M^*) - \sigma_{d+1}(M^*)$, then one has*

$$\max \left\{ \|UU^\top - U^*U^{*\top}\|, \|VV^\top - V^*V^{*\top}\| \right\} \leq \frac{2^{1/2} \max \{ \|E^\top U^{*\top}\|, \|EV^*\| \}}{\sigma_d(M^*) - \sigma_{d+1}(M^*) - \|E\|}.$$

A.4 Bernstein theorems

Theorem 4 (Matrix Bernstein; e.g. Theorem 1.6.2 in [Tropp, 2015](#)). *Let S_1, \dots, S_n be independent, centered random matrices with common dimension $d_1 \times d_2$, and assume that each one is uniformly bounded, that is:*

$$\mathbb{E}\{S_k\} = 0 \quad \text{and} \quad \|S_k\| \leq L_N \quad \text{for each } k = 1, \dots, n.$$

Introduce the sum $S = \sum_k S_k$ and let $v(S)$ denote the variance statistic of the sum:

$$v(S) = \max \left\{ \|\mathbb{E}\{SS^\top\}\|, \|\mathbb{E}\{S^\top S\}\| \right\} = \max \left\{ \left\| \sum_{k=1}^n \mathbb{E}\{S_k S_k^\top\} \right\|, \left\| \sum_{k=1}^n \mathbb{E}\{S_k^\top S_k\} \right\| \right\}.$$

Then

$$\mathbb{P}(\|Z\| \geq t) \leq (d_1 + d_2) \exp \left(-\frac{t^2/2}{v(Z) + Lt/3} \right) \quad \text{for all } t \geq 0.$$

Theorem 5 (Subexponential Bernstein; e.g. Corollary 2.9.2 in [Vershynin, 2018](#)). *Let X_1, \dots, X_n be subexponential, mean zero random variables, and $a = (a_1, \dots, a_n)^\top \in \mathbb{R}^n$. Then, for every $t \geq 0$, we have*

$$\mathbb{P} \left\{ \left| \sum_{i=1}^n a_i X_i \right| \geq t \right\} \leq 2 \exp \left(-c \min \left\{ \frac{t^2}{\left(\max_i \|X_i\|_{\psi_1} \right)^2 \|a\|_2^2}, \frac{t}{\left(\max_i \|X_i\|_{\psi_1} \right) \|a\|_\infty} \right\} \right).$$

A.5 Leave-one-out analysis

Leave-one-out (LOO) analysis is a proof technique used to decouple dependencies between data points. One constructs a LOO counterpart to an estimator and then compares them via a small perturbation.

As an illustrative example, we examine our setting where $\hat{\Lambda}$ is a matrix of Poisson random variables with expectation $\bar{\Lambda}$. Write the SVDs of each of these matrices as

$$\begin{aligned}\hat{\Lambda} &= \hat{U}\hat{\Sigma}\hat{V}^\top + \hat{U}_\perp\hat{\Sigma}_\perp\hat{V}_\perp^\top, \\ \bar{\Lambda} &= \bar{U}\bar{\Sigma}\bar{V}^\top + \bar{U}_\perp\bar{\Sigma}_\perp\bar{V}_\perp^\top,\end{aligned}$$

and suppose that we wish to bound the object $\|(\hat{\Lambda} - \bar{\Lambda})(\mathbf{I} - \bar{V}\bar{V}^\top)\hat{V}\hat{V}^\top\|_{2,\infty}$. We cannot use concentration inequalities here in a standard way as there is a dependency between $\hat{\Lambda}$ and \hat{V} . This problem can be circumvented through LOO analysis.

For each $i \in [NM]$, define a matrix $\hat{\Lambda}^{(i)}$ as

$$\hat{\Lambda}_{jk}^{(i)} = \begin{cases} \hat{\Lambda}_{jk}, & j \neq i, \\ \bar{\Lambda}_{jk}, & j = i \end{cases}.$$

Then $\hat{\Lambda}^{(i)}$ is $\hat{\Lambda}$ with its i -th row replaced with its expectation. That is to say, $\hat{\Lambda}^{(i)}$ is $\hat{\Lambda}$ but with the randomness removed from the i -th row. In this way, we can write $\hat{\Lambda} = \hat{\Lambda}^{(i)} + \mathbf{E}^{(i)}$, where

$$E_{pq}^{(i)} = \begin{cases} \hat{\Lambda}_{pq} - \bar{\Lambda}_{pq}, & p \neq i, \\ 0, & p = i. \end{cases}$$

We compute the singular value decomposition of this de-noised matrix $\hat{\Lambda}^{(i)}$ as

$$\hat{\Lambda}^{(i)} = \hat{U}^{(i)}\hat{\Sigma}^{(i)}\hat{V}^{(i)\top} + \hat{U}_\perp^{(i)}\hat{\Sigma}_\perp^{(i)}\hat{V}_\perp^{(i)\top}.$$

The point of this construction is that $\hat{\Lambda}^{(i)}$, and therefore $\hat{V}^{(i)}\hat{V}^{(i)\top}$, are independent of the i -th row of $\hat{\Lambda}$. To see the benefit of this, consider the following decomposition of our norm

$$\begin{aligned}\|e_i^\top(\hat{\Lambda} - \bar{\Lambda})(\mathbf{I} - \bar{V}\bar{V}^\top)\hat{V}\hat{V}^\top\| &\leq \|e_i^\top(\hat{\Lambda} - \bar{\Lambda})(\mathbf{I} - \bar{P})\hat{P}^{(i)}\| + \|e_i^\top(\hat{\Lambda} - \bar{\Lambda})(\mathbf{I} - \bar{P})(\hat{P} - \hat{P}^{(i)})\|, \\ &= \|(\hat{\Lambda}_{i,*} - \bar{\Lambda}_{i,*})(\mathbf{I} - \bar{P})\hat{P}^{(i)}\| + \|(\hat{\Lambda}_{i,*} - \bar{\Lambda}_{i,*})(\mathbf{I} - \bar{P})(\hat{P} - \hat{P}^{(i)})\|,\end{aligned}$$

where we define $\bar{P} = \bar{V}\bar{V}^\top$, and have analogous definitions for \hat{P} and $\hat{P}^{(i)}$. It is here that we see the power of LOO analysis as we now have the luxury of applying concentration inequalities for sums of independent random variables to the first term as we have decoupled the dependent terms. For the second, we can apply Wedin's Theorem to the operator norm $\|\hat{P} - \hat{P}^{(i)}\|$ which are projections onto very “close” subspaces as they only differ by one row. This argument will be presented in depth when applied in later propositions.

B Key propositions

In this section, we provide several propositions that will be used to prove the main theorems of this work. The proofs in this Appendix combine and extend the standard machinery used to prove results in [Jones and Rubin-Delanchy \(2020\)](#); [Gallagher et al. \(2024\)](#); [Baum et al. \(2024\)](#). Throughout this section, as in the main text, we will write $\hat{\Lambda} \in \mathbb{R}_+^{NM \times NL}$ to be a matrix of independent Poisson random variables with expectation $\bar{\Lambda} \in \mathbb{R}_+^{NM \times NL}$. We will write the SVDs of these matrices as:

$$\begin{aligned}\hat{\Lambda} &= \hat{U}\hat{\Sigma}\hat{V}^\top + \hat{U}_\perp\hat{\Sigma}_\perp\hat{V}_\perp^\top, \\ \bar{\Lambda} &= \bar{U}\bar{\Sigma}\bar{V}^\top + \bar{U}_\perp\bar{\Sigma}_\perp\bar{V}_\perp^\top.\end{aligned}$$

We will write $\hat{\Lambda}^{(i)} \in \mathbb{R}_+^{NM \times NL}$ to be the i -th leave-one-out counterpart of $\hat{\Lambda}$, as detailed in Section A.5, with $\hat{\Lambda}^{(i)}$ having its (p, q) -th entry defined as

$$\hat{\Lambda}_{pq}^{(i)} = \begin{cases} \hat{\Lambda}_{pq}, & p \neq i \\ \bar{\Lambda}_{pq}, & p = q. \end{cases}$$

We write the SVD of $\hat{\Lambda}^{(i)}$ in an analogous way to that of $\hat{\Lambda}$ and $\bar{\Lambda}$.

Proposition 2 provides a high probability decay bound on Poisson random variables that will be used throughout our proofs.

Proposition 2 (Poisson tail bound). *Let $X \sim \text{Poisson}(\lambda)$. Then, for $N \in \mathbb{N}$, for each $\rho > 0$ there exists some β_ρ such that*

$$\mathbb{P}(X < \beta_\rho \log(N)) > 1 - N^{-\rho}.$$

We prove Proposition 2 using a simple application of Markov's inequality and the moment generating function of a Poisson random variable. The next proposition controls the spectral norm between the Poisson random matrix $\hat{\Lambda}$ and its expectation $\bar{\Lambda}$. The bound is seen to grow the N, M_N and L_N .

Proposition 3. $\|\hat{\Lambda} - \bar{\Lambda}\| = \mathcal{O}\left(\max\{M_N, L_N\}^{1/2} M_N N^{1/2} \log^{3/2}(N)\right)$ almost surely.

Proposition 3 is proved by combining Proposition 2 with Bernstein's theorem and Popoviciu's inequality. An application of Borel-Cantelli extends the argument to hold eventually almost surely. Through Proposition 4, we provide control on the growth of the singular values of $\hat{\Lambda}$. In particular, the growth of the eigengap is guaranteed with growing M_N, N and L_N . These bounds hold under Assumption 1 and a simple application of Corollary 7.3.5 from Horn and Johnson (2012).

Proposition 4 (Control of $\sigma_i(\hat{\Lambda})$). *Under Assumption 1, we have*

$$\sigma_1(\hat{\Lambda}), \dots, \sigma_d(\hat{\Lambda}) = \Theta\left(M_N^{1/2} L_N^{1/2} N\right),$$

and

$$\sigma_{d+1}(\hat{\Lambda}) = \mathcal{O}\left(\max\{M_N, L_N\}^{1/2} M_N N^{1/2} \log^{3/2}(N)\right),$$

almost surely.

We require control on the growth of the term $\|\bar{U}^\top(\hat{\Lambda} - \bar{\Lambda})\bar{V}\|_F = \mathcal{O}\left(M_N \log^{3/2}(N)\right)$ as $N \rightarrow \infty$. This is provided by Proposition 5.

Proposition 5. *We have $\|\bar{U}^\top(\hat{\Lambda} - \bar{\Lambda})\bar{V}\|_F = \mathcal{O}\left(M_N \log^{3/2}(N)\right)$, almost surely.*

Proposition 5 is proved by considering the term inside the norm as a sum of scaled, independent random variables and applying Hoeffding's inequality and a union bound.

In Proposition 6, we provide a number of Frobenius and spectral norm bounds that are employed in the proofs of the main theorems.

Proposition 6. *The following bounds hold almost surely:*

1. (a) $\|\hat{U}\hat{U}^\top - \bar{U}\bar{U}^\top\| = \mathcal{O}\left(\max\{M_N, L_N\}^{1/2} M_N^{1/2} L_N^{-1/2} N^{-1/2} \log^{3/2}(N)\right)$,
1. (b) $\|\hat{V}\hat{V}^\top - \bar{V}\bar{V}^\top\| = \mathcal{O}\left(\max\{M_N, L_N\}^{1/2} M_N^{1/2} L_N^{-1/2} N^{-1/2} \log^{3/2}(N)\right)$,
2. (a) $\|\hat{U} - \bar{U}\bar{U}^\top\hat{U}\|_F = \mathcal{O}\left(\max\{M_N, L_N\}^{1/2} M_N^{1/2} L_N^{-1/2} N^{-1/2} \log^{3/2}(N)\right)$,
2. (b) $\|\hat{V} - \bar{V}\bar{V}^\top\hat{V}\|_F = \mathcal{O}\left(\max\{M_N, L_N\}^{1/2} M_N^{1/2} L_N^{-1/2} N^{-1/2} \log^{3/2}(N)\right)$,

3. (a) $\|\bar{\mathbf{U}}^\top \hat{\mathbf{U}} \hat{\Sigma} - \bar{\Sigma} \bar{\mathbf{V}}^\top \hat{\mathbf{V}}\|_F = \mathcal{O} \left(\max\{M_N, L_N\} M_N^{3/2} L_N^{-1/2} \log^3(N) \right)$,
(b) $\|\bar{\Sigma} \bar{\mathbf{U}}^\top \hat{\mathbf{U}} - \bar{\mathbf{V}}^\top \hat{\mathbf{V}} \hat{\Sigma}\|_F = \mathcal{O} \left(\max\{M_N, L_N\} M_N^{3/2} L_N^{-1/2} \log^3(N) \right)$,
4. $\|\bar{\mathbf{U}}^\top \hat{\mathbf{U}} - \bar{\mathbf{V}}^\top \hat{\mathbf{V}}\|_F = \mathcal{O} \left(\max\{M_N, L_N\} M_N L_N^{-1} N^{-1} \log^3(N) \right)$.

Proposition 7 is important as it defines the orthogonal matrix \mathbf{W} , which is key to defining the general linear transformation up to which we recover the latent positions. The result is proved by applying a result from Schönenmann (1966) and parts of Proposition 6.

Proposition 7. *Let $\bar{\mathbf{U}}^\top \hat{\mathbf{U}} + \bar{\mathbf{V}}^\top \hat{\mathbf{V}}$ admit the singular value decomposition*

$$\bar{\mathbf{U}}^\top \hat{\mathbf{U}} + \bar{\mathbf{V}}^\top \hat{\mathbf{V}} = \mathbf{W}_1 \Sigma \mathbf{W}_2,$$

and let $\mathbf{W} = \mathbf{W}_1 \mathbf{W}_2^\top$. Then

$$\max \left\{ \|\bar{\mathbf{U}}^\top \hat{\mathbf{U}} - \mathbf{W}\|_F, \|\bar{\mathbf{V}}^\top \hat{\mathbf{V}} - \mathbf{W}\|_F \right\} = \mathcal{O} \left(\max\{M_N, L_N\} M_N L_N^{-1} N^{-1} \log^3(N) \right),$$

almost surely.

With \mathbf{W} defined, Proposition 8 provides Frobenius norm bounds on terms involving \mathbf{W} , $\hat{\Sigma}$ and $\bar{\Sigma}$. These bounds are employed in proofs of subsequent propositions, in particular Proposition 12.

Proposition 8. *With \mathbf{W} defined as in Proposition 7, we have the following bounds holding almost surely:*

1. $\|\mathbf{W} \hat{\Sigma} - \bar{\Sigma} \mathbf{W}\|_F = \mathcal{O} \left(\max\{M_N, L_N\} M_N^{3/2} L_N^{-1/2} \log^3(N) \right)$,
2. $\|\mathbf{W} \hat{\Sigma}^{1/2} - \bar{\Sigma}^{1/2} \mathbf{W}\|_F = \mathcal{O} \left(\max\{M_N, L_N\} M_N^{5/4} L_N^{-3/4} N^{-1/2} \log^3(N) \right)$,
3. $\|\mathbf{W} \hat{\Sigma}^{-1/2} - \bar{\Sigma}^{-1/2} \mathbf{W}\|_F = \mathcal{O} \left(\max\{M_N, L_N\} M_N^{3/4} L_N^{-5/4} N^{-3/2} \log^3(N) \right)$.

Proposition 9 defines the general linear transformations $\check{\mathbf{K}}$ and $\check{\mathbf{R}}$ that relate the latent position matrices estimated from $\bar{\Lambda}$, namely $\check{\mathbf{X}}$ and $\check{\mathbf{Y}}$, to the true positions $\bar{\mathbf{X}}$ and $\bar{\mathbf{Y}}$. These are key transformations, as they combine with \mathbf{W} to define \mathbf{W}_X and \mathbf{W}_Y in Theorem 1.

Proposition 9. *Define $\check{\mathbf{X}}$ to be $\check{\mathbf{X}} = (\check{\mathbf{X}}_1 \mid \dots \mid \check{\mathbf{X}}^{(m,*)}) \in \mathbb{R}^{NM_N \times d}$ where $\check{\mathbf{X}}^{(m,*)} := M_N \int_{B_m} \mathbf{X}(t) dt \in \mathbb{R}^{N \times d}$. Let the singular value decomposition of $\bar{\Lambda} = \check{\mathbf{X}} \check{\mathbf{Y}}^\top$ be $\bar{\mathbf{U}} \bar{\Sigma} \bar{\mathbf{V}}^\top + \bar{\mathbf{U}}_\perp \bar{\Sigma}_\perp \bar{\mathbf{V}}_\perp^\top$. Define $\check{\mathbf{X}} = \bar{\mathbf{U}} \bar{\Sigma}^{1/2}$ and $\check{\mathbf{Y}} = \bar{\mathbf{V}} \bar{\Sigma}^{1/2}$. Then, there exists matrices $\check{\mathbf{K}} \in \text{GL}(d)$ and $\check{\mathbf{R}} \in \text{GL}(d)$ such that $\check{\mathbf{X}} = \check{\mathbf{X}} \check{\mathbf{K}}$ and $\check{\mathbf{Y}} = \check{\mathbf{Y}} \check{\mathbf{R}}$. Furthermore, we have $\check{\mathbf{K}} \check{\mathbf{R}}^\top = I_d$.*

Proposition 10 provides a bound on the growth of the left and right singular vectors that arise from the leave-one-out analysis. This is needed to provide the decay rates of the remainder terms in Proposition 12.

Proposition 10. *Suppose that $\hat{\Lambda}^{(i)}$ is the matrix formed by setting the i -th row of $\hat{\Lambda}$ equal to $\bar{\Lambda}_{i,*}$. Write the SVD of $\hat{\Lambda}^{(i)}$ as*

$$\hat{\Lambda}^{(i)} = \hat{\mathbf{U}}^{(i)} \hat{\Sigma}^{(i)} \hat{\mathbf{V}}^{(i)\top} + \hat{\mathbf{U}}_\perp^{(i)} \hat{\Sigma}_\perp^{(i)} \hat{\mathbf{V}}_\perp^{(i)\top},$$

and the SVDs of $\hat{\Lambda}$ and $\bar{\Lambda}$ using analogous notation. Then, under Assumption 1.i, we have

$$\|\hat{\mathbf{U}}\|_{2,\infty}, \|\hat{\mathbf{U}}^{(i)}\|_{2,\infty}, \|\hat{\mathbf{V}}\|_{2,\infty}, \|\hat{\mathbf{V}}^{(i)}\|_{2,\infty} = \mathcal{O} \left(\max\{M_N, L_N\}^{1/2} M_N^{1/2} L_N^{-1/2} N^{-1/2} \log^{3/2}(N) \right).$$

The next proposition bounds the spectral norms of the general linear transformations $\check{\mathbf{K}}$ and $\check{\mathbf{R}}$ and also of their inverses. These are needed in the proof of Theorem 1 when we transform from the theoretical latent positions to their estimates.

Proposition 11. *The matrices $\check{\mathbf{K}}$ and $\check{\mathbf{R}}$ as defined in Proposition 9 satisfy:*

- $\|\check{\mathbf{K}}\| = \mathcal{O}\left(M_N^{-1/4}L_N^{1/4}\right)$, $\|\check{\mathbf{K}}^{-1}\| = \mathcal{O}\left(M_N^{1/4}L_N^{-1/4}\right)$,
- $\|\check{\mathbf{R}}\| = \mathcal{O}\left(M_N^{1/4}L_N^{-1/4}\right)$, $\|\check{\mathbf{R}}^{-1}\| = \mathcal{O}\left(M_N^{-1/4}L_N^{1/4}\right)$.

Proposition 12 is key for the proof of Theorem 1. In the theorem, we decompose the two-to-infinity norm into multiple remainders. The following proposition shows that these remainders decay with N and quantifies the rate at which they decay.

Proposition 12. *Define the following:*

$$\begin{aligned} \mathbf{R}_{1,1} &= \bar{\mathbf{U}}(\bar{\mathbf{U}}^\top \hat{\mathbf{U}} \hat{\Sigma}^{1/2} - \bar{\Sigma}^{1/2} \mathbf{W}), & \mathbf{R}_{2,1} &= \bar{\mathbf{V}}(\bar{\mathbf{V}}^\top \hat{\mathbf{V}} \hat{\Sigma}^{1/2} - \bar{\Sigma}^{1/2} \mathbf{W}), \\ \mathbf{R}_{1,2} &= (\mathbf{I} - \bar{\mathbf{U}}\bar{\mathbf{U}}^\top)(\hat{\Lambda} - \bar{\Lambda})(\hat{\mathbf{V}} - \bar{\mathbf{V}}\mathbf{W})\hat{\Sigma}^{-1/2}, & \mathbf{R}_{2,2} &= (\mathbf{I} - \bar{\mathbf{V}}\bar{\mathbf{V}}^\top)(\hat{\Lambda} - \bar{\Lambda})(\hat{\mathbf{U}} - \bar{\mathbf{U}}\mathbf{W})\hat{\Sigma}^{-1/2}, \\ \mathbf{R}_{1,3} &= -\bar{\mathbf{U}}\bar{\mathbf{U}}^\top(\hat{\Lambda} - \bar{\Lambda})\bar{\mathbf{V}}\mathbf{W}\hat{\Sigma}^{-1/2}, & \mathbf{R}_{2,3} &= -\bar{\mathbf{V}}\bar{\mathbf{V}}^\top(\hat{\Lambda} - \bar{\Lambda})\bar{\mathbf{U}}\mathbf{W}\hat{\Sigma}^{-1/2}, \\ \mathbf{R}_{1,4} &= (\hat{\Lambda} - \bar{\Lambda})\bar{\mathbf{V}}(\mathbf{W}\hat{\Sigma}^{-1/2} - \bar{\Sigma}^{-1/2}\mathbf{W}), & \mathbf{R}_{2,4} &= (\hat{\Lambda} - \bar{\Lambda})\bar{\mathbf{U}}(\mathbf{W}\hat{\Sigma}^{-1/2} - \bar{\Sigma}^{-1/2}\mathbf{W}). \end{aligned}$$

With these definitions, the following bounds hold almost surely:

1. $\|\mathbf{R}_{1,1}\|_{2,\infty}, \|\mathbf{R}_{2,1}\|_{2,\infty} = \mathcal{O}\left(\max\{M_N, L_N\}M_N^{3/4}L_N^{-3/4}N^{-1}\log^3(N)\right)$
2. $\|\mathbf{R}_{1,2}\|_{2,\infty}, \|\mathbf{R}_{2,2}\|_{2,\infty} = \mathcal{O}\left(\max\{M_N, L_N\}^{3/2}M_N^{7/4}L_N^{-5/4}N^{-1}\log^{9/2}(N)\right)$,
3. $\|\mathbf{R}_{1,3}\|_{2,\infty}, \|\mathbf{R}_{2,3}\|_{2,\infty} = \mathcal{O}\left(M_N^{1/4}L_N^{-1/4}N^{-1}\log^{3/2}(N)\right)$,
4. $\|\mathbf{R}_{1,4}\|_{2,\infty}, \|\mathbf{R}_{2,4}\|_{2,\infty} = \mathcal{O}\left(\max\{M_N, L_N\}^{3/2}M_N^{7/4}L_N^{-5/4}N^{-1}\log^{9/2}(N)\right)$.

The next two propositions are on the decay of the bias term in Theorem 1 under Assumptions 2.i and 2.ii.

Proposition 13 (Bias decay with Assumption 2.i). *Under Assumption 2.i, we have the following decay:*

$$\|\tilde{\mathbf{X}}^{(m,*)} - \mathbf{X}(t)\|_{2,\infty} = \mathcal{O}(K_N M_N^{-1}).$$

Proposition 14 (Bias decay with Assumption 2.ii). *Under Assumption 2.i, we have the following decay:*

$$\|\tilde{\mathbf{X}}^{(m,*)}\mathbf{W}_m - \mathbf{X}(t)\|_{2,\infty} = \mathcal{O}((K_1 + K_2)M_N^{-1}).$$

C Proof of Theorem 1

The proof of Theorem 1 is constructed using the series of propositions and supplementary results stated in Section B.

The task at hand is to obtain bounds on the following norms:

$$\max_{m \in [M_N]} \sup_{t \in B_m} \|\hat{\mathbf{X}}^{(m,*)}\mathbf{W}_X - \mathbf{X}(t)\|_{2,\infty} \quad \text{and} \quad \|\hat{\mathbf{Y}}\mathbf{W}_Y - \mathbf{Y}\|.$$

To tackle the first of these norms, our strategy is decompose this norm into the sum of two terms as:

$$\max_{m \in [M_N]} \sup_{t \in B_m} \|\hat{\mathbf{X}}^{(m,*)}\mathbf{W}_X - \mathbf{X}(t)\|_{2,\infty} \leq \|\hat{\mathbf{X}}\mathbf{W}_2 - \tilde{\mathbf{X}}\|_{2,\infty} + \max_{m \in [M_N]} \sup_{t \in B_m} \|\tilde{\mathbf{X}}^{(m,*)}\mathbf{W}_1 - \mathbf{X}(t)\|_{2,\infty},$$

with $\mathbf{W}_X = \mathbf{W}_2\mathbf{W}_1$ and $\mathbf{W}_1, \mathbf{W}_2 \in \mathbb{O}(d)$. Note this holds because the two-to-infinity norm of the m -th block is always upper bounded by the two-to-infinity norm of the full matrix. The second term is B_N , and the decay rates of this is proved in Proposition 13.

We begin with the following decomposition:

$$\begin{aligned}
\hat{\mathbf{X}} - \bar{\mathbf{X}}\mathbf{W} &= \hat{\mathbf{U}}\hat{\Sigma}^{1/2} - \bar{\mathbf{U}}\bar{\Sigma}^{1/2}\mathbf{W} \\
&= \hat{\mathbf{U}}\hat{\Sigma}^{1/2} - \bar{\mathbf{U}}\bar{\mathbf{U}}^\top\hat{\mathbf{U}}\hat{\Sigma}^{1/2} + \bar{\mathbf{U}}\left(\bar{\mathbf{U}}^\top\bar{\mathbf{U}}\hat{\Sigma}^{1/2} - \bar{\Sigma}^{1/2}\mathbf{W}\right) \\
&= \hat{\mathbf{U}}\hat{\Sigma}^{1/2} - \bar{\mathbf{U}}\bar{\mathbf{U}}^\top\hat{\mathbf{U}}\hat{\Sigma}^{1/2} + \mathbf{R}_{1,1},
\end{aligned}$$

where $\mathbf{R}_{1,1}$ is defined as in Proposition 12. Continuing, we see

$$\begin{aligned}
\hat{\mathbf{X}} - \bar{\mathbf{X}}\mathbf{W} &= (\hat{\Lambda} - \bar{\Lambda})\hat{\mathbf{V}}\hat{\Sigma}^{-1/2} - (\bar{\mathbf{U}}\bar{\mathbf{U}}^\top\hat{\Lambda} - \bar{\Lambda})\hat{\mathbf{V}}\hat{\Sigma}^{-1/2} + \mathbf{R}_{1,1} \\
&= (\hat{\Lambda} - \bar{\Lambda})\hat{\mathbf{V}}\hat{\Sigma}^{-1/2} - \bar{\mathbf{U}}\bar{\mathbf{U}}^\top(\hat{\Lambda} - \bar{\Lambda})\hat{\mathbf{V}}\hat{\Sigma}^{-1/2} + \mathbf{R}_{1,1} \\
&= (\mathbf{I} - \bar{\mathbf{U}}\bar{\mathbf{U}}^\top)(\hat{\Lambda} - \bar{\Lambda})\hat{\mathbf{V}}\hat{\Sigma}^{-1/2} + \mathbf{R}_{1,1} \\
&= (\mathbf{I} - \bar{\mathbf{U}}\bar{\mathbf{U}}^\top)(\hat{\Lambda} - \bar{\Lambda})[\bar{\mathbf{V}}\mathbf{W} + (\hat{\mathbf{V}} - \bar{\mathbf{V}}\mathbf{W})]\hat{\Sigma}^{-1/2} + \mathbf{R}_{1,1} \\
&= (\hat{\Lambda} - \bar{\Lambda})\bar{\mathbf{V}}\mathbf{W}\hat{\Sigma}^{-1/2} + \mathbf{R}_{1,2} + \mathbf{R}_{1,3} + \mathbf{R}_{1,1} \\
&= (\hat{\Lambda} - \bar{\Lambda})\bar{\mathbf{V}}\bar{\Sigma}^{-1/2}\mathbf{W} + \mathbf{R}_{\mathbf{X}},
\end{aligned}$$

with $\mathbf{R}_{\mathbf{X}} := \mathbf{R}_{1,4} + \mathbf{R}_{1,2} + \mathbf{R}_{1,3} + \mathbf{R}_{1,1}$, and each $\mathbf{R}_{\cdot,\cdot}$ defined as in Proposition 12. By Proposition 12, we know $\|\mathbf{R}_{\mathbf{X}}\|_{2,\infty} = \mathcal{O}\left(\max\{M_N, L_N\}^{3/2}M_N^{7/4}L_N^{-5/4}N^{-1}\log^{9/2}(N)\right)$ almost surely, which says

$$\|\hat{\mathbf{X}} - \bar{\mathbf{X}}\mathbf{W}\|_{2,\infty} \leq \sigma_d(\bar{\Lambda})^{-1/2}\|(\hat{\Lambda} - \bar{\Lambda})\bar{\mathbf{V}}\|_{2,\infty} + \mathcal{O}\left(\max\{M_N, L_N\}^{3/2}M_N^{7/4}L_N^{-5/4}N^{-1}\log^{9/2}(N)\right).$$

Consider the (i, j) -th element of $(\hat{\Lambda} - \bar{\Lambda})\bar{\mathbf{V}}$, which takes the form

$$\left((\hat{\Lambda} - \bar{\Lambda})\bar{\mathbf{V}}\right)_{ij} = \sum_{k=1}^{NL_N} (\hat{\Lambda}_{ik} - \bar{\Lambda}_{ik})\bar{V}_{kj}.$$

Note that $\|\bar{V}_{*,j}\|_\infty \leq 1$ almost surely, and, as argued in the proof of Proposition 3, for large enough N , for all $(i, j) \in \mathcal{X}^{M_N, L_N}$, the event $|\hat{\Lambda}_{ij} - \bar{\Lambda}_{ij}| < M_N \log(N)$ occurs almost surely. We can thus apply Hoeffding's inequality, by which we know

$$\mathbb{P}\left(\left|\sum_{k=1}^{NL_N} (\hat{\Lambda}_{ik} - \bar{\Lambda}_{ik})\bar{V}_{kj}\right| \geq t\right) \leq 2\exp\left(-\frac{2t^2}{\sum_{k=1}^{NL_N} |\bar{V}_{kj}|^2 M_N^2 \log^2(N)}\right) \leq 2\exp\left(-\frac{2t^2}{M_N^2 \log^2(N)}\right),$$

from which it follows that

$$\left|\left((\hat{\Lambda} - \bar{\Lambda})\bar{\mathbf{V}}\right)_{ij}\right| = \mathcal{O}\left(M_N \log^{3/2}(N)\right),$$

almost surely. By taking a union over its d elements, we deduce that $\|((\hat{\Lambda} - \bar{\Lambda})\bar{\mathbf{V}})_{i,*}\| = \mathcal{O}\left(M_N \log^{3/2}(N)\right)$, almost surely. By Proposition 1, we know $\sigma_d(\bar{\Lambda})^{-1/2} = \mathcal{O}\left(M_N^{-1/4}L_N^{-1/4}N^{-1/2}\right)$. Combining, it follows that

$$\sigma_d(\bar{\Lambda})^{-1/2}\|(\hat{\Lambda} - \bar{\Lambda})\bar{\mathbf{V}}\|_{2,\infty} = \mathcal{O}\left(M_N^{3/4}L_N^{-1/4}N^{-1/2}\log^{3/2}(N)\right),$$

almost surely. It follows that

$$\max_{m \in [M]} \|\hat{\mathbf{X}}^{(m,*)} - \bar{\mathbf{X}}^{(m,*)}\mathbf{W}\|_{2,\infty} = \|\hat{\mathbf{X}} - \bar{\mathbf{X}}\mathbf{W}\|_{2,\infty} = \mathcal{O}\left(M_N^{3/4}L_N^{-1/4}N^{-1/2}\log^{3/2}(N)\right).$$

To complete this part of the proof, define $\mathbf{W}_{\mathbf{X}} = \mathbf{W}^{-1}\check{\mathbf{K}}^{-1}$ and note

$$\|\hat{\mathbf{X}}\mathbf{W}_{\mathbf{X}} - \tilde{\mathbf{X}}\|_{2,\infty} \leq \|\hat{\mathbf{X}} - \tilde{\mathbf{X}}\mathbf{W}_{\mathbf{X}}^{-1}\|_{2,\infty}\|\mathbf{W}_{\mathbf{X}}\| = \|\hat{\mathbf{X}} - \bar{\mathbf{X}}\mathbf{W}\|_{2,\infty}\|\mathbf{W}^{-1}\|\|\check{\mathbf{K}}^{-1}\|.$$

Recalling that \mathbf{W} is orthogonal, upon combining with Proposition 11, we obtain the final result

$$\|\hat{\mathbf{X}}\mathbf{W}_X - \tilde{\mathbf{X}}\|_{2,\infty} = \mathcal{O}\left(M_N L_N^{-1/2} N^{-1/2} \log^{3/2}(N)\right),$$

almost surely.

An analogous set of algebraic steps gives

$$\hat{\mathbf{Y}} - \bar{\mathbf{Y}}\mathbf{W} = (\hat{\Lambda} - \bar{\Lambda})^\top \bar{\mathbf{U}} \bar{\Sigma}^{-1/2} \mathbf{W} + \mathbf{R}_Y,$$

where $\mathbf{R}_Y = \mathbf{R}_{2,1} + \mathbf{R}_{2,2} + \mathbf{R}_{2,3} + \mathbf{R}_{2,4}$, with the $\mathbf{R}_{2,*}$ defined as in Proposition 12. The same proposition tells us $\|\mathbf{R}_Y\|_{2,\infty} = \mathcal{O}\left(\max\{M_N, L_N\}^{3/2} M_N^{7/4} L_N^{-5/4} N^{-1} \log^{9/2}(N)\right)$ almost surely. Following the same approach, we consider the (i, j) -th element of $(\hat{\Lambda} - \bar{\Lambda})^\top \bar{\mathbf{U}}$, which takes the form

$$\left((\hat{\Lambda} - \bar{\Lambda})^\top \bar{\mathbf{U}}\right)_{ij} = \sum_{k=1}^{NM} (\hat{\Lambda}_{ki} - \bar{\Lambda}_{ki}) \bar{U}_{kj}.$$

Again, we know $\|\bar{U}_{*,j}\| \leq 1$ almost surely, and, for large enough N , for all $(i, j) \in \mathcal{X}^{N, M_N, L_N}$ the event $|\Lambda_{ij} - \bar{\Lambda}_{ij}| < M_N \log(N)$ occurs almost surely. We can apply Hoeffding's inequality in an analogous way to before to obtain

$$\mathbb{P}\left(\left|\sum_{k=1}^{NM} (\hat{\Lambda}_{ki} - \bar{\Lambda}_{ki}) \bar{U}_{kj}\right| \geq t\right) \leq 2 \exp\left(-\frac{2t^2}{\sum_{k=1}^{NM} |\bar{U}_{kj}|^2 M_N^2 \log^2(N)}\right) \leq 2 \exp\left(-\frac{2t^2}{M_N^2 \log^2(N)}\right),$$

from which it follows as before that

$$\left|\left(\hat{\Lambda} - \bar{\Lambda}\right)^\top \bar{\mathbf{U}}\right|_{i,*} = \mathcal{O}\left(M_N \log^{3/2}(N)\right),$$

almost surely. We deduce

$$\sigma_d(\bar{\Lambda})^{-1/2} \|(\hat{\Lambda} - \bar{\Lambda}) \bar{\mathbf{U}}\|_{2,\infty} = \mathcal{O}\left(M_N^{3/4} L_N^{-1/4} N^{-1/2} \log^{3/2}(N)\right),$$

almost surely. Defining $\mathbf{W}_Y = \mathbf{W}^{-1} \check{\mathbf{R}}^{-1}$ and using Proposition 11, we obtain the result

$$\|\hat{\mathbf{Y}}\mathbf{W}_Y - \mathbf{Y}\|_{2,\infty} = \mathcal{O}\left(M_N^{1/2} N^{-1/2} \log^{3/2}(N)\right),$$

almost surely.

D Proof of Theorem 2

We start with the left embedding, and recall the identities $\mathbf{W}_X = \mathbf{W}^{-1} \check{\mathbf{K}}^{-1}$ and $\tilde{\mathbf{X}} = \bar{\mathbf{X}} \mathbf{K}^{-1}$. We can then write

$$\begin{aligned} N^{1/2} L_N^{1/2} (\hat{\mathbf{X}}\mathbf{W}_X - \tilde{\mathbf{X}}) &= (\hat{\mathbf{X}} - \bar{\mathbf{X}} \check{\mathbf{K}}^{-1} \mathbf{W}_X^{-1}) \mathbf{W}_X \\ &= N^{1/2} L_N^{1/2} (\hat{\mathbf{X}} - \bar{\mathbf{X}} \mathbf{W}) \mathbf{W}_X \\ &= N^{1/2} L_N^{1/2} (\hat{\Lambda} - \bar{\Lambda}) \bar{\mathbf{V}} \bar{\Sigma}^{-1/2} \mathbf{W} \mathbf{W}_X + N^{1/2} L_N^{1/2} \mathbf{R}_X \mathbf{W}_X \\ &= N^{1/2} L_N^{1/2} (\hat{\Lambda} - \bar{\Lambda}) \bar{\mathbf{V}} \bar{\Sigma}^{-1/2} \check{\mathbf{K}}^{-1} + N^{1/2} L_N^{1/2} \mathbf{R}_X \mathbf{W}_X, \end{aligned}$$

where \mathbf{R}_X is defined as in Section C. From our earlier work, we know that the second term on the right-hand side decays vanishes in two-to-infinity norm almost surely.

Note that the definition $\bar{\mathbf{Y}} = \bar{\mathbf{V}}\bar{\Sigma}^{1/2}$ implies that $\bar{\mathbf{V}}\bar{\Sigma}^{1/2} = \bar{\mathbf{Y}}\bar{\Sigma}^{-1} = \bar{\mathbf{Y}}\check{\mathbf{R}}\bar{\Sigma}^{-1}$, and so

$$N^{1/2}L_N^{1/2}(\hat{\Lambda} - \bar{\Lambda})\bar{\mathbf{V}}\bar{\Sigma}^{-1/2}\check{\mathbf{K}}^{-1} = (\hat{\Lambda} - \bar{\Lambda})\bar{\mathbf{Y}}\check{\mathbf{R}}\bar{\Sigma}^{-1}\check{\mathbf{K}}^{-1}.$$

We consider the m -th block:

$$N^{1/2}L_N^{1/2}(\hat{\mathbf{X}}^{(m,*)}\mathbf{W}_{\mathbf{X}} - \tilde{\mathbf{X}}^{(m,*)}) = N^{1/2}L_N^{1/2}(\hat{\Lambda}^{(m,*)} - \bar{\Lambda}^{(m,*)})\bar{\mathbf{Y}}\check{\mathbf{R}}\bar{\Sigma}^{-1}\check{\mathbf{K}}^{-1}.$$

Recall that $\check{\mathbf{K}}\check{\mathbf{R}}^\top = \mathbf{I}_d$ and so we can write

$$\tilde{\mathbf{X}}\check{\mathbf{K}}\bar{\Sigma}\check{\mathbf{K}}^\top\tilde{\mathbf{X}}^\top = \bar{\mathbf{X}}\bar{\Sigma}\bar{\mathbf{X}}^\top = \bar{\Lambda}\bar{\Lambda}^\top = \tilde{\mathbf{X}}\mathbf{Y}^\top\mathbf{Y}\tilde{\mathbf{X}}^\top.$$

It follows that $\check{\mathbf{K}}\bar{\Sigma}\check{\mathbf{K}}^\top = \mathbf{Y}^\top\mathbf{Y}$ and

$$(\check{\mathbf{R}}\bar{\Sigma}^{-1}\check{\mathbf{K}}^{-1})^\top = \check{\mathbf{K}}^{-1}\bar{\Sigma}^{-1}\check{\mathbf{K}}^{-1}\check{\mathbf{R}}\bar{\Sigma}^\top = (\mathbf{Y}^\top\mathbf{Y})^{-1}\check{\mathbf{K}}\check{\mathbf{R}}^\top = (\mathbf{Y}^\top\mathbf{Y})^{-1}.$$

Using this result, we can decompose further and consider the transpose of the i -th row:

$$\begin{aligned} N^{1/2}L_N^{1/2}(\hat{\mathbf{X}}^{(m,*)}\mathbf{W}_{\mathbf{X}} - \tilde{\mathbf{X}}^{(m,*)})_{i,*}^\top &= N^{1/2}L_N^{1/2}(\check{\mathbf{R}}\bar{\Sigma}^{-1}\check{\mathbf{K}}^{-1})^\top[(\hat{\Lambda}^{(m,*)} - \bar{\Lambda}^{(m,*)})\mathbf{Y}]_i^\top \\ &= N^{1/2}L_N^{1/2}(\mathbf{Y}^\top\mathbf{Y})^{-1}\sum_{j=1}^{NL_N}(\hat{\Lambda}_{ij}^{(m,*)} - \bar{\Lambda}_{ij}^{(m,*)})Y_{j,*}^\top \\ &= NL_N(\mathbf{Y}^\top\mathbf{Y})^{-1}\frac{1}{N^{1/2}L_N^{1/2}}\sum_{j=1}^{NL_N}(\hat{\Lambda}_{ij}^{(m,*)} - \bar{\Lambda}_{ij}^{(m,*)})Y_{j,*}^\top. \end{aligned}$$

We first note that as $N \rightarrow \infty$, we have $NL_N(\mathbf{Y}^\top\mathbf{Y})^{-1} \rightarrow \mathbf{Q}_{\mathbf{Y}}^{-1}$ by Assumption 1.ii. Define A_{ij}^m to be the random vector

$$A_{ij}^m = (\hat{\Lambda}_{ij}^{(m,*)} - \bar{\Lambda}_{ij}^{(m,*)})Y_{j,*}^\top,$$

which has covariance given by

$$\text{Cov}(A_{ij}^m) = (\tilde{\mathbf{X}}_{i,*}^{(m,*)}Y_{j,*}^\top)Y_{j,*}^\top Y_{j,*}.$$

Now we define the matrix $\mathbf{C}_{i,m}^N$ to be

$$\mathbf{C}_{i,m}^N = \frac{1}{NL_N}\sum_{j=1}^{NL_N}\text{Cov}(A_{ij}^m),$$

which is invertible by Assumption 3. It follows that

$$\text{Cov}\left(N^{1/2}L_N^{1/2}(\hat{\mathbf{X}}^{(m,*)}\mathbf{W}_{\mathbf{X}} - \tilde{\mathbf{X}}^{(m,*)})_{i,*}^\top\right) = \mathbf{Q}_{\mathbf{X}}^{-1}\mathbf{C}_{i,m}^N(\tilde{\mathbf{X}})\mathbf{Q}_{\mathbf{X}}^{-1}.$$

Because we work with Poisson random variables with intensities that are $\mathcal{O}(1)$, we have for all $u \in \mathbb{R}^d$ that

$$\text{Cov}\left((\hat{\Lambda}_{ij}^{(m,*)} - \bar{\Lambda}_{ij}^{(m,*)})u^\top Y_{j,*}^\top\right) = \mathcal{O}(1) \quad \text{and} \quad \mathbb{E}\left\{ |(\hat{\Lambda}_{ij}^{(m,*)} - \bar{\Lambda}_{ij}^{(m,*)})u^\top Y_{j,*}^\top|^3 \right\} \leq C,$$

uniformly in j and so the Lyapunov condition holds with $\delta = 1$. Consequently, by the multivariate Lindeberg-Feller central limit theorem, we can state that

$$N^{1/2}L_N^{1/2}(\mathbf{Q}_{\mathbf{X}}^{-1}\mathbf{C}_{i,m}^N\mathbf{Q}_{\mathbf{X}}^{-1})^{-1/2}(\hat{\mathbf{X}}^{(m,*)}\mathbf{W}_{\mathbf{X}} - \tilde{\mathbf{X}}^{(m,*)})_{i,*}^\top \rightarrow \mathcal{N}(0, \mathbf{I}_d),$$

in distribution as $N \rightarrow \infty$. Note that this doesn't require that the sequence of $\mathbf{C}_i^{m,N}$ converges, just that they are eventually always invertible.

Similarly, since $\check{\mathbf{K}} = (\tilde{\mathbf{X}}^\top\tilde{\mathbf{X}})^{-1}\tilde{\mathbf{X}}^\top\bar{\mathbf{X}}$ and $\bar{\mathbf{X}}^\top\bar{\mathbf{X}} = \bar{\Sigma}$, we have

$$(\check{\mathbf{K}}\bar{\Sigma}^{-1}\check{\mathbf{R}}^{-1})^\top = \check{\mathbf{R}}^{-1}\bar{\Sigma}^{-1}\bar{\mathbf{X}}^\top\tilde{\mathbf{X}}(\tilde{\mathbf{X}}^\top\tilde{\mathbf{X}})^{-1}$$

$$\begin{aligned}
&= \check{\mathbf{R}}^{-1 \top} \bar{\Sigma}^{-1} \tilde{\mathbf{X}}^\top \tilde{\mathbf{X}} \check{\mathbf{K}}^{-1} (\tilde{\mathbf{X}}^\top \tilde{\mathbf{X}})^{-1} \\
&= \check{\mathbf{R}}^{-1 \top} \bar{\Sigma}^{-1} \bar{\Sigma} \check{\mathbf{K}}^{-1} (\tilde{\mathbf{X}}^\top \tilde{\mathbf{X}})^{-1} \\
&= \check{\mathbf{R}}^{-1 \top} \check{\mathbf{K}}^{-1} (\tilde{\mathbf{X}}^\top \tilde{\mathbf{X}})^{-1} \\
&= (\tilde{\mathbf{X}}^\top \tilde{\mathbf{X}})^{-1}.
\end{aligned}$$

In a completely analogous way, we form the following decomposition:

$$N^{1/2} M_N^{1/2} (\hat{\mathbf{Y}} \mathbf{W}_Y - \mathbf{Y})_{i,*}^\top = NM_N (\tilde{\mathbf{X}}^\top \tilde{\mathbf{X}})^{-1} \frac{1}{N^{1/2} M_N^{1/2}} \sum_{j=1}^{NM_N} (\hat{\Lambda}_{ji}^{(*, \ell)} - \bar{\Lambda}_{ji}^{(*, \ell)}) \tilde{X}_{j,*}^\top.$$

Define the summand

$$B_{ji}^m = (\hat{\Lambda}_{ji}^{(*, \ell)} - \bar{\Lambda}_{ji}^{(*, \ell)}) \tilde{X}_{j,*}^\top,$$

so that we have

$$\text{Cov}(B_{ji}^\ell) = (\tilde{X}_{j,*} Y_{i,*}^{(\ell, *) \top}) \tilde{X}_{j,*}^\top \tilde{X}_{j,*}.$$

If we define the matrices $\mathbf{D}_{i,\ell}^N$ to be

$$\mathbf{D}_{i,\ell}^N = \frac{1}{NM_N} \sum_{j=1}^{NM_N} \text{Cov}(B_{ji}^\ell),$$

which is again eventually always invertible by Assumption 3, we can use an analogous argument to the above to obtain that

$$N^{1/2} M_N^{1/2} (\mathbf{Q}_Y^{-1} \mathbf{D}_{i,\ell}^N \mathbf{Q}_Y^{-1})^{-1/2} (\hat{\mathbf{Y}}^{(m,*)} \mathbf{W}_Y - \tilde{\mathbf{Y}}^{(m,*)})_{i,*}^\top \rightarrow \mathcal{N}(0, \mathbf{I}_d),$$

in distribution as $N \rightarrow \infty$.

E Proofs of key propositions

E.1 Proof of Proposition 1

Write $\mathbf{A}_{NM_N} = \tilde{\mathbf{X}}^\top \tilde{\mathbf{X}} / NM_N$, then entrywise convergence tells us

$$\|\mathbf{A}_{NM_N} - \mathbf{Q}_X\|_F^2 = \sum_{k,\ell=1}^d (A_{NM_N,k\ell} - Q_{X,k\ell})^2 \rightarrow 0,$$

and so $\|\mathbf{A}_{NM_N} - \mathbf{Q}_X\| \leq \|\mathbf{A}_{NM_N} - \mathbf{Q}_X\|_F \rightarrow 0$. Weyl's inequality then says

$$|\lambda_i(\mathbf{A}_{NM_N}) - \lambda_i(\mathbf{Q}_X)| \leq \|\mathbf{A}_{NM_N} - \mathbf{Q}_X\| \rightarrow 0,$$

and hence we have

$$\lambda_i(\tilde{\mathbf{X}}^\top \tilde{\mathbf{X}} / NM_N) \rightarrow \lambda_i(\mathbf{Q}_X) \Rightarrow \sigma_i(\tilde{\mathbf{X}}) / N^{1/2} M_N^{1/2} \rightarrow \lambda_i(\mathbf{Q}_X)^{1/2}.$$

As $\mathbf{Q}_X \succ 0$, we have $\lambda_i(\mathbf{Q}_X) \in (0, \infty)$ and so $\sigma_i(\tilde{\mathbf{X}}) = \Theta(N^{1/2} M_N^{1/2})$ for each $i \leq d$. Clearly, since $\tilde{\mathbf{X}}$ has only d columns, $\sigma_{d+1}(\tilde{\mathbf{X}}) = 0$. For the condition number, we can say

$$\kappa(\tilde{\mathbf{X}}) = \frac{\sigma_1(\tilde{\mathbf{X}})}{\sigma_d(\tilde{\mathbf{X}})} \rightarrow \frac{\lambda_1(\mathbf{Q}_X)^{1/2}}{\lambda_d(\mathbf{Q}_X)^{1/2}} = \mathcal{O}(1).$$

The incoherence parameter can be argued by considering the skinny SVD $\tilde{\mathbf{X}} = \tilde{\mathbf{U}} \tilde{\Sigma} \tilde{\mathbf{V}}^\top$ and that this says $\tilde{\mathbf{U}} = \tilde{\mathbf{X}} \tilde{\mathbf{V}} \tilde{\Sigma}^{-1}$. We then have

$$\|\tilde{\mathbf{U}}\|_{2,\infty} \leq \|\tilde{\mathbf{X}}\|_{2,\infty} \|\tilde{\Sigma}^{-1}\| \leq \mathcal{O}(1) \times N^{-1/2} M_N^{-1/2} \lambda_d(\mathbf{Q}_X),$$

in the limit. The result follows. The same argument holds for \mathbf{Y} .

E.2 Proof of Proposition 2

For any $\theta \in \mathbb{R}$, Markov's inequality gives

$$\mathbb{P}(X \geq k) \leq \frac{\mathbb{E}\{\exp(\theta X)\}}{\exp(\theta k)} = \exp(\lambda \exp(\theta) - \lambda - \theta k),$$

where in the final equality we use the moment generating function of a Poisson random variable. Setting $\theta = 1$ and $k = \beta_\rho \log(n)$, for some $\beta_\rho \in \mathbb{R}$ and $n \in \mathbb{N}$, we see

$$\mathbb{P}(X \geq \beta_\rho \log(n)) \leq n^{-\beta_\rho} \exp(\lambda(e-1)).$$

As λ is does not change with n , if we pick $\beta_\rho = \rho + \lambda(e-1)$ then some algebra yields

$$\mathbb{P}(X < \beta_\rho \log(n)) > 1 - n^{-\rho},$$

as was required.

E.3 Proof of Proposition 3

Define the set $\mathcal{X}^{N,M_N,L_N} = [NM_N] \times [NL_N]$. Let \mathbf{A}_{ij} be the $NM_N \times NL_N$ matrix with entry (i, j) taking the value $A_{ij,ij} = \hat{\Lambda}_{ij} - \bar{\Lambda}_{ij}$ and 0 in all other entries. Clearly $\mathbb{E}\{A_{ij,rs}\} = 0$ for all entries (r, s) . In this proof, we make explicit the upgrade from overwhelming probability to almost surely. We can argue that the events $\{\forall (i, j) \in \mathcal{X}^{N,M_N,L_N}, \hat{\Lambda}_{ij} < M_N \log(N)\}$ occur almost surely as $N \rightarrow \infty$ through a union bound and by invoking the Borel-Cantelli Lemma. Each $\hat{\lambda}_{\ell ij}^m / M_N \sim \text{Poisson}(\bar{\lambda}_{\ell ij}^m / M_N)$, and by Assumption 1.i, we have $\bar{\lambda}_{\ell ij}^m = \mathcal{O}(1)$ which implies that there exists a $\lambda_{\max} > 0$ such that $\bar{\lambda}_{\ell ij}^m \leq \lambda_{\max}$ eventually as $N \rightarrow \infty$. Proposition 2 then tells us that

$$\mathbb{P}\left(\hat{\lambda}_{\ell ij} < (\rho M_N + (e-1)\lambda_{\max}) \log(N)\right) > 1 - N^{-\rho},$$

for any $\rho > 0$. We then have

$$\begin{aligned} & \mathbb{P}\left(\bigcup_{(i,j) \in \mathcal{X}^{N,M_N,L_N}} \left\{ \hat{\Lambda}_{ij} \geq (\rho M_N + (e-1)\lambda_{\max}) \log(N) \right\}\right) \\ & \leq \sum_{(i,j) \in \mathcal{X}^{N,M_N,L_N}} \mathbb{P}\left(\hat{\Lambda}_{ij} \geq (\rho M_N + (e-1)\lambda_{\max}) \log(N)\right) \\ & \leq N^{2-\rho} M_N L_N. \end{aligned}$$

For a large enough choice of ρ , we have $\sum_{N \geq 1} N^{2-\rho} < \infty$, and so Borel-Cantelli says

$$\mathbb{P}\left(\left\{ \exists (i, j) \in \mathcal{X}^{N,M_N,L_N} : \hat{\Lambda}_{ij} \geq M_N \log(N) \right\} \text{ infinitely often}\right) = 0.$$

It follows that for large enough N , the event that every entry of $\hat{\Lambda}$ is bounded by $M \log(N)$ occurs almost surely. Furthermore, by Assumption 1.i, we have that $\bar{\Lambda}_{ij} = \mathcal{O}(1)$. Using the simple bound

$$\|\mathbf{A}_{ij}\| = |\hat{\Lambda}_{ij} - \bar{\Lambda}_{ij}| \leq |\hat{\Lambda}_{ij}| + |\bar{\Lambda}_{ij}|,$$

we combine these results to obtain that for large enough N , for all $(i, j) \in \mathcal{X}^{N,M_N,L_N}$, the event $\|\mathbf{A}_{ij}\| < M_N \log(N)$ occurs almost surely. We can now apply Bernstein's theorem as stated in Theorem 4 to $\mathbf{A} = \sum_{(i,j) \in \mathcal{X}^{N,M_N,L_N}} \mathbf{A}_{ij}$. To apply Bernstein, we need to first bound $v(\mathbf{A})$. To do so, we note that

$$(\mathbf{A}_{ij} \mathbf{A}_{ij}^\top)_{rs} = \sum_{k \in [NL]} A_{ij,rk} A_{ij,sk} = \begin{cases} \left(\hat{\Lambda}_{ij} - \bar{\Lambda}_{ij}\right)^2, & (r, s) = (i, i), \\ 0, & (r, s) \neq (i, i). \end{cases}$$

We then have

$$\sum_{(i,j) \in \mathcal{X}^{M_N, L_N}} \mathbf{A}_{ij} \mathbf{A}_{ij}^\top = \text{diag} \left(\sum_{k \in [NL_N]} \left(\hat{\Lambda}_{1k} - \bar{\Lambda}_{1k} \right)^2, \dots, \sum_{k \in [NL_N]} \left(\hat{\Lambda}_{(NM_N)k} - \bar{\Lambda}_{(NM_N)k} \right)^2 \right),$$

where the notation $B_{(ab)c}$ is to be read as the (ab, c) -th entry of \mathbf{B} . By Popoviciu's inequality, we have $\text{Var} \left\{ \hat{\Lambda}_{ij} \right\} \leq M_N^2 \log^2(N)$ for each $(i, j) \in \mathcal{X}^{N, M_N, L_N}$ almost surely. As we have a diagonal matrix, after expectations and invoking Popoviciu's inequality, it follows

$$\left\| \mathbb{E} \left\{ \sum_{(i,j) \in \mathcal{X}^{N, M_N, L_N}} \mathbf{A}_{ij} \mathbf{A}_{ij}^\top \right\} \right\| \leq NL_N M_N^2 \log^2(N),$$

almost surely. An analogous argument yields

$$\left\| \mathbb{E} \left\{ \sum_{(i,j) \in \mathcal{X}^{N, M_N, L_N}} \mathbf{A}_{ij}^\top \mathbf{A}_{ij} \right\} \right\| \leq NM_N^3 \log^2(N),$$

almost surely. Substituting into Theorem 4, we have that $t \geq 0$:

$$\mathbb{P} \left(\|\hat{\Lambda} - \bar{\Lambda}\| \geq t \right) \leq N(M_N + L_N) \exp \left\{ - \frac{3t^2}{6 \max\{M_N, L_N\} NM_N^2 \log^2(N) + 2M_N t \log(N)} \right\},$$

almost surely. For sufficiently large N , the numerator in the exponential dominates if we select t to be $t = \rho \max\{M_N, L_N\}^{1/2} M_N N^{1/2} \log^{3/2}(N)$. From which it follows that

$$\|\hat{\Lambda} - \bar{\Lambda}\| = \mathcal{O} \left(\max\{M_N, L_N\}^{1/2} M_N N^{1/2} \log^{3/2}(N) \right),$$

with overwhelming probability, and thus eventually almost surely as $N \rightarrow \infty$, as was required.

E.4 Proof of Proposition 4

By Corollary 7.3.5 of [Horn and Johnson \(2012\)](#), for any two matrices \mathbf{A} and \mathbf{B} of the same size, we have

$$\sigma_i(\mathbf{B}) - \|\mathbf{A} - \mathbf{B}\| \leq \sigma_i(\mathbf{A}) \leq \sigma_i(\mathbf{B}) + \|\mathbf{A} - \mathbf{B}\|.$$

Applying this result with $\mathbf{A} = \hat{\Lambda}$ and $\mathbf{B} = \bar{\Lambda}$, applying Proposition 1 and noting that $\sigma_{d+1}(\bar{\Lambda}) = 0$ yields the desired rates.

E.5 Proof of Proposition 5

We can write

$$\left(\bar{\mathbf{U}}^\top (\hat{\Lambda} - \bar{\Lambda}) \bar{\mathbf{V}} \right)_{rs} = \sum_{p=1}^{NM_N} \sum_{q=1}^{NL_N} \bar{U}_{rp}^\top (\hat{\Lambda} - \bar{\Lambda})_{pq} \bar{V}_{qs} = \sum_{p=1}^{NM_N} \sum_{q=1}^{NL_N} \bar{U}_{pr} \bar{V}_{sq} (\hat{\Lambda} - \bar{\Lambda})_{pq},$$

which is the sum of independent random variables with expectation 0 and which are almost surely bounded in magnitude by $|\bar{U}_{pr} \bar{V}_{sq}| M_N \log(N)$ by the argument presented in Proposition 3. Hoeffding's inequality then says

$$\begin{aligned} \mathbb{P} \left(\left| \left(\bar{\mathbf{U}}^\top (\hat{\Lambda} - \bar{\Lambda}) \bar{\mathbf{V}} \right)_{rs} \right| \geq t \right) &\leq \\ 2 \exp \left(- \frac{2t^2}{\sum_{p=1}^{NM_N} \sum_{q=1}^{NL_N} |\bar{U}_{pr} \bar{V}_{sq}|^2 M_N^2 \log^2(N)} \right) &\leq 2 \exp \left(- \frac{2t^2}{M_N^2 \log^2(N)} \right), \end{aligned}$$

where the final inequality follows since $\bar{\mathbf{U}}, \bar{\mathbf{V}}$ are unitary. If we pick $t = cM_N \log^{3/2}(N)$, we obtain

$$\mathbb{P} \left(\left| \left(\bar{\mathbf{U}}^\top (\hat{\Lambda} - \bar{\Lambda}) \bar{\mathbf{V}} \right)_{rs} \right| \geq M_N \log^{3/2}(N) \right) \leq 2N^{-2c^2},$$

and since the matrix is $d \times d$, a union bound gives

$$\|\bar{\mathbf{U}}^\top (\hat{\Lambda} - \bar{\Lambda}) \bar{\mathbf{V}}\|_F = \mathcal{O} \left(M_N \log^{3/2}(N) \right),$$

almost surely.

E.6 Proof of Proposition 6

We prove the results in order:

1. Let $\sigma_1, \dots, \sigma_d$ be the singular values of $\bar{\mathbf{U}}^\top \hat{\mathbf{U}}$ and $\theta_\ell = \cos^{-1}(\sigma_\ell)$ to be the principal angles. Lemma 2.4 of [Chen et al. \(2021\)](#) tells us that the non-zero eigenvalues of $\hat{\mathbf{U}}\hat{\mathbf{U}}^\top - \bar{\mathbf{U}}\bar{\mathbf{U}}^\top$ are equal to $\sin(\theta_\ell)$. By invoking a variant of the Davis-Kahan theorem ([Yu et al., 2014](#), Theorem 4), we find that

$$\|\hat{\mathbf{U}}\hat{\mathbf{U}}^\top - \bar{\mathbf{U}}\bar{\mathbf{U}}^\top\| = \max_{\ell \in [d]} |\sin(\theta_\ell)| \leq \frac{2d^{1/2} \|\hat{\Lambda} - \bar{\Lambda}\| \left(2\sigma_1(\hat{\Lambda}) + \|\hat{\Lambda} - \bar{\Lambda}\| \right)}{\sigma_d(\bar{\Lambda})^2 - \sigma_{d+1}(\bar{\Lambda})^2},$$

for sufficiently large N . Using that $\sigma_{d+1}(\bar{\Lambda}) = 0$, and $\sigma_d(\bar{\Lambda}) = \Omega(NM_N^{1/2}L_N^{1/2})$ by [Proposition 1](#) and [Propositions 3 and 4](#), we obtain

$$\|\hat{\mathbf{U}}\hat{\mathbf{U}}^\top - \bar{\mathbf{U}}\bar{\mathbf{U}}^\top\| = \mathcal{O} \left(\max\{M_N, L_N\}^{1/2} M_N^{1/2} L_N^{-1/2} N^{-1/2} \log^{3/2}(N) \right),$$

almost surely. The second result follows analogously.

2. We use the bound from Part 1 to obtain

$$\begin{aligned} \|\hat{\mathbf{U}} - \bar{\mathbf{U}}\bar{\mathbf{U}}^\top \hat{\mathbf{U}}\|_F &= \|(\hat{\mathbf{U}}\hat{\mathbf{U}}^\top - \bar{\mathbf{U}}\bar{\mathbf{U}}^\top)\hat{\mathbf{U}}\|_F \leq \|\hat{\mathbf{U}}\hat{\mathbf{U}}^\top - \bar{\mathbf{U}}\bar{\mathbf{U}}^\top\|_F \\ &= \mathcal{O} \left(\max\{M_N, L_N\}^{1/2} M_N^{1/2} L_N^{-1/2} N^{-1/2} \log^{3/2}(N) \right), \end{aligned}$$

almost surely. The second result follows analogously.

3. Observe the following

$$\begin{aligned} \bar{\mathbf{U}}^\top \hat{\mathbf{U}}\hat{\Sigma} - \bar{\Sigma}\bar{\mathbf{V}}^\top \hat{\mathbf{V}} &= \bar{\mathbf{U}}^\top (\hat{\Lambda} - \bar{\Lambda}) \hat{\mathbf{V}} \\ &= \bar{\mathbf{U}}^\top (\hat{\Lambda} - \bar{\Lambda}) (\hat{\mathbf{V}} - \bar{\mathbf{V}}\bar{\mathbf{V}}^\top \hat{\mathbf{V}}) + \bar{\mathbf{U}}^\top (\hat{\Lambda} - \bar{\Lambda}) \bar{\mathbf{V}}\bar{\mathbf{V}}^\top \hat{\mathbf{V}}. \end{aligned}$$

Note first that $\|\bar{\mathbf{U}}^\top\|_F = \|\bar{\mathbf{U}}\|_F = d^{1/2} = \mathcal{O}(1)$, and similarly for $\|\bar{\mathbf{V}}^\top \hat{\mathbf{V}}\|_F$. [Propositions 3 and 5](#), coupled with the result of Part 2. above, then yield

$$\begin{aligned} &\|\bar{\mathbf{U}}^\top \hat{\mathbf{U}}\hat{\Sigma} - \bar{\Sigma}\bar{\mathbf{V}}^\top \hat{\mathbf{V}}\|_F \\ &\leq \|\hat{\mathbf{U}}^\top\|_F \|\hat{\Lambda} - \bar{\Lambda}\|_F \|\hat{\mathbf{V}} - \bar{\mathbf{V}}\bar{\mathbf{V}}^\top \hat{\mathbf{V}}\|_F + \|\bar{\mathbf{U}}^\top (\hat{\Lambda} - \bar{\Lambda}) \bar{\mathbf{V}}\|_F \|\bar{\mathbf{V}}^\top \hat{\mathbf{V}}\|_F \\ &= \mathcal{O} \left(\max\{M_N, L_N\} M_N^{3/2} L_N^{-1/2} \log^3(N) \right) + \mathcal{O} \left(M_N \log^{3/2}(N) \right) \\ &= \mathcal{O} \left(\max\{M_N, L_N\} M_N^{3/2} L_N^{-1/2} \log^3(N) \right), \end{aligned}$$

almost surely. The second result follows analogously.

4. Some algebra allows us to write

$$\bar{\mathbf{U}}^\top \hat{\mathbf{U}} - \bar{\mathbf{V}}^\top \hat{\mathbf{V}} = \left[\left(\bar{\mathbf{U}}^\top \hat{\mathbf{U}} \hat{\Sigma} - \bar{\Sigma} \bar{\mathbf{V}}^\top \hat{\mathbf{V}} \right) + \left(\bar{\Sigma} \bar{\mathbf{U}}^\top \hat{\mathbf{U}} - \bar{\mathbf{V}}^\top \hat{\mathbf{V}} \hat{\Sigma} \right) \right] \hat{\Sigma}^{-1} - \bar{\Sigma} (\bar{\mathbf{U}}^\top \hat{\mathbf{U}} - \bar{\mathbf{V}}^\top \hat{\mathbf{V}}) \hat{\Sigma}^{-1},$$

which yields the identity

$$\bar{\mathbf{U}}^\top \hat{\mathbf{U}} - \bar{\mathbf{V}}^\top \hat{\mathbf{V}} + \bar{\Sigma} (\bar{\mathbf{U}}^\top \hat{\mathbf{U}} - \bar{\mathbf{V}}^\top \hat{\mathbf{V}}) \hat{\Sigma}^{-1} = \left[\left(\bar{\mathbf{U}}^\top \hat{\mathbf{U}} \hat{\Sigma} - \bar{\Sigma} \bar{\mathbf{V}}^\top \hat{\mathbf{V}} \right) + \left(\bar{\Sigma} \bar{\mathbf{U}}^\top \hat{\mathbf{U}} - \bar{\mathbf{V}}^\top \hat{\mathbf{V}} \hat{\Sigma} \right) \right] \hat{\Sigma}^{-1} \quad (\text{E.1})$$

Using the definition of $\bar{\Sigma}$ and $\hat{\Sigma}$, we see that the (i, j) th entry of the left-hand side of (E.1) in absolute value is

$$\left| \left(\bar{\mathbf{U}}^\top \hat{\mathbf{U}} - \bar{\mathbf{V}}^\top \hat{\mathbf{V}} + \bar{\Sigma} (\bar{\mathbf{U}}^\top \hat{\mathbf{U}} - \bar{\mathbf{V}}^\top \hat{\mathbf{V}}) \hat{\Sigma}^{-1} \right)_{ij} \right| = \left| \left(\bar{\mathbf{U}}^\top \hat{\mathbf{U}} - \bar{\mathbf{V}}^\top \hat{\mathbf{V}} \right)_{ij} \right| \left(1 + \frac{\sigma_i(\bar{\Lambda})}{\sigma_j(\hat{\Lambda})} \right).$$

We can bound the absolute value of the right-hand side of (E.1) by the Frobenius norm of the full matrix to yield

$$\begin{aligned} \left| \left(\bar{\mathbf{U}}^\top \hat{\mathbf{U}} - \bar{\mathbf{V}}^\top \hat{\mathbf{V}} \right)_{ij} \right| \left(1 + \frac{\sigma_i(\bar{\Lambda})}{\sigma_j(\hat{\Lambda})} \right) &\leq \left(\|\bar{\mathbf{U}}^\top \hat{\mathbf{U}} \hat{\Sigma} - \bar{\Sigma} \bar{\mathbf{V}}^\top \hat{\mathbf{V}}\|_F + \|\bar{\Sigma} \bar{\mathbf{U}}^\top \hat{\mathbf{U}} - \bar{\mathbf{V}}^\top \hat{\mathbf{V}} \hat{\Sigma}\|_F \right) \|\hat{\Sigma}^{-1}\|_F \\ &= \mathcal{O} \left(\max\{M_N, L_N\} M_N L_N^{-1} N^{-1} \log^3(N) \right) \end{aligned}$$

almost surely, where we have used the result of Part 3 above and Proposition 4. Noticing that $1 + \sigma_i(\bar{\Lambda})/\sigma_j(\hat{\Lambda}) > 1$ gives the desired result.

E.7 Proof of Proposition 7

From Schönemann (1966), we have that

$$\mathbf{W} = \underset{\mathbf{W} \in \mathbb{O}(d)}{\operatorname{argmin}} \left[\|\bar{\mathbf{U}}^\top \hat{\mathbf{U}} - \mathbf{W}\|_F^2 + \|\bar{\mathbf{V}}^\top \hat{\mathbf{V}} - \mathbf{W}\|_F^2 \right]. \quad (\text{E.2})$$

Denote the SVD of $\bar{\mathbf{U}}^\top \hat{\mathbf{U}}$ by $\mathbf{W}_{U,1} \Sigma_{\mathbf{W}} \mathbf{W}_{U,2}^\top$ and define the $d \times d$ orthogonal matrix $\mathbf{W}_U = \mathbf{W}_{U,1} \mathbf{W}_{U,2}^\top$. Then, with $\sigma_1, \dots, \sigma_d$ defined as in Part 1 of Proposition 6, we have

$$\begin{aligned} \|\bar{\mathbf{U}}^\top \hat{\mathbf{U}} - \mathbf{W}_U\|_F &= \|\Sigma_{\mathbf{U}} - \mathbf{I}\|_F = \left(\sum_{i=1}^d (1 - \sigma_i)^2 \right)^{1/2} \leq \sum_{i=1}^d (1 - \sigma_i) \leq \sum_{i=1}^d (1 - \sigma_i^2) \\ &= \sum_{i=1}^d \sin^2(\theta_i) \leq d \|\hat{\mathbf{U}} \hat{\mathbf{U}}^\top - \bar{\mathbf{U}} \bar{\mathbf{U}}^\top\|^2 \\ &= \mathcal{O} \left(\max\{M_N, L_N\} M_N L_N^{-1} N^{-1} \log^3(N) \right), \end{aligned}$$

where we invoke Part 1 of Proposition 6. Combining with Part 4 of the same proposition, we find

$$\begin{aligned} \|\bar{\mathbf{V}}^\top \hat{\mathbf{V}} - \mathbf{W}_U\|_F &\leq \|\bar{\mathbf{V}}^\top \hat{\mathbf{V}} - \bar{\mathbf{U}}^\top \hat{\mathbf{U}}\|_F + \|\bar{\mathbf{U}}^\top \hat{\mathbf{U}} - \mathbf{W}_U\|_F \\ &= \mathcal{O} \left(\max\{M_N, L_N\} M_N L_N^{-1} N^{-1} \log^3(N) \right) \end{aligned}$$

Combining these results gives us

$$\begin{aligned} \|\bar{\mathbf{U}}^\top \hat{\mathbf{U}} - \mathbf{W}\|_F^2 + \|\bar{\mathbf{V}}^\top \hat{\mathbf{V}} - \mathbf{W}\|_F^2 &\leq \|\bar{\mathbf{V}}^\top \hat{\mathbf{V}} - \mathbf{W}_U\|_F^2 + \|\bar{\mathbf{U}}^\top \hat{\mathbf{U}} - \mathbf{W}_U\|_F^2 \\ &= \mathcal{O} \left(\max\{M_N, L_N\}^2 M_N^2 L_N^{-2} N^{-2} \log^6(N) \right), \end{aligned}$$

where we have used that \mathbf{W} is the minimiser of (E.2), which yields the desired bound.

E.8 Proof of Proposition 8

We address the bounds in order:

1. Observe that

$$\begin{aligned} \mathbf{W}\hat{\Sigma} - \bar{\Sigma}\mathbf{W} &= (\mathbf{W} - \bar{\mathbf{U}}^\top \hat{\mathbf{U}})\hat{\Sigma} + \bar{\mathbf{U}}^\top \hat{\mathbf{U}}\hat{\Sigma} - \bar{\Sigma}\mathbf{W} \\ &= (\mathbf{W} - \bar{\mathbf{U}}^\top \hat{\mathbf{U}})\hat{\Sigma} + (\bar{\mathbf{U}}^\top \hat{\mathbf{U}}\hat{\Sigma} - \bar{\Sigma}\hat{\mathbf{V}}^\top \hat{\mathbf{V}}) + \bar{\Sigma}(\hat{\mathbf{V}}^\top \hat{\mathbf{V}} - \mathbf{W}). \end{aligned}$$

Combining Propositions 7, 4 and 1 says that

$$\|(\mathbf{W} - \bar{\mathbf{U}}^\top \hat{\mathbf{U}})\hat{\Sigma}\|_F, \|\bar{\Sigma}(\hat{\mathbf{V}}^\top \hat{\mathbf{V}} - \mathbf{W})\|_F = \mathcal{O}\left(\max\{M_N, L_N\}M_N^{3/2}L_N^{-1/2}\log^3(N)\right),$$

and that

$$\|\bar{\mathbf{U}}^\top \hat{\mathbf{U}}\hat{\Sigma} - \bar{\Sigma}\hat{\mathbf{V}}^\top \hat{\mathbf{V}}\|_F = \mathcal{O}\left(\max\{M_N, L_N\}M_N^{3/2}L_N^{-1/2}\log^3(N)\right),$$

from which the result follows.

2. We prove this by bounding the absolute value of the (i, j) -th entry. We see

$$\begin{aligned} \left(\mathbf{W}\hat{\Sigma}^{1/2} - \bar{\Sigma}^{1/2}\mathbf{W}\right)_{ij} &= W_{ij} \left[\sigma_i(\hat{\Sigma})^{1/2} - \sigma_j(\bar{\Sigma})^{1/2}\right] \\ &= \frac{W_{ij} \left[\sigma_i(\hat{\Sigma}) - \sigma_j(\bar{\Sigma})\right]}{\sigma_i(\hat{\Sigma})^{1/2} + \sigma_j(\bar{\Sigma})^{1/2}} \\ &= \frac{\left(\mathbf{W}\hat{\Sigma} - \bar{\Sigma}\mathbf{W}\right)_{ij}}{\sigma_i(\hat{\Sigma})^{1/2} + \sigma_j(\bar{\Sigma})^{1/2}}. \end{aligned}$$

Using the result from Part 1, and Propositions 1 and 4, we see

$$\left|\left(\mathbf{W}\hat{\Sigma}^{1/2} - \bar{\Sigma}^{1/2}\mathbf{W}\right)_{ij}\right| \leq \frac{\left|\left(\mathbf{W}\hat{\Sigma} - \bar{\Sigma}\mathbf{W}\right)_{ij}\right|}{\sigma_d(\bar{\Sigma})^{1/2}} = \mathcal{O}\left(\max\{M_N, L_N\}M_N^{5/4}L_N^{-3/4}N^{-1/2}\log^3(N)\right).$$

The result follows from summing over the d^2 elements of the matrix.

3. Following the same approach, we get

$$\left(\mathbf{W}\hat{\Sigma}^{-1/2} - \bar{\Sigma}^{-1/2}\mathbf{W}\right)_{ij} = \frac{W_{ij} \left(\sigma_i(\bar{\Lambda})^{1/2} - \sigma_j(\hat{\Lambda})^{1/2}\right)}{\sigma_i(\bar{\Lambda})^{1/2}\sigma_j(\hat{\Lambda})^{1/2}} = \frac{\left(\mathbf{W}\hat{\Sigma}^{1/2} - \bar{\Sigma}^{1/2}\mathbf{W}\right)_{ij}}{\sigma_i(\bar{\Lambda})^{1/2}\sigma_j(\hat{\Lambda})^{1/2}}.$$

Taking the Frobenius norm and using the bounds from Part 2 and Propositions 1 and 4, we obtain

$$\|\mathbf{W}\hat{\Sigma}^{-1/2} - \bar{\Sigma}^{-1/2}\mathbf{W}\|_F = \mathcal{O}\left(\max\{M_N, L_N\}M_N^{3/4}L_N^{-5/4}N^{-3/2}\log^3(N)\right).$$

E.9 Proof of Proposition 9

Define $\Pi_{\tilde{\mathbf{X}}} = (\tilde{\mathbf{X}}^\top \tilde{\mathbf{X}})^{1/2}$ and $\Pi_{\mathbf{Y}} = (\mathbf{Y}^\top \mathbf{Y})^{1/2}$. Note that

$$(\bar{\mathbf{X}}\bar{\Sigma}^{1/2})^\top (\bar{\mathbf{X}}\bar{\Sigma}^{1/2}) = \bar{\mathbf{U}}\bar{\Sigma}^2\bar{\mathbf{U}}^\top = \bar{\Lambda}\bar{\Lambda}^\top = \tilde{\mathbf{X}}\mathbf{Y}^\top \mathbf{Y}\tilde{\mathbf{X}}^\top = (\tilde{\mathbf{X}}\Pi_{\mathbf{Y}})^\top (\tilde{\mathbf{X}}\Pi_{\mathbf{Y}}).$$

This implies the existence of some orthogonal matrix $\mathbf{Q} \in \mathbb{O}(d)$ such that

$$\bar{\mathbf{X}}\bar{\Sigma}^{1/2} = \tilde{\mathbf{X}}\Pi_{\mathbf{Y}}\mathbf{Q},$$

then $\check{\mathbf{K}} := \mathbf{\Pi}_Y \mathbf{Q} \bar{\Sigma}^{-1/2} \in \text{GL}(d)$ satisfies the required definition. Similarly, we write

$$\left(\bar{\mathbf{Y}} \bar{\Sigma}^{1/2}\right) \left(\bar{\mathbf{Y}} \bar{\Sigma}^{1/2}\right)^\top = \bar{\mathbf{V}} \bar{\Sigma}^2 \bar{\mathbf{V}} = \bar{\Lambda} \bar{\Lambda}^\top = \mathbf{Y} \tilde{\mathbf{X}}^\top \tilde{\mathbf{X}} \mathbf{Y}^\top = (\mathbf{Y} \mathbf{\Pi}_{\tilde{\mathbf{X}}}) (\mathbf{Y} \mathbf{\Pi}_{\tilde{\mathbf{X}}})^\top.$$

In turn, this implies the existence of $\mathbf{Q}^* \in \mathbb{O}(d)$ such that

$$\bar{\mathbf{Y}} \bar{\Sigma}^{1/2} = \mathbf{Y} \mathbf{\Pi}_{\tilde{\mathbf{X}}} \mathbf{Q}^*,$$

and so $\check{\mathbf{R}} := \mathbf{\Pi}_{\tilde{\mathbf{X}}} \mathbf{Q}^* \bar{\Sigma}^{-1/2} \in \text{GL}(d)$ is the matrix required. Further note

$$\tilde{\mathbf{X}} \check{\mathbf{K}} \check{\mathbf{R}}^\top \mathbf{Y}^\top = \tilde{\mathbf{X}} \bar{\mathbf{Y}}^\top = \bar{\Lambda} = \tilde{\mathbf{X}} \mathbf{Y}^\top.$$

Multiplying on the left by $(\tilde{\mathbf{X}}^\top \tilde{\mathbf{X}})^{-1} \tilde{\mathbf{X}}^\top$ and on the right by $\mathbf{Y} (\mathbf{Y}^\top \mathbf{Y})^{-1}$ yields $\check{\mathbf{L}} \check{\mathbf{R}}^\top = \mathbf{I}_d$.

E.10 Proof of Proposition 10

We will show the result for $\hat{\mathbf{U}}^{(i)}$, with the other results being shown in an analogous manner. Note that for a matrix \mathbf{A} with orthonormal columns, we can write

$$\|\mathbf{A} \mathbf{A}^\top e_i\|^2 = e_i^\top \mathbf{A}^\top \mathbf{A} \mathbf{A} \mathbf{A}^\top e_i = e_i^\top \mathbf{A} \mathbf{A}^\top e_i = (\mathbf{A} \mathbf{A}^\top)_{ii} = \|A_{i,*}\|^2.$$

We can use this identity along with Wedin's Theorem, as stated in Theorem 3, say

$$\begin{aligned} \|\hat{\mathbf{U}}_{i,*}^{(i)}\| &= \|(\hat{\mathbf{U}}^{(i)} \hat{\mathbf{U}}^{(i)\top}) e_i\| \leq \|(\hat{\mathbf{U}}^{(i)} \hat{\mathbf{U}}^{(i)\top} - \bar{\mathbf{U}} \bar{\mathbf{U}}^\top) e_i\| + \|\bar{\mathbf{U}}_{i,*}\| \\ &\leq \|\hat{\mathbf{U}}^{(i)} \hat{\mathbf{U}}^{(i)\top} - \bar{\mathbf{U}} \bar{\mathbf{U}}^\top\| + \|\bar{\mathbf{U}}_{i,*}\| \\ &\leq \frac{\max \left\{ \|(\hat{\Lambda}^{(i)} - \bar{\Lambda})^\top \bar{\mathbf{U}}\|, \|(\hat{\Lambda}^{(i)} - \bar{\Lambda}) \bar{\mathbf{V}}\| \right\}}{\sigma_d(\bar{\Lambda}) - \sigma_{d+1}(\bar{\Lambda}) - \|\hat{\Lambda}^{(i)} - \bar{\Lambda}\|} + \|\bar{\mathbf{U}}_{i,*}\|. \end{aligned}$$

We look to bound the growth of the first term. Define the row-deletion operator $\mathbf{P}^{(i)} := \mathbf{I} - e_i e_i^\top$, which is symmetric and idempotent. We can then write

$$\hat{\Lambda}^{(i)} - \bar{\Lambda} = \mathbf{P}^{(i)} (\hat{\Lambda} - \bar{\Lambda}),$$

and so we can bound each of the terms in the numerator as

$$\|(\hat{\Lambda}^{(i)} - \bar{\Lambda})^\top \bar{\mathbf{U}}\| = \|(\hat{\Lambda} - \bar{\Lambda})^\top \mathbf{P}^{(i)} \bar{\mathbf{U}}\| \leq \|\hat{\Lambda} - \bar{\Lambda}\|,$$

and

$$\|(\hat{\Lambda}^{(i)} - \bar{\Lambda})^\top \bar{\mathbf{V}}\| = \|\mathbf{P}^{(i)} (\hat{\Lambda} - \bar{\Lambda}) \bar{\mathbf{V}}\| \leq \|\hat{\Lambda} - \bar{\Lambda}\|,$$

both of which are $\mathcal{O}\left(\max\{M_N, L_N\}^{1/2} M_N N^{1/2} \log^{3/2}(N)\right)$ by Proposition 3. The denominator, by our assumption on the singular values of $\bar{\Lambda}$ and Proposition 3, is $\mathcal{O}\left(M_N^{1/2} L_N^{1/2} N\right)$, and so it follows

$$\|\hat{\mathbf{U}}_{i,*}^{(i)}\| \leq \mathcal{O}\left(\max\{M_N, L_N\}^{1/2} M_N^{1/2} L_N^{-1/2} N^{-1/2} \log^{3/2}(N)\right) + \|\bar{\mathbf{U}}_{i,*}\|.$$

By Proposition 1, we know $\mu(\bar{\Lambda}) = \mathcal{O}(1)$, and so we can bound $\|\bar{\mathbf{U}}_{i,*}\| = \mathcal{O}(M_N^{-1/2} N^{-1/2})$. The result follows.

E.11 Proof of Proposition 11

Recall the definitions $\check{\mathbf{K}} = \Pi_{\mathbf{Y}} \mathbf{Q} \bar{\Sigma}^{-1/2}$ and $\check{\mathbf{R}} = \Pi_{\tilde{\mathbf{X}}} \mathbf{Q}^* \bar{\Sigma}^{-1/2}$. By Proposition 1, we have

$$\|\bar{\Sigma}^{1/2}\| = \mathcal{O}\left(M_N^{1/4} L_N^{1/4} N^{1/2}\right), \quad \|\bar{\Sigma}^{-1/2}\| = \mathcal{O}\left(N^{-1/2} M_N^{-1/4} L_N^{-1/4}\right),$$

Since the entries of $\tilde{\mathbf{X}}$ and \mathbf{Y} are bounded by Assumption 1.i and $\Pi_{\tilde{\mathbf{X}}}$ and $\Pi_{\mathbf{Y}}$ have the same singular values as $\tilde{\mathbf{X}}$ and \mathbf{Y} , respectively, we see

$$\|\Pi_{\tilde{\mathbf{X}}}\| = \mathcal{O}\left(N^{1/2} M_N^{1/2}\right), \quad \|\Pi_{\mathbf{Y}}\| = \mathcal{O}\left(N^{1/2} L_N^{1/2}\right),$$

By the rank d assumption of $\tilde{\mathbf{X}}$ and \mathbf{Y} paired with Proposition 1, we have

$$\|\Pi_{\tilde{\mathbf{X}}}^{-1}\| = \mathcal{O}\left(M_N^{-1/2} N^{-1/2}\right), \quad \|\Pi_{\mathbf{Y}}^{-1}\| = \mathcal{O}\left(L_N^{-1/2} N^{-1/2}\right).$$

It follows that

$$\begin{aligned} \|\check{\mathbf{K}}\| &\leq \|\Pi_{\mathbf{Y}}\| \|\mathbf{Q}\| \|\bar{\Sigma}^{-1/2}\| = \mathcal{O}\left(M_N^{-1/4} L_N^{1/4}\right), \quad \|\check{\mathbf{K}}^{-1}\| \leq \|\bar{\Sigma}^{1/2}\| \|\mathbf{Q}^{-1}\| \|\Pi_{\mathbf{Y}}^{-1}\| = \mathcal{O}\left(M_N^{1/4} L_N^{-1/4}\right) \\ \|\check{\mathbf{R}}\| &\leq \|\Pi_{\tilde{\mathbf{X}}}\| \|\mathbf{Q}^*\| \|\bar{\Sigma}^{-1/2}\| = \mathcal{O}\left(M_N^{1/4} L_N^{-1/4}\right), \quad \|\check{\mathbf{R}}^{-1}\| \leq \|\bar{\Sigma}^{1/2}\| \|\mathbf{Q}^{*-1}\| \|\Pi_{\tilde{\mathbf{X}}}^{-1}\| = \mathcal{O}\left(M_N^{-1/4} L_N^{1/4}\right). \end{aligned}$$

E.12 Proof of Proposition 12

We will prove the results for $\mathbf{R}_{1,\ell}$, for $\ell = 1, 2, 3, 4$, with $\mathbf{R}_{2,\ell}$ following analogously unless otherwise stated.

1. By Proposition 1, we have $\mathcal{O}(1)$ growth of the incoherence of $\bar{\Lambda}$, and so $\|\bar{\mathbf{U}}\|_{2,\infty} = \mathcal{O}\left(M_N^{-1/2} N^{-1/2}\right)$. It follows that

$$\begin{aligned} \|\mathbf{R}_{1,1}\|_{2,\infty} &\leq \|\bar{\mathbf{U}}\|_{2,\infty} \|\bar{\mathbf{U}}^\top \hat{\mathbf{U}} \hat{\Sigma}^{1/2} - \bar{\Sigma}^{1/2} \mathbf{W}\| \\ &\leq \|\bar{\mathbf{U}}\|_{2,\infty} \left(\|(\bar{\mathbf{U}}^\top \hat{\mathbf{U}} - \mathbf{W}) \hat{\Sigma}^{1/2}\|_F + \|\mathbf{W} \hat{\Sigma}^{1/2} - \bar{\Sigma}^{1/2} \mathbf{W}\|_F \right). \end{aligned}$$

Using Propositions 4 and 7 for the first term and Proposition 8 for the second, we obtain the desired bound.

2. Define $\mathbf{M}_1 = \bar{\mathbf{U}} \bar{\mathbf{U}}^\top (\hat{\Lambda} - \bar{\Lambda})(\hat{\mathbf{V}} - \bar{\mathbf{V}} \mathbf{W}) \hat{\Sigma}^{-1/2}$ and $\mathbf{M}_2 = (\hat{\Lambda} - \bar{\Lambda})(\hat{\mathbf{V}} - \bar{\mathbf{V}} \mathbf{W}) \hat{\Sigma}^{-1/2}$ so that $\mathbf{R}_{1,2} = \mathbf{M}_2 - \mathbf{M}_1$ and we can bound $\|\mathbf{R}_{1,2}\|_{2,\infty} \leq \|\mathbf{M}_1\|_{2,\infty} + \|\mathbf{M}_2\|_{2,\infty}$.

Bound on \mathbf{M}_1 :

For the first norm, we split as:

$$\begin{aligned} \|\mathbf{M}_1\|_{2,\infty} &\leq \|\bar{\mathbf{U}}\|_{2,\infty} \|\hat{\Lambda} - \bar{\Lambda}\| \|\hat{\mathbf{V}} - \bar{\mathbf{V}} \mathbf{W}\| \|\hat{\Sigma}^{-1/2}\| \\ &\leq \|\hat{\mathbf{V}} - \bar{\mathbf{V}} \mathbf{W}\| \mathcal{O}\left(\max\{M_N, L_N\}^{1/2} M_N^{1/4} L_N^{-1/4} N^{-1/2} \log^{3/2}(N)\right), \end{aligned}$$

where we have used the bound on $\|\bar{\mathbf{U}}\|_{2,\infty}$ and Propositions 3 and 4. We then observe that by Propositions 6 and 7 we have

$$\begin{aligned} \|\hat{\mathbf{V}} - \bar{\mathbf{V}} \mathbf{W}\| &\leq \|\hat{\mathbf{V}} - \bar{\mathbf{V}} \bar{\mathbf{V}}^\top \hat{\mathbf{V}}\| + \|\bar{\mathbf{V}}(\bar{\mathbf{V}}^\top \hat{\mathbf{V}} - \mathbf{W})\| \\ &= \mathcal{O}\left(\max\{M_N, L_N\}^{1/2} M_N^{1/2} L_N^{-1/2} N^{-1/2} \log^{3/2}(N)\right) \\ &\quad + \mathcal{O}\left(\max\{M_N, L_N\} M_N L_N^{-1} N^{-1} \log^3(N)\right) \\ &= \mathcal{O}\left(\max\{M_N, L_N\}^{1/2} M_N^{1/2} L_N^{-1/2} N^{-1/2} \log^{3/2}(N)\right) \end{aligned}$$

Combining gives

$$\|\mathbf{M}_1\|_{2,\infty} = \mathcal{O} \left(\max\{M_N, L_N\} M_N^{3/4} L_N^{-3/4} N^{-1} \log^3(N) \right), \quad (\text{E.3})$$

almost surely.

Bound on \mathbf{M}_2 :

Note that we can write

$$\mathbf{M}_2 = \underbrace{(\hat{\Lambda} - \bar{\Lambda})(\mathbf{I} - \bar{\mathbf{V}}\bar{\mathbf{V}}^\top)\hat{\mathbf{V}}\hat{\Sigma}^{-1/2}}_{\mathbf{T}_1} + \underbrace{(\hat{\Lambda} - \bar{\Lambda})\bar{\mathbf{V}}(\bar{\mathbf{V}}^\top\hat{\mathbf{V}} - \mathbf{W})\hat{\Sigma}^{-1/2}}_{\mathbf{T}_2}.$$

We bound $\|\mathbf{T}_2\|_{2,\infty}$ using Propositions 3, 4 and 7 and that $\|\mathbf{T}_2\|_{2,\infty} \leq \|\mathbf{T}_2\|$:

$$\begin{aligned} \|\mathbf{T}_2\|_{2,\infty} &\leq \|\hat{\Lambda} - \bar{\Lambda}\| \|\bar{\mathbf{V}}\| \|(\bar{\mathbf{V}}^\top\hat{\mathbf{V}} - \mathbf{W})\| \|\hat{\Sigma}^{-1/2}\| \\ &= \mathcal{O} \left(\max\{M_N, L_N\}^{3/2} M_N^{7/4} L_N^{-5/4} N^{-1} \log^{9/2}(N) \right). \end{aligned}$$

For \mathbf{T}_1 , first note that we can write

$$\|\mathbf{T}_1\|_{2,\infty} \leq \underbrace{\|(\hat{\Lambda} - \bar{\Lambda})(\mathbf{I} - \bar{\mathbf{V}}\bar{\mathbf{V}}^\top)\hat{\mathbf{V}}\hat{\mathbf{V}}^\top\|_{2,\infty}}_{\mathbf{T}_3} \underbrace{\|\hat{\mathbf{V}}\hat{\Sigma}^{-1/2}\|}_{\mathbf{T}_4}. \quad (\text{E.4})$$

We have

$$\|\mathbf{T}_4\| \leq \|\hat{\mathbf{V}}\| \|\hat{\Sigma}^{-1/2}\| = \mathcal{O} \left(M_N^{-1/4} L_N^{-1/4} N^{-1/2} \right), \quad (\text{E.5})$$

and so it remains only to bound the norm of \mathbf{T}_3 . Define $\bar{\mathbf{P}} = \bar{\mathbf{V}}\bar{\mathbf{V}}^\top$, $\hat{\mathbf{P}} = \hat{\mathbf{V}}\hat{\mathbf{V}}^\top$ and $\mathbf{E} = \hat{\Lambda} - \bar{\Lambda}$, so that $\mathbf{T}_3 = \mathbf{E}(\mathbf{I} - \bar{\mathbf{P}})\hat{\mathbf{P}}$. We look to obtain a bound on

$$\|\mathbf{T}_3\|_{2,\infty} = \max_{i \in [NM]} \|e_i^\top \mathbf{T}_3\|,$$

where e_i is the i -th standard basis vector. There is a dependence between $\hat{\mathbf{P}}$ and \mathbf{E} that prevents the application of standard concentration inequalities. To circumvent this, we proceed using a leave-one-out argument. For each $i \in [NM_N]$, define a matrix $\hat{\Lambda}^{(i)}$ as

$$\hat{\Lambda}_{jk}^{(i)} = \begin{cases} \hat{\Lambda}_{jk}, & j \neq i, \\ \bar{\Lambda}_{jk} & j = i \end{cases}.$$

Then $\hat{\Lambda}^{(i)}$ is $\hat{\Lambda}$ with its i -th row replaced with its expectation. That is to say, $\hat{\Lambda}^{(i)}$ is $\hat{\Lambda}$ but with the randomness removed from the i -th row. In this way, we can write $\hat{\Lambda} = \hat{\Lambda}^{(i)} + \mathbf{E}^{(i)}$, where

$$E_{pq}^{(i)} = \begin{cases} \hat{\Lambda}_{pq} - \bar{\Lambda}_{pq}, & p \neq i, \\ 0, & p = i. \end{cases}$$

We compute the singular value decomposition of this de-noised matrix $\hat{\Lambda}^{(i)}$ as

$$\hat{\Lambda}^{(i)} = \hat{\mathbf{U}}^{(i)} \hat{\Sigma}^{(i)} \hat{\mathbf{V}}^{(i)\top} + \hat{\mathbf{U}}_\perp^{(i)} \hat{\Sigma}_\perp^{(i)} \hat{\mathbf{V}}_\perp^{(i)\top},$$

and define $\hat{\mathbf{P}}^{(i)} = \hat{\mathbf{V}}^{(i)} \hat{\mathbf{V}}^{(i)\top}$. It is important to note that this construction ensures that $\hat{\Lambda}^{(i)}$, and therefore $\hat{\mathbf{P}}^{(i)}$, is independent of the i -th row of \mathbf{E} .

Recall that we are trying to bound each $\|e_i^\top \mathbf{T}_3\|$. With these new definitions, for a given $i \in [NM_N]$, we consider a decomposition of the row norm as

$$\|e_i^\top \mathbf{T}_3\| \leq \underbrace{\|e_i^\top \mathbf{E}(\mathbf{I} - \bar{\mathbf{P}})\hat{\mathbf{P}}^{(i)}\|}_{\mathbf{T}_5} + \underbrace{\|e_i^\top \mathbf{E}(\mathbf{I} - \bar{\mathbf{P}})(\hat{\mathbf{P}} - \hat{\mathbf{P}}^{(i)})\|}_{\mathbf{T}_6}.$$

We start by bounding $\|T_6\|$. To do so, we note

$$\|T_6\| \leq \|e_i^\top \mathbf{E}\| \|\mathbf{I} - \bar{\mathbf{P}}\| \|\hat{\mathbf{P}} - \hat{\mathbf{P}}^{(i)}\| = \|e_i^\top \mathbf{E}\| \|\hat{\mathbf{P}} - \hat{\mathbf{P}}^{(i)}\|. \quad (\text{E.6})$$

Wedin's Theorem, as stated in Theorem 3, tells us

$$\begin{aligned} \|\hat{\mathbf{P}} - \hat{\mathbf{P}}^{(i)}\| &= \|\hat{\mathbf{V}}\hat{\mathbf{V}}^\top - \hat{\mathbf{V}}^{(i)}\hat{\mathbf{V}}^{(i)\top}\| \leq \frac{2^{1/2} \max \left\{ \|\mathbf{E}^{(i)\top} \hat{\mathbf{U}}^{(i)}\|, \|\mathbf{E}^{(i)} \hat{\mathbf{V}}^{(i)}\| \right\}}{\sigma_d(\hat{\Lambda}^{(i)}) - \sigma_{d+1}(\hat{\Lambda}^{(i)}) - \|\mathbf{E}^{(i)}\|} \\ &= \frac{2^{1/2} \max \left\{ \|(\hat{\Lambda}_{i,*} - \bar{\Lambda}_{i,*})^\top e_i^\top \hat{\mathbf{U}}^{(i)}\|, \|(\hat{\Lambda}_{i,*} - \bar{\Lambda}_{i,*}) \hat{\mathbf{V}}^{(i)}\| \right\}}{\sigma_d(\hat{\Lambda}^{(i)}) - \sigma_{d+1}(\hat{\Lambda}^{(i)}) - \|\hat{\Lambda}_{i,*} - \bar{\Lambda}_{i,*}\|} \end{aligned} \quad (\text{E.7})$$

We first consider the numerator of (E.7) and bound each of the terms inside of the max operator. For the second of the numerator terms, we note that the k th element of the vector $(\hat{\Lambda}_{i,*} - \bar{\Lambda}_{i,*})\hat{\mathbf{V}}^{(i)}$ takes the form $\sum_{j=1}^{NL_N} (\hat{\Lambda}_{i,*} - \bar{\Lambda}_{i,*})_j \hat{V}_{jk}^{(i)}$. By construction, each element of $\hat{\mathbf{V}}^{(i)}$ is independent of the vector $(\hat{\Lambda}_{i,*} - \bar{\Lambda}_{i,*})$, and so we can invoke a standard subexponential Bernstein inequality, as stated in Theorem 5, using that a centred Poisson random variable is subexponential. By the definition of an SVD, the k th column of $\hat{\mathbf{V}}^{(i)}$ satisfies $\|\hat{V}_{*,k}^{(i)}\| = 1$ and $\|\hat{V}_{*,k}^{(i)}\|_\infty \leq 1$, almost surely. Under Assumption 1.i, the subexponential norm of each vector entry is bounded. That is $\|(\hat{\Lambda}_{i,j} - \bar{\Lambda}_{i,j})/M_N\|_{\psi_1} = \mathcal{O}(1)$ for each $j \in [NL_N]$. We can thus apply Theorem 5 to $\sum_{j=1}^{NL_N} (\hat{\Lambda}_{i,j} - \bar{\Lambda}_{i,j}) \hat{V}_{jk}^{(i)}$ to get that for any $t \geq 0$,

$$\mathbb{P} \left(\left| \sum_{j=1}^{NL_N} (\hat{\Lambda}_{ij} - \bar{\Lambda}_{ij}) \hat{V}_{jk}^{(i)} \right| \geq Mt \right) \leq \exp \left(-C_{1,k}^{(i)} \min \left\{ \frac{t^2}{C_{2,k}^{(i)}}, \frac{t}{C_{3,k}^{(i)}} \right\} \right),$$

almost surely, for some constants $C_{1,k}^{(i)}, C_{2,k}^{(i)}, C_{3,k}^{(i)} > 0$. For large t , the quadratic term dominates and so the bound reduces to

$$\mathbb{P} \left(\left| \sum_{j=1}^{NL_N} (\hat{\Lambda}_{ij} - \bar{\Lambda}_{ij}) \hat{V}_{jk}^{(i)} \right| \geq Mt \right) \leq \exp \left(-C_{4,k}^{(i)} t \right).$$

Choosing $t = C_{5,k}^{(i)} \log(N)$, taking a union bound over the d (a constant) elements of the vector $(\hat{\Lambda}_{i,*} - \bar{\Lambda}_{i,*})\hat{\mathbf{V}}^{(i)}$ and invoking that $\|(\hat{\Lambda}_{i,*} - \bar{\Lambda}_{i,*})\hat{\mathbf{V}}^{(i)}\| \leq d^{1/2} \|(\hat{\Lambda}_{i,*} - \bar{\Lambda}_{i,*})\hat{\mathbf{V}}^{(i)}\|_\infty$ shows

$$\|(\hat{\Lambda}_{i,*} - \bar{\Lambda}_{i,*})\hat{\mathbf{V}}^{(i)}\| = \mathcal{O}(M_N \log(N)), \quad (\text{E.8})$$

almost surely.

For the first term, we cannot apply the same technique as we do not reduce to the norm of a length d vector of weighted Poisson random variables. This raises issues with controlling the spectral norm. We note the following decomposition of the operator norm in the case of a rank-one matrix: for $a \in \mathbb{R}^m$ and $b \in \mathbb{R}^n$, we have $\|ab^\top\| = \|a\| \|b\|$. We can apply this to write the first term of the numerator, up to the multiplicative constant, as $\|\hat{\Lambda}_{i,*} - \bar{\Lambda}_{i,*}\| \|\hat{U}_{i,*}^{(i)}\|$. The second term is bounded by Proposition 10. We can then use that the two-to-infinity norm is upper bounded by the spectral norm, and so Proposition 3 says that $\|\hat{\Lambda}_{i,*} - \bar{\Lambda}_{i,*}\| = \mathcal{O}(\max\{M_N, L_N\}^{1/2} M_N N^{1/2} \log^{3/2}(N))$ almost surely. It follows that

$$\|(\hat{\Lambda}_{i,*} - \bar{\Lambda}_{i,*})e_i^\top \mathbf{U}^{(i)}\| = \mathcal{O}(\max\{M_N, L_N\} M_N^{3/2} L_N^{-1/2} \log^3(N)). \quad (\text{E.9})$$

Comparing (E.9) and (E.8), we see that the numerator of (E.7) is

$$2^{1/2} \max \left\{ \|(\hat{\Lambda}_{i,*} - \bar{\Lambda}_{i,*})e_i^\top \mathbf{U}^{(i)}\|, \|(\hat{\Lambda}_{i,*} - \bar{\Lambda}_{i,*})\hat{\mathbf{V}}^{(i)}\| \right\} = \mathcal{O}(\max\{M_N, L_N\} M_N^{3/2} L_N^{-1/2} \log^3(N)), \quad (\text{E.10})$$

almost surely.

Next we bound the denominator of (E.7). To do so, we again recall Corollary 7.3.5 of Horn and Johnson (2012), which implies that for any two matrices \mathbf{A} and \mathbf{B} of the same size, we have

$$\sigma_i(\mathbf{B}) - \|\mathbf{A} - \mathbf{B}\| \leq \sigma_i(\mathbf{A}) \leq \sigma_i(\mathbf{B}) + \|\mathbf{A} - \mathbf{B}\|.$$

This tells us,

$$\sigma_d(\hat{\mathbf{\Lambda}}) - \|\hat{\mathbf{\Lambda}}^{(i)} - \hat{\mathbf{\Lambda}}\| \leq \sigma_d(\hat{\mathbf{\Lambda}}^{(i)}) \leq \sigma_d(\hat{\mathbf{\Lambda}}) + \|\hat{\mathbf{\Lambda}}^{(i)} - \hat{\mathbf{\Lambda}}\|.$$

Propositions 3 and 4 the combine to tells us

$$\begin{aligned} \Theta(M_N^{1/2} L_N^{1/2} N) - \mathcal{O}(\max\{M_N, L_N\}^{1/2} M_N N^{1/2} \log^{3/2}(N)) \\ \leq \sigma_d(\hat{\mathbf{\Lambda}}^{(i)}) \leq \Theta(M_N^{1/2} L_N^{1/2} N) + \mathcal{O}(\max\{M_N, L_N\}^{1/2} M_N N^{1/2} \log^{3/2}(N)), \end{aligned}$$

almost surely, and so $\sigma_d(\hat{\mathbf{\Lambda}}^{(i)}) = \Omega(M_N^{1/2} L_N^{1/2} N)$. Similarly, we see

$$\begin{aligned} \mathcal{O}(\max\{M_N, L_N\}^{1/2} M_N N^{1/2} \log^{3/2}(N)) - \mathcal{O}(\max\{M_N, L_N\}^{1/2} M_N N^{1/2} \log^{3/2}(N)) \\ \leq \sigma_{d+1}(\hat{\mathbf{\Lambda}}^{(i)}) \leq \mathcal{O}(\max\{M_N, L_N\}^{1/2} M_N N^{1/2} \log^{3/2}(N)) + \mathcal{O}(\max\{M_N, L_N\}^{1/2} M_N N^{1/2} \log^{3/2}(N)), \end{aligned}$$

and so $\sigma_{d+1}(\hat{\mathbf{\Lambda}}^{(i)}) = \mathcal{O}(\max\{M_N, L_N\}^{1/2} M_N N^{1/2} \log^{3/2}(N))$. It follows that

$$\left(\sigma_d(\hat{\mathbf{\Lambda}}^{(i)}) - \sigma_{d+1}(\hat{\mathbf{\Lambda}}^{(i)}) - \|\hat{\Lambda}_{i,*} - \bar{\Lambda}_{i,*}\| \right)^{-1} = \mathcal{O}\left(M_N^{-1/2} L_N^{-1/2} N^{-1}\right), \quad (\text{E.11})$$

almost surely. Combining We can then combine (E.10) and (E.11), we find

$$\|\hat{\mathbf{P}} - \hat{\mathbf{P}}^{(i)}\| = \mathcal{O}\left(\max\{M_N, L_N\}^{1/2} M_N L_N^{-1} N^{-1} \log^3(N)\right), \quad (\text{E.12})$$

almost surely. Finally, upon noting that the two-to-infinity norm is bounded by the spectral norm, we combine (E.12) with Proposition 3, we can bound $\|T_6\|$ as decomposed in (E.6):

$$\|T_6\| = \mathcal{O}\left(\max\{M_N, L_N\} M_N^2 L_N^{-1} N^{-1/2} \log^{9/2}(N)\right), \quad (\text{E.13})$$

almost surely.

To bound $\|T_5\|$, we note

$$\|T_5\| \leq \|e_i^\top \mathbf{E}(\mathbf{I} - \bar{\mathbf{P}})\hat{\mathbf{V}}^{(i)}\| = \|(\hat{\Lambda}_{i,*} - \bar{\Lambda}_{i,*})(\mathbf{I} - \bar{\mathbf{P}})\hat{\mathbf{V}}^{(i)}\|.$$

By construction, the random matrix $\hat{\mathbf{V}}^{(i)}$ is independent of $(\hat{\Lambda}_{i,*} - \bar{\Lambda}_{i,*})$ and so we will look to apply concentration inequalities We have

$$\begin{aligned} \|(\mathbf{I} - \bar{\mathbf{P}})\hat{\mathbf{V}}^{(i)}\| &\leq \|(\mathbf{I} - \bar{\mathbf{P}})\hat{\mathbf{V}}\| + \min_{\mathbf{W} \in \mathbb{O}(d)} \|(\mathbf{I} - \bar{\mathbf{P}})\| \|\hat{\mathbf{V}}^{(i)} - \hat{\mathbf{V}}\mathbf{W}\| \\ &= \|(\mathbf{I} - \bar{\mathbf{P}})\hat{\mathbf{V}}\| + \min_{\mathbf{W} \in \mathbb{O}(d)} \|\hat{\mathbf{V}}^{(i)} - \hat{\mathbf{V}}\mathbf{W}\|, \end{aligned}$$

which is valid as the triangle inequality will hold for any \mathbf{W} , and we use its assumed orthogonality to remove it from the first of the two norms. By Proposition 6, the first term satisfies

$$\|(\mathbf{I} - \bar{\mathbf{P}})\hat{\mathbf{V}}\| = \|\hat{\mathbf{V}} - \bar{\mathbf{V}}\bar{\mathbf{V}}^\top \hat{\mathbf{V}}\| = \mathcal{O}\left(\max\{M_N, L_N\}^{1/2} M_N^{1/2} L_N^{-1/2} N^{-1/2} \log^{3/2}(N)\right), \quad (\text{E.14})$$

almost surely. We use (E.12) to bound the second term by noting that we can write

$$\min_{\mathbf{W} \in \mathbb{O}(d)} \|\hat{\mathbf{V}}^{(i)} - \hat{\mathbf{V}}\mathbf{W}\| \leq \|\hat{\mathbf{P}} - \hat{\mathbf{P}}^{(i)}\| = \mathcal{O}\left(\max\{M_N, L_N\}^{1/2} M_N L_N^{-1} N^{-1} \log^3(N)\right). \quad (\text{E.15})$$

Combining (E.14) and (E.15), we find

$$\|(\mathbf{I} - \bar{\mathbf{P}})\hat{\mathbf{V}}^{(i)}\| = \mathcal{O}\left(\max\{M_N, L_N\}^{1/2} M_N^{1/2} L_N^{-1/2} N^{-1/2} \log^{3/2}(N)\right),$$

almost surely. In particular, as this matrix is of maximal rank d , we have

$$\|(\mathbf{I} - \bar{\mathbf{P}})\hat{\mathbf{V}}^{(i)}\|_{2,\infty} \leq \|(\mathbf{I} - \bar{\mathbf{P}})\hat{\mathbf{V}}^{(i)}\|_F \leq d^{1/2} \|(\mathbf{I} - \bar{\mathbf{P}})\hat{\mathbf{V}}^{(i)}\|,$$

and so we obtain almost sure bounds on the Frobenius and two-to-infinity norms.

We know $\|[(\mathbf{I} - \bar{\mathbf{P}})\hat{\mathbf{V}}^{(i)}]_{*,k}\|, \|[(\mathbf{I} - \bar{\mathbf{P}})\hat{\mathbf{V}}^{(i)}]_{*,k}\|_\infty$ decay at least as fast as $\|(\mathbf{I} - \bar{\mathbf{P}})\hat{\mathbf{V}}^{(i)}\|_F$. So, after recalling that the subexponential norm of $(\hat{\Lambda}_{i,k} - \bar{\Lambda}_{i,k})/M_N$ is $\mathcal{O}(1)$, we again apply Theorem 5 as before to say

$$\mathbb{P}\left(\left|\sum_{j=1}^{NL_N} (\hat{\Lambda}_{i,j} - \bar{\Lambda}_{i,j}) Q_{jk}^{(i)}\right| \geq Mt\right) \leq \exp\left(-D_{1,k}^{(i)} \min\left\{\frac{t^2 L_N N}{D_{2,k}^{(i)} \max\{M_N, L_N\} M_N \log^3(N)}, \frac{t L_N^{1/2} N^{1/2}}{D_{3,k}^{(i)} \max\{M_N, L_N\}^{1/2} M_N^{1/2} \log^{3/2}(N)}\right\}\right),$$

for constants $D_{1,k}^{(i)}, D_{2,k}^{(i)}, D_{3,k}^{(i)} > 0$. The linear regime dominates with a choice of

$$t = D_{5,k}^{(i)} \max\{M_N, L_N\}^{1/2} M_N^{1/2} L_N^{-1/2} N^{-1/2} \log^{5/2}(N).$$

Taking a union bound over the d elements of the vector as before, it follows that

$$\|T_5\| = \mathcal{O}\left(\max\{M_N, L_N\}^{1/2} M_N^{3/2} L_N^{-1/2} N^{-1/2} \log^{5/2}(N)\right), \quad (\text{E.16})$$

almost surely. Combining (E.13) with (E.16), we finally obtain the desired bound on $\|e_i^\top \mathbf{T}_3\|$ of:

$$\|e_i^\top \mathbf{T}_3\| = \mathcal{O}\left(\max\{M_N, L_N\}^{1/2} M_N^{3/2} L_N^{-1/2} N^{-1/2} \log^{5/2}(N)\right), \quad (\text{E.17})$$

almost surely independently of i . We couple (E.17) with (E.5) using the upper bound of (E.4) to bound $\|\mathbf{T}_1\|_{2,\infty}$ as

$$\|\mathbf{T}_1\|_{2,\infty} = \mathcal{O}\left(\max\{M_N, L_N\}^{1/2} M_N^{5/4} L_N^{-3/4} N^{-1} \log^{5/2}(N)\right),$$

almost surely. Finally, we combine our bounds on \mathbf{T}_1 and \mathbf{T}_2 to bound the two-to-infinity norm of \mathbf{M}_2 as

$$\|\mathbf{M}_2\|_{2,\infty} = \mathcal{O}\left(\max\{M_N, L_N\}^{3/2} M_N^{7/4} L_N^{-5/4} N^{-1} \log^{9/2}(N)\right), \quad (\text{E.18})$$

almost surely. Using (E.18) with the bound on $\|\mathbf{M}_2\|_{2,\infty}$ in (E.3), we obtain the stated result. The result for $\mathbf{R}_{2,2}$ follows analogously.

3. We see that

$$\begin{aligned} \|\mathbf{R}_{1,3}\|_{2,\infty} &\leq \|\bar{\mathbf{U}}\|_{2,\infty} \|\bar{\mathbf{U}}^\top (\hat{\Lambda} - \bar{\Lambda}) \bar{\mathbf{V}} \mathbf{W} \hat{\Sigma}^{-1/2}\| \\ &\leq \|\bar{\mathbf{U}}\|_{2,\infty} \|\bar{\mathbf{U}}^\top (\hat{\Lambda} - \bar{\Lambda}) \bar{\mathbf{V}}\|_F \|\mathbf{W} \hat{\Sigma}^{-1/2}\|_F. \end{aligned}$$

We know $\|\bar{\mathbf{U}}\|_{2,\infty} = \mathcal{O}\left(M_N^{-1/2} N^{-1/2}\right)$, and by Proposition 4 we have the bound $\|\mathbf{W} \hat{\Sigma}^{-1/2}\|_F = \mathcal{O}\left(N^{-1/2} M_N^{-1/4} L_N^{-1/4}\right)$. Combining these with Proposition 5 gives the desired result on $\|\mathbf{R}_{1,3}\|_{2,\infty}$. The bound on $\|\mathbf{R}_{2,3}\|_{2,\infty}$ follows analogously.

4. We get

$$\|\mathbf{R}_{1,4}\|_{2,\infty} \leq \|\hat{\Lambda} - \bar{\Lambda}\| \|\bar{V}\|_F \|\mathbf{W} \hat{\Sigma}^{-1/2} - \bar{\Sigma}^{-1/2} \mathbf{W}\|_F.$$

We can invoke Propositions 3 and 8 to write

$$\begin{aligned} \|\mathbf{R}_{1,4}\|_{2,\infty} &= \mathcal{O} \left(\max\{M_N, L_N\}^{1/2} M_N N^{1/2} \log^{3/2}(N) \max\{M_N, L_N\} N^{-3/2} M_N^{3/4} L_N^{-5/4} \log^3(N) \right) \\ &= \mathcal{O} \left(\max\{M_N, L_N\}^{3/2} M_N^{7/4} L_N^{-5/4} N^{-1} \log^{9/2}(N) \right). \end{aligned}$$

E.13 Proof of Proposition 13

For some $t_m \in B_m$, we can write the following:

$$\|\tilde{\mathbf{X}}^{(m,*)} - \mathbf{X}(t)\|_{2,\infty} = M_N \int_{B_m} \|\mathbf{X}(s) - \mathbf{X}(t_m)\|_{2,\infty} ds + \|\mathbf{X}(t_m) - \mathbf{X}(t)\|_{2,\infty}.$$

By Assumption 2.i, we can then say

$$\|\tilde{\mathbf{X}}^{(m,*)} - \mathbf{X}(t)\|_{2,\infty} \leq M_N K \int_{B_m} |t_m - s| ds + K|t_m - t| \leq M_N K \int_{B_m} M_N^{-1} ds + K M_N^{-1} = \mathcal{O}(K M_N^{-1}).$$

E.14 Proof of Proposition 14

Define \mathbf{W}_m to be

$$\mathbf{W}_m \in \underset{\mathbf{Q} \in \mathbb{O}(d)}{\operatorname{argmin}} \|\mathbf{P}(t_m) \tilde{\mathbf{X}}^{(m,*)} \mathbf{Q} - \mathbf{X}(t_m)\|_{2,\infty},$$

and decompose our norm into the following two terms:

$$\|\tilde{\mathbf{X}}^{(m,*)} \mathbf{W}_m - \mathbf{X}(t)\|_{2,\infty} \leq \|(\mathbf{I} - \mathbf{P}(t)) \tilde{\mathbf{X}}^{(m,*)} \mathbf{W}_m\|_{2,\infty} + \|\mathbf{P}(t) \tilde{\mathbf{X}}^{(m,*)} \mathbf{W}_m - \mathbf{X}(t)\|_{2,\infty}.$$

Note that \mathbf{W}_m is guaranteed to exist as $\mathbb{O}(d)$ is compact and the mapping is continuous as it is a composition of a linear map and the continuous two-to-infinity norm. For the first of these terms, we use that the two-to-infinity norm is invariant upon right multiplication by an orthogonal matrix and that $\mathbf{X}(u) = \mathbf{P}(u)$ to write

$$(\mathbf{I} - \mathbf{P}(t)) \tilde{\mathbf{X}}^{(m,*)} = M_N \int_{B_m} (\mathbf{I} - \mathbf{P}(t)) \mathbf{P}(u) \mathbf{X}(u) du.$$

We then use the following equality:

$$\|(\mathbf{I} - \mathbf{P}(t)) \mathbf{P}(u)\|_{2,\infty} = \|\mathbf{P}(u)^2 - \mathbf{P}(t) \mathbf{P}(u)\|_{2,\infty} = \|\mathbf{P}(u) - \mathbf{P}(t)\|_{2,\infty},$$

to bound our expression as

$$\begin{aligned} \|(\mathbf{I} - \mathbf{P}(t)) \tilde{\mathbf{X}}^{(m,*)} \mathbf{W}_m\|_{2,\infty} &\leq M_N \int_{B_m} \|(\mathbf{I} - \mathbf{P}(t)) \mathbf{P}(u)\|_{2,\infty} \|\mathbf{X}(u)\|_{2,\infty} du, \\ &\leq M_N \int_{B_m} \|\mathbf{P}(u) - \mathbf{P}(t)\|_{2,\infty} \|\mathbf{X}(u)\|_{2,\infty} du, \\ &\leq M_N \int_{B_m} \|\mathbf{P}(u) - \mathbf{P}(t)\|_{2,\infty} du \times \mathcal{O}(1), \\ &\leq M_N K_1 \int_{B_m} |t - u| du \times \mathcal{O}(1), \\ &\leq K_1 / (2M_N) \times \mathcal{O}(1) \\ &= \mathcal{O}(K_1 M_N^{-1}). \end{aligned}$$

where we invoked Assumptions 1.i and 2.ii. The second term we decompose as follow:

$$\begin{aligned}\|\mathbf{P}(t)\tilde{\mathbf{X}}^{(m,*)}\mathbf{W}_m - \mathbf{X}(t)\|_{2,\infty} &\leq \|(\mathbf{P}(t) - \mathbf{P}(t_m))\tilde{\mathbf{X}}^{(m,*)}\|_{2,\infty} + \|\mathbf{P}(t_m)\tilde{\mathbf{X}}^{(m,*)}\mathbf{W}_m - \mathbf{X}(t_m)\|_{2,\infty} \\ &\quad + \|\mathbf{X}(t_m) - \mathbf{X}(t)\|_{2,\infty}.\end{aligned}$$

The first term is clearly $\mathcal{O}(K_1 M_N^{-1})$. The third term is bounded as

$$\begin{aligned}\|\mathbf{X}(t_m) - \mathbf{X}(t)\|_{2,\infty} &\leq \|\mathbf{P}(t_m)(\mathbf{X}(t_m) - \mathbf{X}(t))\|_{2,\infty} + \|(\mathbf{I} - \mathbf{P}(t_m))\mathbf{X}(t)\|_{2,\infty}, \\ &\leq K_2|t_m - t| + K_1|t_m - t| \times \mathcal{O}(1), \\ &= \mathcal{O}((K_1 + K_2)M_N^{-1}).\end{aligned}$$

Finally, the second term is bounded by invoking the definition of \mathbf{W}_m to say

$$\|\mathbf{P}(t_m)\tilde{\mathbf{X}}^{(m,*)}\mathbf{W}_m - \mathbf{X}(t_m)\|_{2,\infty} \leq \|\mathbf{P}(t_m)\tilde{\mathbf{X}}^{(m,*)} - \mathbf{X}(t_m)\|_{2,\infty} = \mathcal{O}(K_1 M^{-1}).$$

Combining, we see

$$\|\mathbf{P}(t)\tilde{\mathbf{X}}^{(m,*)}\mathbf{W}_m - \mathbf{X}(t)\|_{2,\infty} = \mathcal{O}((K_1 + K_2)M_N^{-1}),$$

and so

$$\|\tilde{\mathbf{X}}^{(m,*)}\mathbf{W}_m - \mathbf{X}(t)\|_{2,\infty} = \mathcal{O}((K_1 + K_2)M_N^{-1}).$$

This result is clearly uniform over t and m and the result follows.